PHYSICAL REVIEW
LETTERS

VOLUME 3 SEPTEMBER 15, 1959 NUMBER 6

TIME-DEPENDENT PAIR CORRELATIONS IN LIQUID LEAD

B. N. Brockhouse and N. K. Pope
Physics Division, Atomic Energy of Canada Limited, Chalk River, Ontario, Canada
(Received August 17, 1959)

Van Hove has proposed that the atomic motions in liquids can be studied in terms of a time-dependent pair correlation function, obtainable by Fourier transformation of neutron scattering measurements over neutron energy and momentum.[1] This pair correlation function $G(\vec{r}, t)$ is "classically" the average number density at the point $\vec{r}$ at the time t, when it is known that there was an atom at the origin at time 0. It is a natural extension of the instantaneous pair correlation function $g(\vec{r})$, first obtained by Fourier inversion of x-ray scattering measurements; in fact its value at time zero is given by $G(\vec{r}, 0) = g(\vec{r}) + \delta(\vec{r})$. The correlation function has been discussed further by other workers.[2-4] It has been studied experimentally for the rather special case of water,[2,5-7] but not in full generality. In this Letter we present the first experimental determination of $G(\vec{r}, t)$ for a simple liquid, liquid lead at a temperature (620°K) just above its melting point.

For the particular case of neutron scattering by a classical monatomic liquid, the partial differential scattering cross section per atom has the form

$$\frac{d^2\sigma}{d\Omega dE'} \equiv \frac{b^2}{\hbar}\frac{k'}{k_0} S(Q,\omega), \qquad (1)$$

where b is the coherent scattering length, $\vec{k}_0$ and $\vec{k}'$ are the ingoing and outgoing neutron wave vectors, and E_0 and E' are the ingoing and outgoing neutron energies. $Q \equiv |\vec{k}_0 - \vec{k}'|$ is the magnitude of the change of wave vector, and $\hbar\omega \equiv E_0 - E'$ is the change of neutron energy. The Van Hove correlation function is given by

$$G(r,t) = \frac{1}{2\pi^2}\int_0^\infty i(Q,t)\,\frac{\sin Qr}{Qr}\,Q^2 dQ, \qquad (2)$$

where

$$i(Q,t) = \int_{-\infty}^{\infty} S(Q,\omega)\cos\omega t\, d\omega. \qquad (3)$$

The fact that the function S depends only on the magnitude of the vector Q is shown by writing S as a function of Q, not $\vec{Q}$. In the same way G is written as a function of r, not $\vec{r}$.

Hereafter r will be given in angstroms, Q in reciprocal angstroms, t in units of 10^{-13} second, and units will be omitted.

In our experiments so far, about fifty energy distributions of monoenergetic neutrons scattered by liquid lead have been measured, using neutrons of wavelengths 1.36 A (Series I), and 2.22 A (Series II) from a crystal spectrometer at the NRU reactor, and neutrons of wavelength 4.13 A (Series III) from the rotating-crystal spectrometer,[8] also at NRU. The results were in agreement with limited studies on liquid lead already reported.[9-11] Series I were complete energy distributions and covered a range of Q from 1 to 7 A^{-1}. The distributions of Series II and III were limited to energies near the incoming energy and to values of Q from 1 to 4 for Series II and 2 to 2.2 for Series III. Several typical energy distributions are shown in Fig. 1, together with resolution functions obtained from the elastic inco-

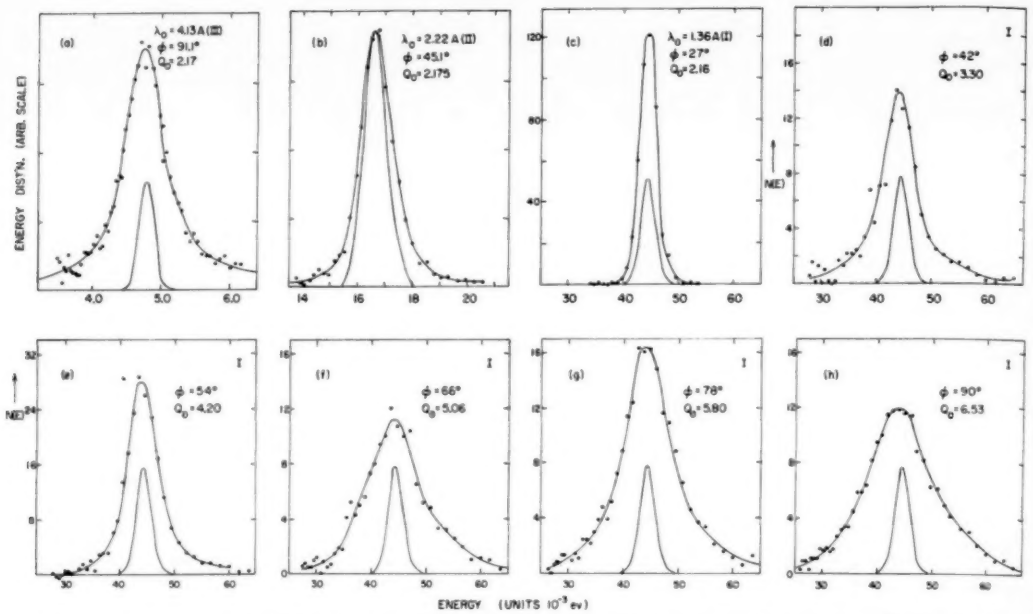
ENERGY DISTN. (ARB. SCALE)
ENERGY (UNITS 10^{-3} ev)
(a) λ_0 = 4.13 A (III) ϕ = 91.1° Q_0 = 2.17
(b) λ_0 = 2.22 A (II) ϕ = 45.1° Q_0 = 2.175
(c) λ_0 = 1.36 A (I) ϕ = 27° Q_0 = 2.16
(d) ϕ = 42° Q_0 = 3.30
(e) ϕ = 54° Q_0 = 4.20
(f) ϕ = 66° Q_0 = 5.06
(g) ϕ = 78° Q_0 = 5.80
(h) ϕ = 90° Q_0 = 6.53

FIG. 1. A selection of energy distributions of neutrons scattered from liquid lead at 620°K, each with its resolution function (appropriate to the incident energy). All patterns have been corrected for background, for container scattering, for instrument sensitivity, and all except (a) for multiple scattering. [Figure 1 (a) is thought to contain ~ 10% multiple scattering.] The factor k'/k_0 of Eq. (1) has also been removed. Figures 1 (a), (b), and (c) show energy distributions obtained under different resolutions at the main diffraction peak. In Fig. 1 (b) the resolution function has been normalized at the peak to illustrate the energy broadening. Figures 1 (a) and (b) are in agreement that the half-width at half maximum of the distribution is $\sim 3.5\times 10^{-4}$ ev, compared with the 8×10^{-4} ev expected on simple arguments of diffusion broadening by small motions [references 2 and 3]. The shape is roughly Lorentzian. Figures (c) to (h) show Series I distributions at different values of Q_0. The intensities are consistently normalized but note the different ordinate scales.

herent scattering by vanadium metal.

The flat specimen of liquid lead has a transmission of ~78%. The energy distributions thus contained a component due to multiple scattering which amounted[12] to about 29% of the distributions at large Q. The integrated intensity[12] and energy distribution of this component were assumed to be isotropic. The average of distributions obtained at small angles of scattering ($Q<1.4$) was taken to be the multiple scattering component, and was subtracted point-by-point from the other distributions of the same series.

In constructing the function $S(Q,\omega)$ from the experimental data several approximations were made, which will be removed in the final analysis. (1) The wave vector change was assumed to be independent of the outgoing energy, and to depend only on the angle of scattering ϕ; that is $Q=Q_0 \equiv 2k_0 \sin(\phi/2)$. (2) No correction for the resolution in Q space was applied. (3) The energy resolution was assumed to be constant in a given series of measurements. It was then possible to remove the resolution from the transformed function $i(Q,t)$ by simple division, rather than by unfolding it from $S(Q,\omega)$. In the present context these approximations are not serious. The measurements of the angular distribution by Sharrah and Smith[9] were used to extrapolate the functions $i(Q,t)$ for small t to $Q \simeq 9$.

In Fig. 2 a selection of the functions $i(Q,t)$ and $G(r,t)$ are presented as computed from the measurements. The part of $G(r,t)$ representing the atom which at $t=0$ is at the origin, called the self-correlation function,[1] is plotted on different scales from the remainder of $G(r,t)$.

De Gennes[4] has shown in a very general way that the mean square energy transfer is related to the angular distribution $i(Q,0)$ by the expression

$$i(Q,0) = (k_B T/M)(\hbar Q)^2/(\hbar\omega)^2, \qquad (4)$$

where k_B is Boltzmann's constant and M is the

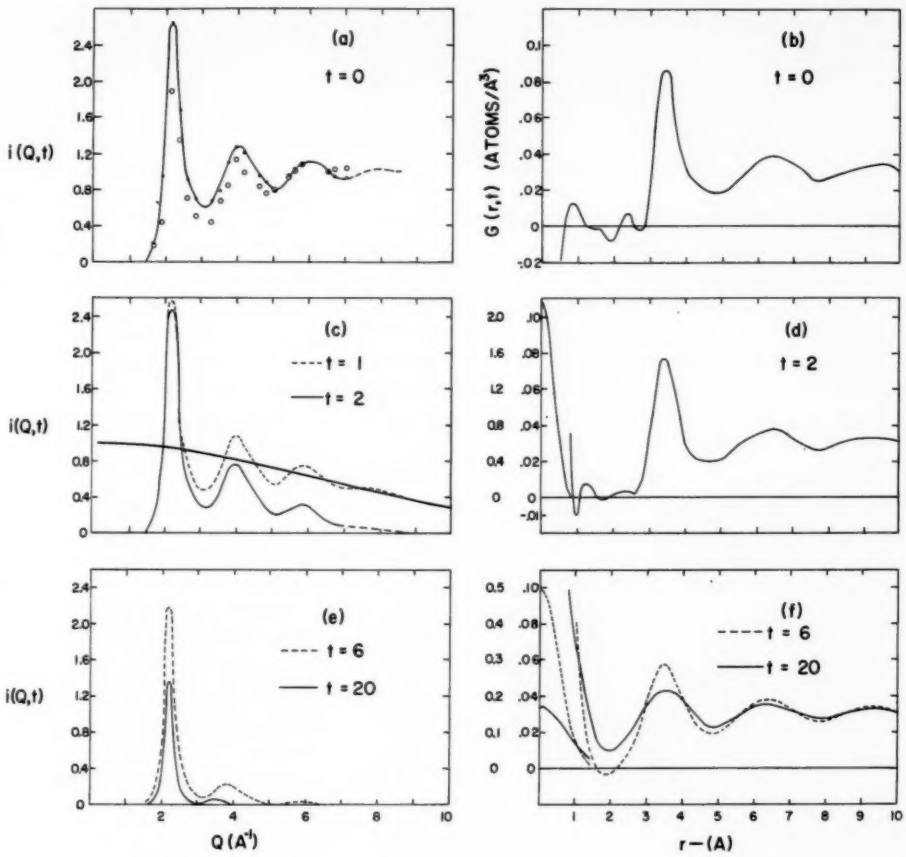

FIG. 2. A selection of smoothed curves of $i(Q,t)$ vs Q, and curves of $G(r,t)$ vs r for values of $t = 0$, 1, 2, 6, and 20×10^{-13} sec. The closed circles in Fig. 2(a) show the experimental points for the integrated intensities $i(Q, 0)$ of Series I. The open circles in Fig. 2(a) are values of $i(Q, 0)$ calculated following Eq. (4). Note that the left-hand scales in Figs. 2(d) and 2(f) apply to the self-correlation functions.

mass of the atom. This relation can be used as a rather stringent test of the consistency of experimental data. Figure 2(a) shows the function $i(Q, 0)$ as measured directly (Series I), and as computed from the measured mean square energy transfers by means of Eq. (4). The agreement is considered to be reasonably good.

For a classical system at small times, the self-correlation function is expected to be independent[1,2] of the state of the system—whether solid, liquid, or gas. Under these conditions, for small t and large Q, the function $i(Q,t)$ takes the form for a perfect gas

$$i(Q,t) = \exp[-(k_B T/2M)Q^2t^2]. \quad (5)$$

In Fig. 2(c) the measured curve for $i(Q,1)$ is shown, together with a curve calculated from Eq. (5) for $t = 1$, to which the measured curve indeed appears to be asymptotic.

The radius at half maximum of the self-correlation function, and the half-widths at half maximum of the first peak in the pair correlation function—the correlation function for first neighbors—are plotted as functions of time in Fig. 3. The half-width of the correlation function for first neighbors was taken somewhat arbitrarily to be the difference between 3.50 A and the position at half maximum on the inward edge of the peak. Also shown are calculated curves[2,3] for the radius at half maximum of the self-correlation functions of a perfect gas, and of a diffusing atom making infinitesimally small jumps and having the measured[13] coefficient of self-diffusion 2.5×10^{-5} cm²/sec.

From Figs. 2 and 3, $G(r,t)$ may be followed in some detail. At $t = 0$ the instantaneous pair correlation is in good agreement with that obtained by Sharrah and Smith.[9] At small times, up to $t = 2$, the principal effect is the rapid motion outwards of the atom at the origin at gas velocities. For t from 2 to 8, the atom at the origin and the

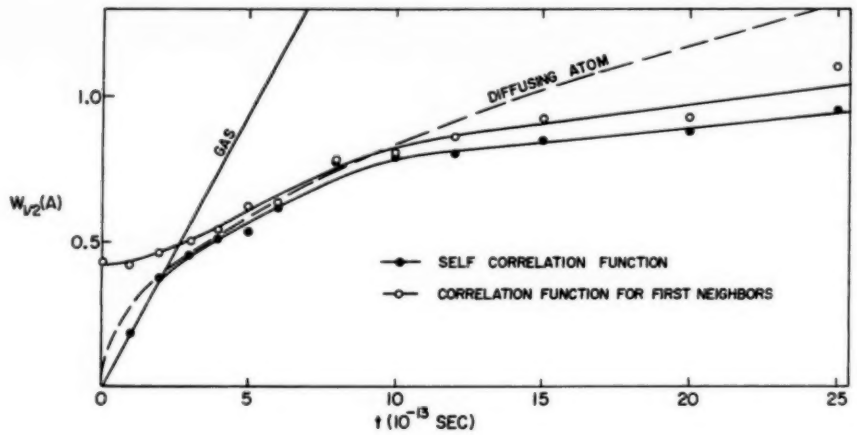

FIG. 3. The radius at half maximum of the self-correlation function (closed circles) and the half-width at half maximum of the correlation function for first neighbors (open circles) as functions of the time.

atoms in the first shell move in a somewhat complicated way. At times $t \gtrsim 8\times10^{-13}$ sec the atoms seem to be settling down into a diffusive type of motion, but the rate of diffusion appears to be less than the rate of self-diffusion measured by tracers. This suggests that, in addition to the small motions ("jitter") of the atoms, which show up as a continuous diffusive expansion of the correlation functions, there also occur significant numbers of comparatively large diffusion "jumps." Such behavior was previously postulated[2] to explain the results on water. The distribution of "jump sizes" could possibly be studied by means of the shapes of the correlation functions. The present results, however, are not sufficiently precise for this to be possible.

Details of the experiments and of the analysis will be published on conclusion of the work.

[1]L. Van Hove, Phys. Rev. 95, 249 (1954).
[2]B. N. Brockhouse, Suppl. Nuovo cimento 9, 45 (1958).
[3]G. H. Vineyard, Phys. Rev. 110, 999 (1958).
[4]P. G. de Gennes, Physica (to be published).
[5]Brugger, McClellan, Streetman, and Evans, Nuclear Sci. and Eng. 5, 99 (1959).
[6]B. N. Brockhouse, Phys. Rev. Letters 2, 287 (1959).
[7]Hughes, Palevsky, Kley, and Tunkelo, Phys. Rev. Letters 3, 91 (1959).
[8]B. N. Brockhouse, Bull. Am. Phys. Soc. 3, 233 (1958).
[9]P. C. Sharrah and G. P. Smith, J. Chem. Phys. 21, 228 (1953).
[10]B. N. Brockhouse, Phys. Rev. 98, 1171(A) (1955).
[11]Pelah, Whittemore, and McReynolds, Phys. Rev. 113, 767 (1959).
[12]G. H. Vineyard, Phys. Rev. 96, 93 (1954); Brockhouse, Corliss, and Hastings, Phys. Rev. 98, 1721 (1955).
[13]L. D. Hall and S. Rothman, Trans. Am. Inst. Mining, Met., Petrol. Engrs. 206, 199 (1956).

KNIGHT SHIFT IN SUPERCONDUCTORS*

Richard A. Ferrell†
United States Naval Ordnance Laboratory, White Oak, Silver Spring, Maryland
and University of Maryland, College Park, Maryland
(Received July 31, 1959)

The theory of Townes et al.[1] of the Knight shift in the frequency of nuclear resonance in a metal predicts a fractional change of

$$\frac{\Delta H}{H} = \frac{8\pi}{3} \frac{\langle |\psi_F(0)|^2 \rangle_{Av}}{n_a} \chi, \qquad (1)$$

where χ is the magnetic spin susceptibility per unit volume, n_a is the atomic density, and the square of the wave function is evaluated at the nucleus and averaged over the Fermi surface.[2] The measurements of Reif[3] and of Androes and Knight[4] indicate shifts for superconducting mercury and tin almost as large as that for the metals in the normal state. This would seem to indicate according to Eq. (1) that the supercon-

ducting and normal susceptibilities are practically equal, even at zero temperature (which is the case to which we limit ourselves). This interpretation conflicts with the theory of Bardeen et al.,[5] which establishes a strict energy gap and a vanishing spin susceptibility for the superconducting ground state.[6] The exact pairing of electrons in momentum space has been relaxed by Heine and Pippard[7] to permit spin excitations and a susceptibility almost as large in the superconducting as in the normal state. It is not impossible that this modification of the BCS theory does indeed provide the correct explanation of the finite Knight shift for superconductors. But on the other hand, there is a danger that when the details of this modification are worked out, a discrepancy may arise with the specific heat. If the spin excitations which are allowed by Heine and Pippard prove to have appreciable statistical weight, they will yield a measurable contribution to the specific heat, in disagreement with experiment. Furthermore, evidence against the existence of the spin excitations is provided by the marked increase in the nuclear spin relaxation time in superconducting aluminum, as the temperature is decreased.[8]

The purpose of the present note is to propose an alternative explanation of the Knight shift in superconductors which is free of the above difficulties. We assume that low-lying excitations do not exist for a bulk superconductor, for which the susceptibility can indeed be taken to be zero. But we present some theoretical considerations which indicate that for a finite sample the susceptibility should rise when the geometrical dimensions are made smaller than the coherence length, to a value comparable to that in the normal state. This proposed size dependence is quite plausible, since it is generally accepted that the superconducting state depends in a very essential way on long-range correlations.

In order to establish that the superconducting Knight shift should be expected to possess a size dependence, it is convenient to avoid calculating the susceptibility directly, and instead to consider an alternative way of computing the shift. The effect results from an interference of two perturbing terms H' and H'' in the Hamiltonian for the electron system. The first represents the interaction between the electron spins and the laboratory magnetic field, and the second that between the electron spins and the nuclear magnetic moment. The part of the perturbed ground-state energy which depends in second order upon the interference of the two perturbations is given by

$$\Delta E = \sum_{n\neq 0} \frac{H_{0n}' H_{n0}'' + H_{0n}'' H_{n0}'}{E_0 - E_n}, \qquad (2)$$

where the matrix elements are taken with respect to the unperturbed stationary states of energy E_n. This equation can be interpreted in two ways. One can imagine that H' produces a change ψ' in the wave function and that the energy of the perturbation H'' is then computed as an expectation value with respect to this perturbed wave function. This corresponds to Eq. (1), where the laboratory field first polarizes the electron gas, which then acts upon the nucleus. Alternatively, one can think of H'' as producing a different change ψ'', and can then use this wave function for computing the expectation value of H'. In other words, one can first "turn on" the nuclear magnetic moment, which then becomes "dressed" with a polarization cloud which changes its g factor and consequently its resonance frequency in the laboratory field. The latter picture has some merit conceptually, since in actual fact it is never possible to turn off the nuclear moment; the laboratory field is, of course, at one's disposal. We are therefore motivated to calculate the total magnetic moment induced in the electron gas by the nuclear magnetic dipole.

For our argument it is essential to establish the spatial distribution of the magnetization. We give the result of a calculation using the simple free-electron model, where the wave functions are plane waves. The nucleus is considered to be only a magnetic dipole; its Coulomb field is ignored. By applying Born's approximation we obtain a magnetization density[9] of

$$M(r) = (4\mu\chi/3r^2) j_1(2k_0 r), \qquad (3)$$

where the spherical Bessel's function is

$$j_1(x) = \frac{\sin x}{x^2} - \frac{\cos x}{x}. \qquad (4)$$

μ is the nuclear magnetic dipole moment, k_0 the wave number at the top of the Fermi sea, and r the radial distance from the nucleus. This magnetization density can be integrated to give a total induced magnetic dipole moment in the vicinity of the nucleus whose ratio to the inducing nuclear moment is equal to

$$\frac{\Delta\mu}{\mu} = \frac{4\pi}{\mu}\int_0^\infty M(r) r^2 dr = \frac{8\pi}{3}\chi. \qquad (5)$$

In the present model the square of the wave function equals the atomic density, so that the Knight shift predicted by Eqs. (1) and (5) is identical. This agreement was to be expected because of the equivalence of the two different ways of computing the energy change given by Eq. (2). But this second way of computing the Knight shift has the advantage of providing an intuitive picture for the effect. The magnetization density times $4\pi r^2$ is plotted in Fig. 1, which shows that most of the effect comes from close distances (high-energy virtual excitations). The arrow in Fig. 1 indicates approximately one-half of the average interelectron separation, and it is very natural to assume that the magnetization density at distances from the nucleus of this order of magnitude is completely unaffected by the superconducting transition.

The transition to the superconducting state can be expected to have an effect on the polarization cloud only over distances of the order of the coherence length, which is hundreds or thousands of times greater than the mean radius of the cloud shown in Fig. 1. To illustrate this, a very crude energy-gap model suffices. Let us modify the free-electron model by leaving all the matrix elements unchanged but by replacing all excitation energies less than $\hbar k_0 \kappa/m$, by this quantity itself. The reciprocal of the parameter κ, which specifies the gap energy, is a rough measure of the coherence length. With this change, an additional contribution to the magnetization density appears of the form

$$M'(r) = -\frac{4\mu\chi}{3\pi r^2}\frac{1-\cos\kappa r}{\kappa r^2}. \tag{6}$$

(Here we have omitted a fluctuating term proportional to $\cos 2k_0 r$ which gives no net magnetization.) Integrating over this, we find an additional induced moment corresponding to a fractional change in the nuclear g factor of

$$\frac{\Delta\mu'}{\mu} = -\frac{8\pi}{3}\chi. \tag{7}$$

Adding this contribution to that found in Eq. (5) above, we obtain a vanishing net Knight shift, as expected for a strict energy-gap model which can possess no bulk susceptibility. But it is essential to note that the density of the compensating cloud described by Eq. (6) is extremely low compared to that of Eq. (2) at distances from the nucleus of the order of interatomic dimensions. It is only by integrating out to radii of the order of the coherence length that we produce a cancellation of the close-in cloud responsible for the normal Knight shift.

Because of the boundary effects, it is difficult to give a rigorous treatment of the compensating cloud set up in a small sample. For simplicity, imagine that the nucleus is at the center of a sphere of diameter L much less than $\xi_0 \approx \kappa^{-1}$, the coherence length. As a first approximation we can take the magnetization density at any distance less than $L/2$ to be the same as that which would exist around the nucleus in a bulk sample. Then it follows from the preceding paragraph that the superconducting fractional decrease in the Knight shift is of the order of $L/\xi_0 \ll 1$. But this is much too crude a treatment, as can be seen from the following transport picture:[10] The magnetization cloud in a bulk sample is established by electrons which interact with the nucleus and then carry the effect of the perturbation radially outward. In a small sample, these electrons will be reflected back at the surface and will build up a magnetization larger by the factor f, the number of times that they can be scattered before the spin-orbit force flips their spin.[11] Thus we obtain, to within a multiplicative numerical constant, the following rough equality for the normal-superconducting difference:

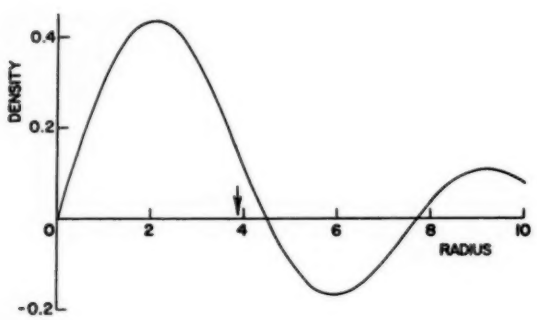

FIG. 1. Radial magnetization density vs radius r, measured in units of $(2k_0)^{-1}$ [or $(4\pi)^{-1}$ times the deBroglie wavelength at the Fermi surface]. The ordinate is proportional to $(dr)^{-1}$ times the magnetization contained between spheres of radius r and $r+dr$. The curve represents the polarization cloud surrounding a point magnetic dipole (nucleus) in a free-electron gas and is given by $j_1(2k_0 r)$. The arrow indicates a radius roughly equal to one-half of the average interelectron separation, within which most of the polarization cloud is contained. The superconducting transition cannot affect this cloud, which changes the total magnetic moment of the "dressed" nucleus and consequently yields the Knight shift, because it arises from virtual excitation to states very far above the energy gap.

$$(\Delta H_n - \Delta H_s)/\Delta H_n \approx fL/\xi_0. \quad (8)$$

(This equation applies only when L is less than ξ_0/f. For larger values of L, $\Delta H_s/\Delta H_n$ approaches zero.) Substituting from reference 4 the values $(\Delta H_n - \Delta H_s)/\Delta H_n = 0.27$ and $L \approx 100$ A (a weighted geometrical mean value of the diameter and thickness of the platelets), and $\xi_0 = 2500$ A from reference 5, we obtain $f \approx 6$, a reasonable value.

Summarizing, we have seen that the Knight shift results from a normal magnetization cloud, which is closely bound to the nucleus and is the same in both the normal and superconducting states, and a diffuse compensating cloud which appears only in the superconducting state and is of very great linear dimensions. Since only a fraction of this cloud is contained in a small sample, the superconducting shift is expected to be smaller than but comparable to the normal shift. The actual magnitude of the decrease has been interpreted in Eq. (8) as being dependent on the spin-orbit coupling. It should be emphasized that the spin-orbit force is quite essential, since it is only by means of it that the total electron spin ceases to be a good quantum number. It then becomes possible for the magnetic field to mix in virtual excitations from above the gap, yielding a nonvanishing susceptibility. Since the spin-orbit coupling is very strongly dependent on atomic number, f may be expected to be very large for a light element, which should consequently show a Knight shift very much reduced in the superconducting state, in definite contrast to the nearly full shift exhibited by the heavy elements. It would be highly desirable to test experimentally this aspect of Eq. (8), as well as the linear dependence on L.

We wish to thank Dr. T. Day, Dr. F. Stern, Dr. J. Sucher, and especially Dr. M. Tinkham for several useful discussions.

---

*This work was carried out by the author partly at the U. S. Naval Ordnance Laboratory and in part with the support of the Office of Naval Research under contract with the University of Maryland.

†Present address: CERN, Geneva, Switzerland. (Permanent address: University of Maryland, College Park, Maryland.)

[1]Townes, Herring, and Knight, Phys. Rev. 77, 852 (1950).

[2]For further discussion see W. D. Knight, in Solid State Physics, edited by F. Seitz and D. Turnbull (Academic Press, New York, 1956), Vol. 2, p. 97.

[3]F. Reif, Phys. Rev. 106, 208 (1957).

[4]G. M. Androes and W. D. Knight, Phys. Rev. Letters 2, 386 (1959).

[5]Bardeen, Cooper, and Schrieffer, Phys. Rev. 108, 1175 (1957).

[6]K. Yosida, Phys. Rev. 110, 769 (1958).

[7]V. Heine and A. B. Pippard, Phil. Mag. 3, 1046 (1958).

[8]A. G. Redfield, Phys. Rev. Letters 3, 85 (1959).

[9]This expression is essentially identical to that found by Ruderman and Kittel for the indirect exchange coupling of nuclear magnetic moments by conduction electrons [M. A. Ruderman and C. Kittel, Phys. Rev. 96, 99 (1959)].

[10]The author is greatly endebted to Dr. M. Tinkham for bringing this feature of the problem to his attention.

[11]The considerations involved here are analogous to those which enter into the calculation of the current in a thin film under the assumption of almost perfect specular reflection at the surfaces. See, for example, J. R. Schrieffer, Phys. Rev. 106, 47 (1957).

MAGNETIC EFFECTS ON SHEAR WAVE ATTENUATION IN SINGLE CRYSTAL COPPER

J. R. Neighbours* and G. A. Alers
Scientific Laboratory, Ford Motor Company, Dearborn, Michigan
(Received August 7, 1959)

Recently there has been much interest in the effects of a magnetic field on ultrasonic attenuation at low temperatures, and much experimental work has been directed toward the study of longitudinal[1] waves. To our knowledge, resonances in the attenuation of shear waves in single crystals have not been previously reported in detail. These are of interest because recently published theories[2,3] predict the existence of oscillations in the attenuation versus magnetic field data only for certain orientations of field, polarization, and propagation directions. In particular no oscillations should be observed when the magnetic field is parallel to the polarization direction, although the attenuation should decrease with increasing magnetic field. Our preliminary observations show that oscillations occur in shear wave attenuation when the field is either

parallel or perpendicular to the particle motion. The measurements also indicate that the effective mean free path of the electrons depends on the polarization of the sound wave with which they interact.

The ultrasonic generating apparatus was the same as has been previously described.[4] Several accurately oriented [110] crystals were cut from a single crystal ingot[5] of very pure copper, and the measurements were performed with the crystals immersed in a liquid helium bath between the pole pieces of an A.D.L. electromagnet. The experimental arrangement was such that the direction of propagation, [110], was always perpendicular to the applied field, and this field could be made either parallel or perpendicular to the acoustic polarization. The maximum applied field was 15.0 kilogauss. Our measurements were similar to others reported,[1] except that here the attenuation was measured by observing the change in echo height displayed on an oscilloscope as the field was changed.

For the polarization along a [001] direction, the wave velocity is determined by the elastic constant $C = C_{44}$, while for a $[\bar{1}10]$ polarization, the constant $C' = \frac{1}{2}(C_{11} - C_{12})$ determines the velocity. At the same frequency the latter will have a shorter wavelength by a factor of nearly two. Figure 1 shows relative changes in attenuation for the C' mode, for 15.9 Mc/sec ($\lambda = 0.106$ mm) and 25.5 Mc/sec ($\lambda = 0.066$ mm), plotted as a function of λH on an (inverted) reciprocal scale. $H_\parallel$ and $H_\perp$ refer to the direction of the applied magnetic field with respect to the acoustic polarization. In all cases, H was perpendicular to the direction of propagation. For the low-frequency waves two maxima in attenuation are apparent for $H_\parallel$ and none for $H_\perp$ which is contrary to the predictions. At the higher frequency, prominent oscillations are apparent for both orientations of applied field. The disconnected parts of the curves represent very large maxima in attenuation, since they correspond to the observed echo disappearing into the noise and no longer being discernable.

Attenuation changes for the C mode are shown in Fig. 2. As would be expected from the longer wavelengths involved, these data show a smaller effect than that observed for the C' mode. No oscillation was observed at 15.9 Mc/sec ($\lambda = 0.19$ mm) for either orientation of magnetic field. At the higher frequency (25.9 Mc/sec)($\lambda = 0.116$ mm) one peak was observed for $H_\parallel$ and two peaks for $H_\perp$.

Several of the different experimental arrangements which have been used are listed in Table I. The column headed longitudinal mode lists the orientations used by Morse et al.[1] and the other columns show the orientations used in the present work. Inspection of the table shows that the

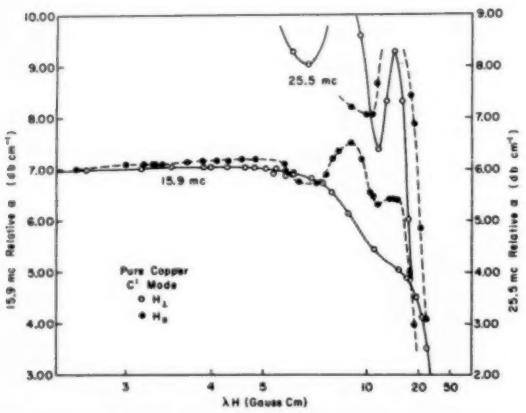

FIG. 1. Attenuation of shear waves in copper at 4.2°K plotted as a function of λH on an inverted reciprocal scale. The propagation direction is parallel to [110] and the acoustic polarization is parallel to $[\bar{1}10]$. The notations $H_\parallel$ and $H_\perp$ refer to the direction of the applied magnetic field with respect to the acoustic polarization. At 15.9 Mc/sec, $\lambda = 0.106$ mm, and at 25.5 Mc/sec, $\lambda = 0.066$ mm. The zero of the attenuation scale was set at 15 kilogauss.

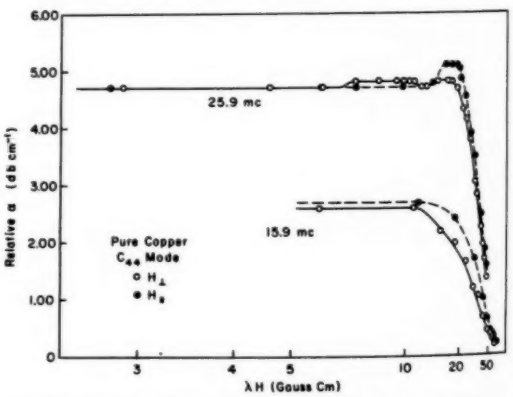

FIG. 2. Attenuation of shear waves in copper at 4.2°K plotted as a function of λH on an inverted reciprocal scale. The propagation direction is parallel to [110] and the acoustic polarization is parallel to [001]. The notations $H_\parallel$ and $H_\perp$ refer to the direction of the applied magnetic field with respect to the acoustic polarization. At 15.9 Mc/sec, $\lambda = 0.19$ mm, and at 25.9 Mc/sec, $\lambda = 0.116$ mm. The zero of the attenuation scale was set at 15 kilogauss.

Table I. Orientations of the electron orbits, magnetic fields, and acoustic waves with respect to the cubic crystal axes.

	Longitudinal mode [100] propagation		C mode [110] propagation		C' mode [110] propagation	
	$H_{\parallel}$	$H_{45°}$	$H_{\parallel}$	$H_{\perp}$	$H_{\parallel}$	$H_{\perp}$
Acoustic polarization	[100]	[100]	[001]	[001]	$[\bar{1}10]$	$[\bar{1}10]$
Normal to plane of orbit	[100]	[110]	[001]	$[\bar{1}10]$	$[\bar{1}10]$	[001]

C mode with $H_{\parallel}$ and the longitudinal mode with $H_{\parallel}$ are equivalent. The observed maximum for the C mode with $H_{\parallel}$ occurs at a λH value very close to that observed for the longitudinal mode, so the measurements for this mode appear to be in agreement with previous results. Although the plane of the electron orbit for the C' mode with $H_{\perp}$ is the same as in the two above cases, the acoustic polarization and thus the induced electric fields are in a different direction. It is observed that this difference in polarization direction causes the maxima and minima in attenuation to occur at different λH values. The above comparisons cannot be interpreted in terms of the existing theories because no maxima are predicted in the $H_{\parallel}$ cases.

The current theories do predict that the attenuation maxima and minima should be periodic in $(\lambda H)^{-1}$. Theoretically this period is equal to one fourth the electronic charge divided by the electron momentum. The results of Figs. 1 and 2 give values of momentum in agreement with the value previously found for copper[1] ($p = 1.16 \times 10^{-19}$ g cm/sec). However, the data are not sufficiently precise to detect differences between orbits in (100) and (110) type planes. Another theoretical prediction is that the λH value at which the first maximum occurs as well as the zero-field value of the attenuation depends upon the electron mean free path L. Since one crystal was used for all measurements, one would expect the same L to apply to both modes. However, Figs. 1 and 2 show that the first maxima occur at different λH values, and the total relative attenuation changes associated with similar wavelengths (25.9 Mc/sec for C and 15.9 Mc/sec for C') differ by more than can be explained by the methods of measurement. Based on the existing theories, the effective mean free path for the two polarization directions would have to be different even though the waves propagate in the same direction in the same crystal.

One of the crystals cut from the ingot was cold worked by reducing its height five percent in compression. The influence of this deformation on the attenuation phenomena was examined by observing the C' mode at 15.7 megacycles per second. It was found that such deformation had very little effect on the total change in attenuation resulting from the application of a 15-koe magnetic field. However, it did eliminate the oscillations and made the difference between the $H_{\parallel}$ and $H_{\perp}$ cases very small. Such a result is in agreement with theory, which predicts that the attenuation oscillations are very sensitive to the electron mean free path whereas the total attenuation is only a slowly varying function of L/λ.

According to theory,[3] there should be little or no effect of a magnetic field on a longitudinal wave when the field, polarization, and propagation directions are all parallel. On the other hand, when the field is perpendicular to the propagation direction, attenuation changes are expected. In a crystal oriented such that the magnetic field and propagation directions were along [111], an attenuation decrease of only 0.09 db/cm was barely observed when the applied field was changed from 0 to 15 koe. For the field oriented at right angles to the [111] propagation direction at 15-koe field decreased the attenuation by 0.9 db/cm. No oscillations were observed in this case, presumably because the wavelength of 0.19 mm was too large by about a factor of two for oscillations to be visible in these specimens.

Much of this work was stimulated by conversations with Professor R. W. Morse. The authors are grateful to him and Dr. W. A. Harrison for communicating their results prior to publication.

---

*Present address: U. S. Naval Postgraduate School, Monterey, California.

[1]J. D. Gavenda and R. W. Morse, Bull. Am. Phys. Soc. 3, 167 (1959); T. Olsen and R. W. Morse, Bull. Am. Phys. Soc. 3, 167 (1959); R. W. Morse and J. D.

Gavenda, Phys. Rev. Letters 2, 250 (1959).
[2]M. H. Cohen. Bull. Am. Phys. Soc. 3, 167 (1959).
[3]W. A. Harrison, General Electric Research Laboratory Memo No. MB-32 (unpublished).
[4]R. L. Forgacs, Proceedings of the National Electronics Conference, Chicago, October, 1958 (to be published), Vol. XIV, p. 1.

[5]Grown from 99.999% American Smelting and Refining Company copper by D. O. Thompson of the Oak Ridge National Laboratory.

SCATTERING FACTOR FOR OUTER ELECTRONS IN ORDERED Fe_3Al

Y. Komura
Osaka City University, Osaka, Japan

and

Y. Tomiie and R. Nathans*
Osaka University, Nakanoshima, Osaka, Japan
(Received August 27, 1959)

The number of localized $3d$ electrons in metallic iron has recently been the subject of some controversy. Weiss and DeMarco[1] originally directed attention to the problem as a result of the unexpectedly low value of (2.3 ± 0.3) $3d$ electrons quoted by them. Their result was based on x-ray single-crystal measurements. Batterman[2] subsequently reported an atomic scattering factor for iron which was in substantial agreement with the free-atom calculations of Freeman (six $3d$ electrons). This determination was based on an analysis of cold-worked powder samples. Weiss and DeMarco[3] repeated Batterman's procedure, and again found a low number of $3d$ electrons, in confirmation of their single-crystal analysis.

We have made single-crystal measurements on ordered Fe_3Al which indicate that the outer electron configuration of the iron atoms in this alloy is very close to that calculated for the free iron atom. Since the magnetic scattering data[4] from ordered Fe_3Al support the notion that no large difference in the $3d$ electron configuration is expected between the iron atoms in this ordered alloy and those in pure iron, our results can be taken to confirm Batterman's conclusion.

The procedure used in our measurements is essentially the same as that of Weiss and De Marco. We measure the absolute scattering factors for a number of the low-angle superlattice peaks. The coherent scattering cross section for these peaks can be written as

$$\sigma = K(f_{\mathrm{Ar}} + f_{3d} - f_{\mathrm{Al}})^2,$$

where f_{Ar} is the contribution of the argon core, f_{3d} is the contribution of the outer electron, and f_{Al} is the scattering amplitude of aluminum atoms. For f_{Ar} and f_{Al} we make use of Freeman's recently published calculations, while f_{3d} is the quantity to be determined. We note that since we are looking at difference peaks, the effect of the aluminum is to cancel out a portion of the argon core electrons, thereby making the the observed scattering cross sections more dependent on the magnitude of the f_{3d} contribution.

The two outstanding difficulties in making precise estimates of the scattering cross section from single-crystal intensities are the problems of correction for sizable extinction effects and surface roughness. The use of comparatively low-reflectivity superlattice reflections has reduced significantly the problem of extinction. In fact, a wavelength analysis of the strongest of the superlattice reflections showed the extinction corrections to be negligible to within the $\pm 3\%$ accuracy of the measurements. The problem of the surface roughness, for which it is difficult to make accurate corrections, was avoided altogether by using a very thin crystal ($t = 0.014$ cm) in a transmission geometry.

Although these two principal problems have been effectively eliminated in the experimental arrangement, in measuring the absolute scattering in the superlattice reflections of an ordered alloy, additional parameters enter into the final determination. In the expression given above for the coherent scattering cross section, K is dependent on S^2, the long-range order parameter. Moreover, a difference in the Debye-Waller temperature factors between the iron and aluminum atoms increases the sensitivity of these peaks to the assumed values, the sensitivity being higher at higher Bragg angles. We have used neutron analysis, where the nuclear scattering

Table I. Comparison of experimental and calculated F_{hkl}^2 values.

hkl	$\sin\theta/\lambda$	F_{hkl}^2 experimental	F_{hkl}^2 calculated (six 3d electrons)		F_{hkl}^2 calculated (2.3 3d electrons)
111	0.1495	2110 ± 100[a]	Al	2339	1177
			Al^+	2370	1200
			Al^{++}	2469	1270
			Al^{+++}	2621	1381
200	0.1726	2006 ± 100	Al	2160	1183
			Al^+	2190	1205
			Al^{++}	2238	1242
			Al^{+++}	2331	1310
311	0.2860	1280 ± 60		1343	893
222	0.2990	1242 ± 60		1282	869
511	0.4489	603 ± 30		635	482

[a]The uncertainties given here represent the accumulated standard deviations in the x-ray and neutron measurements.

amplitudes are known and independent of angle on the same sample, to evaluate S^2 and to determine the effect of the unequal Debye-Waller factors.

Briefly stated, the experimental arrangement consisted of measuring the integrated intensities from the first five superlattice reflections using monochromatized Mo K radiation. A small collimated x-ray beam, falling well within the area of the crystal, was used. Absorption coefficients were measured directly and checks made on the uniformity of the sample. The reflectivities were placed on an absolute basis by comparison of the direct and scattered intensities. The numerous other checks involved in making a precise measurement of absolute scattering factor will be described in more detail in a forthcoming publication.

A list of the measured F_{hkl}^2 values for the first five superlattice reflections based on the neutron result of $S^2 = 0.75$ is given in Table I. Also given are the F_{hkl}^2 values calculated from Freeman's free-atom form factor (six 3d electrons) and those based on the Weiss-DeMarco estimate of 2.3 3d electrons. The calculated values have been corrected for temperature effects using $B_{Fe} = 0.345$, $B_{Al} = 0.450$. The discrepancy between our results and those calculated from the Weiss and DeMarco estimate of 2.3 3d electrons is quite evident, and amounts to differences of 25% or more.

---

*Fulbright Lecturer on leave from Pennsylvania State University. Present address: Brookhaven National Laboratory, Upton, New York.

[1]R. J. Weiss and J. J. DeMarco, Revs. Modern Phys. 30, 59 (1958).

[2]Boris W. Batterman, Phys. Rev. Letters 2, 47 (1959).

[3]R. J. Weiss and J. J. DeMarco, Phys. Rev. Letters 2, 148 (1959).

[4]Nathans, Pigott, and Shull, J. Phys. Chem. Solids 6, 38 (1958).

PHOTOSENSITIVE SPIN RESONANCE IN CdS*

J. Lambe, J. Baker, and C. Kikuchi
Willow Run Laboratories, The University of Michigan, Ann Arbor, Michigan
(Received August 21, 1959)

The phenomena of trapping of free carriers has long played an important role in the interpretation of various luminescent and photoconductive properties of solids. However, it has not always been possible to obtain definitive information about the nature of the trapping center. The purpose of this paper is to report the direct observation of a trapping center and its identification using the techniques of paramagnetic resonance. The experiments described here were carried out on CdS crystals containing traces of iron impurities.

The sample was placed in a cavity[1] of an X-band EPR (electron paramagnetic resonance) spectrometer such that the sample could be illuminated at 4.2°K through a hole in the cavity while EPR measurements were being made. When the sample was first placed in the cavity at 4.2°K, little or no signal was observed. After illumination with visible light, a large spin-resonance signal was observed as shown in Fig. 1. By irradiating with infrared light the signal could be removed. It was found that light in the region around 5500 A was most effective in producing the spin resonance, while 2-micron radiation was most effective in removing the signal. In all cases the light level was kept quite low to avoid any heating effects. At 77°K and 300°K no spin-resonance effects were observed.

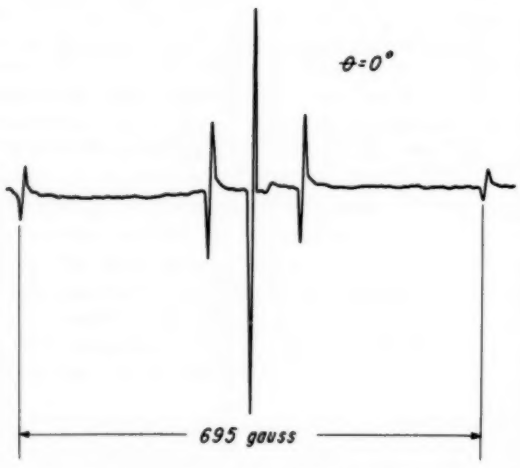

FIG. 1. Spectra obtained at 4.2°K after crystal was irradiated with visible light. The center line is at a position equivalent to $g=2.01$.

The structure and the angular dependence of the observed spin-resonance signal[2] indicate that the spin of the photosensitive center is $\frac{5}{2}$. When the c axis is parallel to the magnetic field, a simple 5-line spectrum with the weak satellites lying outside the strong ones is obtained. At 90°, the weak satellites lie inside the strong ones. Such a spectrum can be explained by a combination of a cubic and axial crystalline electric fields. The analysis of the spectra for 0° and 90° indicate that $D/a_0 \sim -0.5$, with $|D| = 30\times10^{-4}$ cm^{-1}, $g=2.01$. Here $3a_0$ is the ground-state splitting in zero field, with the doublet lying lowest. For intermediate angles, the satellites split into doublets, which is expected for a paramagnetic center of spin $\frac{5}{2}$ occupying inequivalent sites. It is interesting to note that the central $-\frac{1}{2}\leftrightarrow\frac{1}{2}$ line is also split into a doublet; calculations indicate that this is due to a second-order effect. Spectroscopic analysis indicated that iron concentration might be as high as 0.01%. Thus the photosensitive center is assigned tentatively to Fe^{3+}.

We interpret these effects as follows: Fe^{3+} is present in the CdS as an impurity. Its spin resonance is not observed, possibly being too broad. When free electrons and holes are produced by irradiation, the Fe^{2+} traps a hole and becomes Fe^{3+} which is readily observed since it is an S-state ion. The electrons must be trapped elsewhere. The action of the 2-micron infrared radiation is then to restore the electron back to the Fe^{3+} converting it to Fe^{2+}. The 2-micron light may release an electron from some other trap or may move it from the valence band into the Fe^{3+}. This point is not yet settled. In the latter case one could obtain directly the energy separation between the Fe^{3+} level and the valence band.

These measurements thus demonstrate directly the phenomena of trapping in photoconductors as well as the untrapping by infrared radiation. This technique should thus be extremely useful in testing various models of phosphors and photoconductors.

We wish to thank Mr. R. Ager for his technical assistance and Dr. Y. T. Sihvonen of the General

Motors Research Laboratories for a gift of single crystals of CdS.

*This research was supported by the Air Force Office of Scientific Research.

[1]J. Lambe and R. Ager, Rev. Sci. Instr. 30, 599 (1959).

[2]L. M. Matarrese and C. Kikuchi, J. Phys. Chem. Solids 1, 117 (1956); C. Kikuchi, Phys. Rev. 100, 1243 (1955).

ELECTRONIC SPECTRA OF EXCHANGE-COUPLED ION PAIRS IN CRYSTALS

A. L. Schawlow, D. L. Wood, and A. M. Clogston
Bell Telephone Laboratories, Murray Hill, New Jersey

(Received July 16, 1959)

Trivalent chromium ions (Cr^{3+}) in many insulating crystal lattices fluoresce with the emission of sharp lines near 7000 angstroms. The strongest emission lines in this region are well understood from crystal field theory as transitions from a ^2E excited state to the $^4A_2$ ground state.[1] In MgO there is one ^2E line since in a strictly cubic field the degeneracy of the upper level is not split. In ruby (Al_2O_3), however, there are two ^2E lines due to the lifting of the upper level degeneracy by the trigonal component of the crystal field. The ground state is also split in ruby, but by a much smaller amount which is not usually resolved in the optical spectrum.

It has been known for many years that within a few hundred cm^{-1} of the ^2E lines there are other sharp lines and bands which are not accounted for by the crystal field theory.[2,3] It has been suggested[2,4] that these "satellites" are caused by transitions to excited lattice vibrational states, followed by the emission of a phonon, and this is probably correct for the broader band satellites. This suggestion does not fit the observations for the sharp lines, since at 4.2°K the satellite lines have different spacing in emission from those in absorption and the crossover point between absorption and emission does not coincide with the ^2E lines. One would expect the same satellite spacings in both emission and absorption, since the vibrational frequencies are a property of the host lattice, which is not changed by the electronic transition within the impurity atom. Vibrations of the O-Cr-O complex, which would change with excitation of the chromium ion, would not have frequencies less than 80 cm^{-1} from the crossover point.

We wish to propose that the satellite lines are not due to individual chromium ions, but to chromium ions paired with a neighboring chromium ion or with some other crystal defect. If the concentration of chromium is, say, 1 atomic percent, there is a probability varying from 3% to 12% depending on the local symmetry that a given ion will find another Cr^{3+} ion among its nearest neighbors. If there is any clustering of chromium ions, this probability will be still greater. Between such neighboring ions there will be strong exchange forces. Indeed, the exchange forces lead to antiferromagnetism in Cr_2O_3.

If the satellite lines are due to randomly distributed nearest neighbor pairs, at low concentrations of Cr^{3+} their intensity relative to the main lines should be proportional to the concentration. As shown in Fig. 1, this behavior has been observed in the fluorescence spectrum of ruby. At very low concentrations the satellites are vanish-

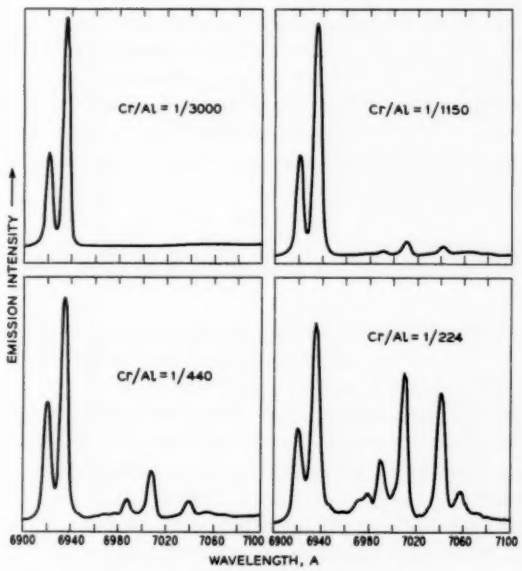

FIG. 1. Fluorescence spectrum of ruby at 77°K with different chromium concentrations (photoelectric recording at low resolution).

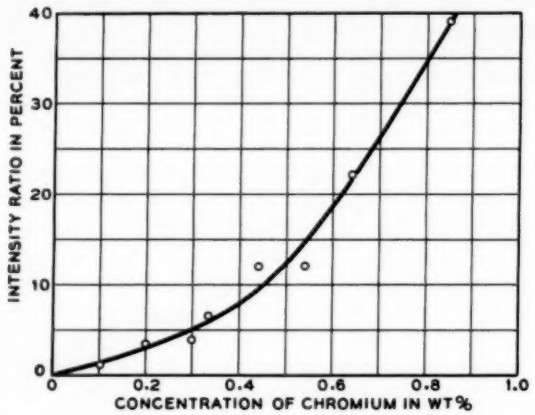

FIG. 2. Intensity ratio of strongest satellite (7010 A) to main line (6934 A) in ruby as a function of chromium concentration.

ingly faint, while at about 1% Cr^{3+}, they approach the main lines in intensity. In Fig. 2 the ratio of intensity for the strongest satellite (7010 A) relative to that of the main line is plotted against concentration. The curve shows a linear increase in the ratio at first, but then a faster rise. This may be due to the fact that pairs may remove the excitation from isolated atoms, since the lowest excited pair state lies lower than the corresponding state of the isolated atom.

The basis on which these spectra are being analyzed may be summarized briefly as follows: Ignoring the very small ground-state splitting, we may consider each chromium ion of a pair to be in a fourfold degenerate state of spin 3/2. The interactions between the spins will be represented by a Hamiltonian

$$H = 2J\vec{S}_1 \cdot \vec{S}_2 + J_x S_{1x} S_{2x} + J_y S_{1y} S_{2y} + J_z S_{1z} S_{2z},$$

with $J_x + J_y + J_z = 0$.[5,6] The observed Curie-Weiss Θ of the homologous compound Cr_2O_3 is 1070°K,[7] which corresponds to a value of J equal to 50 cm^{-1} and an exchange field of 3×10^6 oersteds. Measurements[8] of the paramagnetic resonance line width in Cr_2O_3 above its Curie point yield a value of about 1000 oersteds. If the usual formula for exchange-narrowed line width[9] is applied, we see that the ratio of the anisotropic exchange terms J_x, J_y, J_z above to the isotropic term J cannot be larger than 10^{-2}. We propose initially to ignore these terms. The isotropic coupling term will then split the ground state into terms of total spin $S = 3, 2, 1, 0$.

Consider now the excited state where one ion of a chromium pair has been excited into the ^2E state. In MgO, this ion may be considered as occupying two degenerate states of spin 1/2, each of which will also be coupled by exchange to the ground state of the second ion. The excited state will then be split into two terms of total spin 2 or 1. If J is positive, the excited state $S = 1$ will lie lower than $S = 2$ and at sufficiently low temperatures will be the only one populated. It will be observed to fluoresce into the ground states of $S = 2$, 1, and 0, observing the selection rule $\Delta S = 0, \pm 1$. If J is negative, there will also be three possible lines. A calculation has been made of the intensity of these transitions and will be reported later.

In the case of Al_2O_3 an exact analysis of the observed spectrum has not yet been achieved, probably for the following reasons. The ^2E state is split by the combined action of spin-orbit coupling and the axial field. If the splitting were much larger than the exchange energy, the analysis of the pair states would be simple. In fact, the axial splitting and exchange are comparable, which complicates the interpretation of this spectrum. The analysis of the ruby spectrum is also made difficult by the existence of several nonequivalent types of chromium pairs.

In MgO, the Cr^{3+} fluorescence shows two groups of satellite lines, one of which varies with concentration somewhat like those of ruby. The other group persists to fairly low concentrations, and may be caused by selective pairing of a Cr^{3+} ion with whatever compensates the excess charge.[10,11] Since a large fraction of the chromium ions have their charge compensation nearby, it may be relatively rare for two uncompensated chromium ions to be near neighbors. Thus this spectrum involves the various kinds of charge compensation as well as chromium exchange interactions.

Efforts are continuing to obtain a detailed interpretation of the observed fluorescence spectrum and to study spectra produced by pairs of dissimilar atoms.

We wish to thank Professor G. H. Dieke for allowing us to see Jacobs' unpublished thesis. We also wish to thank A. D. Liehr and M. Peter for helpful discussions, and G. E. Devlin for assistance with the experiments. We are indebted to Miss S. M. Vincent for determining the chromium concentration by the method of x-ray

fluorescence.

[1]S. Sugano and Y. Tanabe, J. Phys. Soc. (Japan) 9, 766 (1954).
[2]O. Deutschbein, Ann. Physik 14, 712 (1932); 20, 828 (1934).
[3]S. F. Jacobs, thesis, Johns Hopkins University, Baltimore, 1957 (unpublished).
[4]R. S. Krishnan, Proc. Indian Acad. Sci. A26, 450 (1947).
[5]J. M. Baker and B. Bleaney, Paris Conference on Low-Temperature Physics, 1955 (Centre National de la Recherche Scientifique, and UNESCO, Paris, 1956).
[6]Griffiths, Owen, Park, and Partridge, Phys. Rev. 108, 1345 (1957).
[7]L. R. Maxwell and T. R. McGuire, Revs. Modern Phys. 25, 279 (1953).
[8]Nagamiya, Yosida, and Kubo, Advances in Physics, edited by N. F. Mott (Taylor and Francis, Ltd., London, 1955), Vol. 4, p. 14.
[9]P. W. Anderson and P. R. Weiss, Revs. Modern Phys. 25, 269 (1953).
[10]J. E. Wertz and P. Auzins, Phys. Rev. 106, 484 (1957).
[11]J. H. E. Griffiths and J. W. Orton, Proc. Phys. Soc. (London) 73, 948 (1959).

PARAMAGNETIC RESONANCE DETECTION OF THE OPTICAL EXCITATION OF AN INFRARED STIMULABLE PHOSPHOR

R. S. Title
Research Laboratory, International Business Machines Corporation, Poughkeepsie, New York
(Received August 20, 1959)

The effect of the optical excitation of a phosphor may in certain cases manifest itself by a change in the paramagnetic resonance spectrum of the phosphor. Attempts to observe such changes in inorganic phosphors have previously been made by Hershberger[1] and Low[2] without success. This Letter describes an experiment in which paramagnetic resonance absorption was used to observe the optical excitation of the infrared stimulable phosphor SrS:Eu, Sm.

The physical properties of this phosphor have been widely investigated, the most extensive investigations being those carried out by Keller et al.[3] One of the properties of this phosphor is its ability to store energy when optically excited with ultraviolet or blue radiation. This stored energy may subsequently be released by irradiation with either infrared (970 mμ) or orange (590 mμ) wavelengths.

A simplified band-theory model was proposed by Keller[3] to explain this and other properties of SrS:Eu, Sm. In brief, europium is present in the SrS lattice as Eu^{2+} and samarium as Sm^{3+}. Excitation by ultraviolet radiation corresponds to SrS base absorption with the formation of an electron-hole pair. The electron is subsequently trapped by the Sm^{3+} which becomes Sm^{2+} and the hole trapped at the europium site giving Eu^{3+}. Excitation by blue radiation results in a direct ionization of Eu^{2+} to Eu^{3+} with the electron subsequently being trapped by the Sm^{3+} site. In the case of either ultraviolet or blue excitation the net effect is to change Eu^{2+} to Eu^{3+} and Sm^{3+} to Sm^{2+}. The Eu^{2+} has an $^8S_{7/2}$ ground state which is paramagnetic.[2] The Eu^{3+} ground state is $^7F_0$ and is nonmagnetic. Excitation of this phosphor should therefore manifest itself by a diminution in the Eu^{2+} paramagnetic spectrum.

The stored energy may be exhausted by irradiating with the wavelength which removes an electron from the Sm^{2+} site to the conduction band. The Sm^{2+} may be ionized in two ways and hence there are two wavelengths, 970 mμ and 590 mμ, that may be used.[3]

A diminution in the magnitude of the Eu^{2+} paramagnetic spectrum when optically excited has been observed for a SrS:Eu, Sm phosphor of the following composition: SrS, 6% $SrSO_4$, 6% CaF_2, 0.02% Eu, and 0.02% Sm. The percentages are in terms of molar percent. The preparation has been described in reference 3. A Varian Associates 4500 EPR spectrometer was used. The rectangular cavity that was used operated in the TE_{102} mode and had one end removed and replaced with a stainless steel screen, 96×96 mesh, which allowed light to irradiate the sample in the cavity. The powder sample was mounted on a 0.9- by 0.4-inch Teflon button placed along the region of maximum H_1 field at the middle of the cavity. An Osram xenon arc lamp *XBO* 1001 combined with a Bausch and Lomb 33-86-40 grating monochromator were used to irradiate the sample. All measurements were made at room temperature.

A plot of the relative stored energy against wavelength of the exciting light was made in the

following way. The sample was first brought to its exhausted state by irradiating with 970-mμ light for four minutes. The light was removed and the paramagnetic spectrum of Eu^{2+} in the exhausted sample was plotted. The sample was then irradiated with the particular wavelength of exciting light for four minutes. The light was removed. The Eu^{2+} paramagnetic spectrum was replotted, the diminution in its intensity being proportional to the stored energy in the phosphor. The sample was then once again exhausted with 970-mμ light before a second exciting wavelength was used. The results are given in Fig. 1. The heights have been corrected for constant number of exciting photons. The graph of Fig. 1 agrees favorably with that found by Keller, Mapes, and Cheroff[3] who used as a measure of the stored energy the intensity of the light emitted by the sample when 970-mμ light was incident on it.

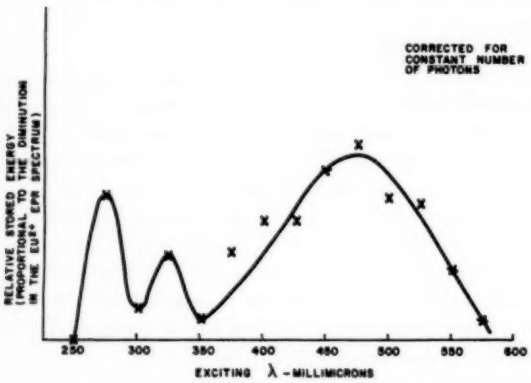

FIG. 1. Relative stored energy as measured by the diminution in the Eu^{2+} paramagnetic spectrum versus exciting wavelength.

As a measure of the efficiency of optical excitation it is noted that at the point of maximum optical excitation, 475 mμ, the Eu^{2+} paramagnetic spectrum decreased by 13% in magnitude. This should be taken as a lower limit of the efficiency as the light absorption is not uniform throughout the sample, decreasing exponentially from the surface inward. We plan to measure the variation of efficiency as a function of the relative europium and samarium concentrations. The experiment will also be repeated at liquid helium temperatures looking for a change in the Sm paramagnetic spectrum.

It may be added that 590-mμ light was found to be equally as effective as 970-mμ light in exhausting the phosphor, which agrees with the results of Keller and Pettit.[3]

In conclusion the use of paramagnetic resonance absorption to detect the optical excitation provides an independent verification of the simplified band-theory model proposed by Keller[3] for this phosphor.

The author wishes to acknowledge the encouragement and interest of Dr. S. P. Keller and Dr. W. V. Smith, and wishes to thank Mr. J. Kucza for material preparation.

[1]W. D. Hershberger, J. Chem. Phys. 24, 168 (1956); W. D. Hershberger and H. N. Liefer, Phys. Rev. 88, 714 (1952).

[2]B. Bleaney and W. Low, Proc. Phys. Soc. (London) A68, 55 (1955); W. Low, Phys. Rev. 98, 426 (1955).

[3]Keller, Mapes, and Cheroff, Phys. Rev. 108, 663 (1957); S. P. Keller and G. D. Pettit, Phys. Rev. 111, 1533 (1958); S. P. Keller, Phys. Rev. 113, 1415 (1959).

TRITIUM AS A PRODUCT OF FISSION*

E. L. Albenesius
Savannah River Laboratory, E. I. du Pont de Nemours and Company, Aiken, South Carolina
(Received August 19, 1959)

Evidence is described that indicates that the triton is a previously unrecognized fission product. Tritium was shown to be present in a ratio of one triton per $(1-2)\times10^4$ fissions in samples of irradiated natural and enriched uranium and in an irradiated mixture of transuranium isotopes. The triton-to-fission ratio was within a factor of two for these samples even though the concentrations of tritium per gram of irradiated material ranged over a factor of one thousand.

The lithium content of the irradiated uranium was proved not to be the source of the tritium; neither was the tritium present as the result of diffusion from the tritiated heavy water moderator of the Savannah River piles. Confirmation of the triton as a product of fission may contribute to the understanding of ternary fission and may have a practical application to burnup analysis.

A search of the literature of ternary fission showed that the formation of the triton in fission

had not been observed or postulated, although ejection of an alpha particle for approximately each 300 fissions had been well established.[1,2] Proton emission had also been suspected although this appeared unlikely from a theoretical standpoint.[1,3]

Recent data collected at the Savannah River Laboratory suggest that a direct correlation exists between triton formation and the number of fissions. These data were taken on irradiated samples of natural and enriched uranium and on an irradiated sample of fissionable transuranium nuclides. In each case, aliquots of nitric acid solutions of the irradiated material were made alkaline with sodium hydroxide, distilled, diluted, and analyzed for tritium with a Packard "Tri-Carb" liquid scintillation spectrometer. For these three cases, the observed frequency of formation was one triton per $(1-2)\times10^4$ fissions.

Three experiments were carried out to provide proof that the radioactive species being measured was tritium, that the presence of tritium was not due to irradiation of a lithium impurity in the uranium fuel, and that the tritium did not come from the heavy water moderator system of the piles:

(1) A sample of water from the acid solution in which irradiated natural uranium had been dissolved was converted to hydrogen and the gas was diffused through a palladium barrier. The diffusate was reoxidized to water and the expected activity was verified by means of liquid scintillation counting.

(2) The lithium content of the uranium fuel was determined. A 100-gram sample of natural uranium from a typical fuel element was dissolved in nitric acid and the uranium was precipitated by means of pyridine as $UO_4\cdot 2H_2O$. The supernate, which contained any possible lithium impurity in solution, was evaporated to dryness and the residue analyzed by emission spectrography. The lithium content of the uranium was found to be 0.01 ppm, less than 6% of the amount required to produce the levels of tritium observed in irradiated natural uranium.

(3) The third experiment was more qualitative. A sample of enriched uranium as U_3O_8, with a lithium content of <0.2 ppm, was irradiated in a graphite-moderated experimental reactor which contained no heavy water. The sample was dissolved in nitric acid and the water was separated by distillation from alkaline solution. The water was then reacted with hot zinc to produce hydrogen that was diffused through a palladium barrier. The diffusate was reoxidized to water and counted in the liquid scintillation counter. An estimated 10^{15} fissions in the original sample were found to produce about 2×10^{-3} μC of tritium, a ratio of about one triton per 3×10^4 fissions. Less than 4% of the observed activity could be attributed to the irradiation of lithium-6.

It is postulated on the basis of these findings that like the alpha particle, the triton is produced by direct emission in ternary fission.

Further experiments are planned to establish the frequency of formation with a greater degree of accuracy over a wide range of exposure for a variety of fissionable nuclides and to investigate, as a possible application, tritium analysis as an index of fuel "burnup."

The author wishes to acknowledge the interest of H. M. Kelley, G. Dessauer, and D. S. St. John, whose guidance and suggestions greatly encouraged this study, the diligent efforts of R. S. Ondrejcin and R. C. Milham in development of the key laboratory data, the assistance of F. E. Kinard in sample irradiation, and the cooperation of several members of the Health Physics Section of the Savannah River Plant, including W. S. Curlee, R. S. Denham, J. H. Horton, and L. D. Martin, in cross-checking data and in providing the counting service for the samples.

---

*The information contained in this article was developed during the course of work under a contract with the U. S. Atomic Energy Commission.

[1]D. L. Hill, Phys. Rev. 87, 1049 (1952).

[2]C. E. Fulmer and B. L. Cohen, Phys. Rev. 108, 370 (1957).

[3]D. L. Hill and J. A. Wheeler, Phys. Rev. 89, 1102 (1953).

DISTRIBUTION OF TOTAL RADIATION WIDTHS OF Cu^{59}

J. H. Carver
Australian National University, Canberra, Australia

and

G. A. Jones
Atomic Energy Research Establishment, Harwell, England
(Received August 24, 1959)

Proton capture experiments have been very successful in determining radiation widths among the light nuclei but it is technically difficult to extend such observations beyond this region, owing to the rapid decrease in level spacing with increasing atomic weight. Exceptions to this general rule occur near the closed shells. In the present experiments we have studied the reaction $Ni^{58}(p,\gamma)Cu^{59}$ for proton energies E_p up to 4.3 Mev. The spacing of the resonances for this reaction is unusually wide, being ~40 kev at E_p = 1.6 Mev and ~10 kev at E_p = 4.3 kev.[1] The wide spacing arises partly from the low Q value (3.42 Mev)[2] and, more importantly, from the proximity of the $N=Z=28$ closed shells.

Isotopically separated targets of Ni^{58} were bombarded with protons from the Harwell electrostatic generator, the targets having a thickness of 3 kev for 3-Mev protons. The total radiation widths for 158 resonances with $E_p > 1.6$ Mev were obtained by measuring the yield of 81-sec Cu^{59} using a NaI(Tl) spectrometer to detect the annihilation radiation. It was assumed that the targets were thicker than the intrinsic widths of the resonances and that $\Gamma_p \gg \Gamma_\gamma$. The observed resonances correspond to excited states in Cu^{59} having a range of J values which is expected to be limited, in this energy region, by the moment-of-inertia "cutoff" rather than by penetrability. The J dependence of Lang and Le Couteur[3] suggests that 94% of the levels have $J \leq \frac{7}{2}$. The quantity $g\Gamma_\gamma$ is determined from the yield measurements where g is the usual statistical weight factor. The average value of $g\Gamma_\gamma$ increases systematically with increasing excitation energy as shown in Fig. 1. This average energy dependence has been removed from the frequency distribution $P(g\Gamma_\gamma/\langle g\Gamma_\gamma\rangle_{Av})$ shown in Fig. 2. The data have been corrected for the loss of small resonances by multiplying the observed distribution by the probability of observing a level of a given size at a given energy. The errors include the estimated uncertainties in the loss correction as well as statistical uncertainties.

The frequency distribution $P(g\Gamma_\gamma/\langle g\Gamma_\gamma\rangle_{Av})$ has been compared in Fig. 2 with the chi-squared distributions with ν degrees of freedom described by Porter and Thomas.[4] A maximum-likelihood

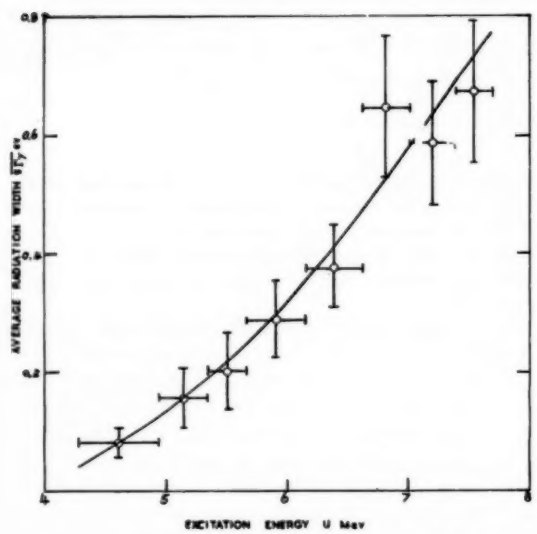

FIG. 1. Variation with excitation energy U of the average total radiation width ($\langle g\Gamma_\gamma\rangle_{Av}$) of Cu^{59}.

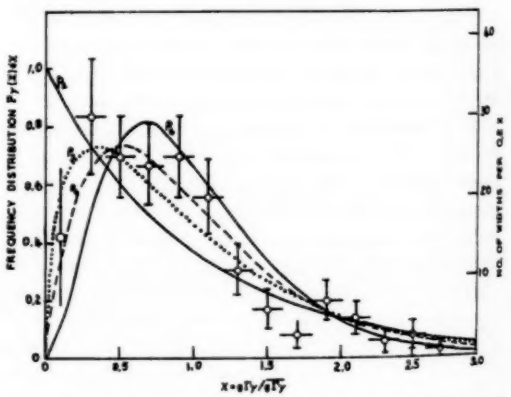

FIG. 2. Frequency distribution of 158 total radiation widths of Cu^{59} as a function of $x = g\Gamma_\gamma/\langle g\Gamma_\gamma\rangle_{Av}$. Corrections have been made for the loss of small levels. The smooth curves are the chi-squared distributions $P_\nu(x)dx$.

analysis gives $\nu = 2.9 \pm 0.6$ with the uncertainty arising mainly from the loss correction. The wide dispersion in the present set of total radiation widths is in marked contrast with the almost constant values which have been found in neutron studies of the heavy nuclei.[5] According to the Porter-Thomas theory[4] these almost constant values are a consequence of the large number (~100) of partial radiation widths. In the present case the derived value of ν indicates that if the theory is correct, about three partial widths on the average make up the bulk of the total radiation width. For these radioactive measurements the total radiation width includes only those gamma-ray transitions from the capturing state which are not followed by particle emission. Thus, primary transitions, which leave the nucleus with more than ~4 Mev of residual excitation, are excluded since these would most likely be followed by proton re-emission. The high-energy primary gamma-ray transitions are further enhanced by the energy dependence of the radiative probability which may either be taken to follow an ϵ^3 law or inferred from photodisintegration data. A calculation, using the measured Cu^{59} level density, suggests that for excitations of the capturing state of 4.5-7.5 Mev, 80-65% of the transitions populate the seven known Cu^{59} levels below 2.4 Mev. This is qualitatively in agreement with the result $\nu \approx 3$ since spin factors will further reduce the effective number of partial widths. A direct check can be obtained by observing the gamma-ray spectra from the resonances and a preliminary study indicates that on the average less than five partial widths are important. It appears, therefore, that the Porter-Thomas theory[4] accounts satisfactorily for the distribution of these total radiation widths.

One of us (J.H.C.) is indebted to Dr. E. Bretscher and Dr. E. B. Paul for the facilities made available to him while visiting Harwell.

[1]J. H. Carver and G. A. Jones (to be published).
[2]J. W. Butler and C. R. Gossett, Phys. Rev. 108, 1473 (1957).
[3]J. M. B. Lang and K. J. Le Couteur, Proc. Phys. Soc. (London) A67, 586 (1954).
[4]C. E. Porter and R. G. Thomas, Phys. Rev. 104, 483 (1956).
[5]J. S. Levin and D. J. Hughes, Phys. Rev. 101, 1328 (1956).

SEARCH FOR HIGHER-ORDER EFFECTS IN ALLOWED BETA DECAY*

R. M. Steffen
Department of Physics, Purdue University, Lafayette, Indiana
(Received August 6, 1959)

The ordinary theory of beta decay predicts an isotropic beta-gamma directional correlation for allowed beta transitions, since only s-wave leptons contribute to the decay. Under certain conditions, however, the relative contributions of p and d waves by virtue of their interference with s waves may become large enough to lead to measurable effects, e.g., to a small anisotropy in an allowed beta-gamma directional correlation. These higher-order effects are characterized by the presence of cross terms of the allowed matrix elements with second forbidden matrix elements. The dominant contributions are expected to arise from cross terms of $\int\vec{\sigma}$ with the relativistic momentum type second forbidden matrix elements $\int\vec{\alpha}\times\vec{r}$ and $i\int\gamma_5\vec{r}$. The latter were estimated by Morita[1] to be of the order $M^{-1}\int\vec{\sigma}$ (M = nucleon mass in units of the electron mass m). Recently, Gell-Mann[2] proposed a beta-decay theory which, as compared to the old theory, involves an additional term caused by the beta decay through the meson cloud of the nucleon. In Gell-Mann's theory $\int\vec{\alpha}\times\vec{r}$ is estimated to be of the order $M^{-1}(\mu_p - \mu_n)\int\vec{\sigma}$.

The anisotropy $a = [W(180°) - W(90°)]/W(90°)$ of the beta-gamma directional correlation is proportional to p^2/W in both theories.[1,3] Thus these higher order effects should be noticeable at very large beta energies ($W \geq 10$). Such a measurement has been reported.[4] A different situation in which the effects may be enhanced is encountered in the case of allowed beta transitions with large ft values, where the magnitude of the allowed matrix elements are considerably reduced and thus the influence of $\int\vec{\alpha}\times\vec{r}$ and $i\int\gamma_5\vec{r}$ may be relatively more pronounced.[3]

The anisotropy values to be expected for some beta-gamma cascades were computed using

Table I. Anisotropies $a=[W(180°)-W(90°)]/W(90°)$ of allowed $\beta-\gamma$ directional correlations.

$\beta-\gamma$ cascade	Theoretical anisotropy (%) with $\int\vec{\sigma}$ nominal Morita	Theoretical anisotropy (%) with $\int\vec{\sigma}$ nominal Gell-Mann	Theoretical anisotropy (%) with $\int\vec{\sigma}$ reduced Morita	Experimental anisotropy (%)
Na^{24} $4^+(\beta^-)4^+(\gamma)2^+(\gamma)0^+$ $\log ft=6.1$ ($E_\beta=1.1$ Mev)	+0.04	+0.11	+0.25	+0.02 ± 0.04
Sc^{46} $4^+(\beta^-)4^+(\gamma)2^+(\gamma)0^+$ $\log ft=6.2$ ($E_\beta=0.2$ Mev)	+0.01	+0.03	0.07	+0.02 ± 0.04
Co^{60} $5^+(\beta^-)4^+(\gamma)2^+(\gamma)0^+$ $\log ft=7.3$ ($E_\beta=0.2$ Mev)	-0.003	-0.01	-0.07	-0.03 ± 0.04
Na^{22} $3^+(\beta^+)2^+(\gamma)0^+$ $\log ft=7.4$ ($E_\beta=0.35$ Mev)	-0.0008 (-0.005)	+0.013	-0.02 (-0.12)	(a) -0.27 ± 0.05 (b) -0.25 ± 0.08 (c) -0.30 ± 0.08 (d) -0.18 ± 0.04 Average -0.27 ± 0.04

Morita's formulas,[1] and are listed in columns two and three of Table I. The values in column four were calculated by taking into account the reduction of $\int\vec{\sigma}$ which was estimated on the basis of a nominal log*ft* value for an allowed transition of 4.5. The contribution of the Fermi component in the beta transitions of Na^{24} and Sc^{46} were taken from a previous paper.[5]

The anisotropies in Gell-Mann's theory for the cases of large *ft* values are much more difficult to estimate. In Gell-Mann's theory

$$\int\vec{\alpha}\times\vec{r}\sim\frac{\mu_p-\mu_n}{M}\int\vec{\sigma}+\frac{1}{M}\int\vec{l}\tau_+ + \text{possible other terms.}$$

If the main matrix element $\int\vec{\sigma}$ is reduced, the first term is presumably also reduced and the second term may become important. It is difficult to estimate the contribution of this latter term and so no attempt will be made to do so.

The pronounced difference of the Na^{22} anisotropy in Gell-Mann's and Morita's theory arises from a partial cancellation of the contributions of $\int\vec{\alpha}\times\vec{r}$ and $i\int\gamma_5\vec{r}$ in the latter. If one assumes that only $i\int\gamma_5\vec{r}$ contributes in this particular case, one obtains the values indicated in parentheses.

Measurements of the beta-gamma directional correlations were performed on the nuclides listed in Table I with the vacuum chamber and the scintillation counter arrangement shown in Fig. 1. The concidence spectrometer was of the usual fast-slow type. The beta sources were less than 30 $\mu g/cm^2$ thick and were mounted on 0.9-mg/cm^2 Mylar films. The data were carefully corrected for the presence of gamma-gamma coincidences.

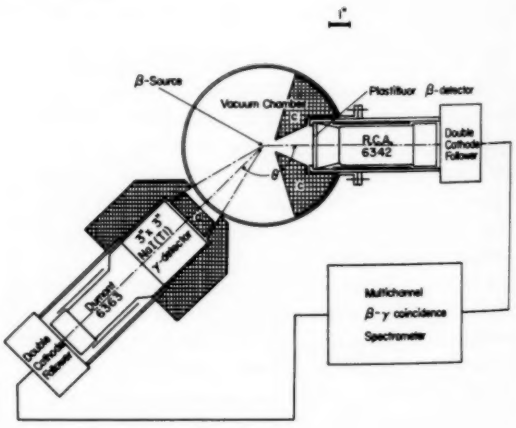

FIG. 1. Vacuum chamber and counter arrangement for beta-gamma directional correlation measurements. The lead shields (c) and the lead absorber (d) were only used in the Na^{22} measurements (c) and (d), respectively.

The execution of the beta-gamma directional correlation measurements on the positron emitter Na^{22} required special precautions. The annihilation radiation resulting from the positrons stopped in the beta detector, if accepted by the gamma detector, gives rise to a beta-gamma coincidence rate, which is dependent on the relative positions of the beta and the gamma detector. Although the energy window of the gamma detector accepts only the photopeak of the 1.28-Mev gamma radiation which follows the positron decay, the aforementioned effect must be considered because a fraction of the annihilation radiation reaches the gamma detector simultaneously with the 1.28-Mev gamma ray and may be detected by virtue of superposition of the annihilation photopeak on the Compton distribution of the 1.28-Mev gamma ray. This effect adds, in general, more genuine coincidences to the beta-gamma coincidence rate, if the beta and gamma detector axes are at 90° or 270°, than if they are at 180°. In other words, the effect gives rise to an apparent negative anisotropy, which is of the order of ~0.1%. In order to take this superposition effect into consideration and also in order to test for possible instrumental distortions the beta-gamma correlation of Na^{22} was measured under various experimental conditions. In measurement (a) the effect was eliminated by arranging the counters in such a way that the effective solid angle subtended by the gamma counter at the beta scintillator was the same at $\theta = 90°$ (or 270°) and at $\theta = 180°$. Measurements (b), (c), and (d) were performed in a different counter arrangement and corrections were applied for the presence of the superposition effect. Furthermore in measurements (c) and (d) the superposition effect was considerably reduced by placing lead wedges between the counters (c), or by placing a $\frac{1}{2}$-inch lead absorber in front of the gamma detector (d) (see Fig. 1).

The results of the beta-gamma anisotropy measurements are summarized in Table I. The errors quoted in Table I can be considered as maximum errors. The statistical errors are three times smaller.

Within experimental errors there is no indication of an anisotropy in Na^{24}, Sc^{46}, and Co^{60}. The disagreement between the experimental anisotropy result of Na^{24} and the values calculated in columns three and four of Table I may indicate that not only the $\int\vec{\sigma}$ matrix elements, but also the momentum type matrix elements $\int\vec{\alpha}\times\vec{r}$ and $i\int\gamma_5\vec{r}$ are reduced considerably in this beta transition. Thus these data are inconclusive as far as the Gell-Mann theory is concerned.

The small anisotropy measured in Na^{22} is of the opposite sign to that predicted by the Gell-Mann theory. Thus the effect cannot be attributed to the Gell-Mann term. It rather seems likely that the anisotropy is caused by cross terms of the allowed matrix elements with other second forbidden matrix elements which are unusually large in this particular case. The presence of an anisotropy in the Na^{22} beta-gamma correlation may be related to the fact that the Na^{22} positron spectrum shows deviations from the allowed shape.[6]

The author is indebted to Dr. R. L. Lewis for some very informative correspondence on the problem of higher-order effects in allowed beta decay and to Dr. R. W. King for many discussions.

---

*This research was supported by the U. S. Atomic Energy Commission.

[1]M. Morita, Phys. Rev. 113, 1584 (1959).

[2]M. Gell-Mann, Phys. Rev. 111, 362 (1958).

[3]J. Bernstein and R. L. Lewis, Phys. Rev. 112, 232 (1958).

[4]Boehm, Soergel, and Stech, Phys. Rev. Letters 1, 77 (1958).

[5]R. M. Steffen, Phys. Rev. (to be published).

[6]Hamilton, Langer, and Smith, Phys. Rev. 112, 2012 (1958).

7.656-Mev $E0$ TRANSITION IN C^{12}†

David E. Alburger*
Oak Ridge National Laboratory, Oak Ridge, Tennessee
and
Brookhaven National Laboratory, Upton, New York
(Received August 25, 1959)

The 7.656-Mev second excited state[1] of C^{12} is involved in theories[2,3] of helium burning and element synthesis in red giant stars. The cores of such stars are thought to consist mostly of helium which can combine into unstable Be^8 with an equilibrium ratio of Be^8 to He^4 of $\sim 10^{-9}$. As the next step in the process, Be^8 resonantly captures an alpha particle into the 7.656-Mev level in C^{12} whose spin-parity assignment is most probably 0+. Energy generation and element synthesis can occur if the 7.656-Mev level decays to the ground state of C^{12} rather than breaking up again into three He^4 nuclei.

Three modes of decay are open to the 7.656-Mev level, namely alpha-particle emission to Be^8, emission of a 3.2-Mev $E2$ gamma ray to the 2+ first excited state of C^{12} at 4.433 Mev, and the emission of nuclear pairs to the 0+ ground state. Assuming that the 7.656-Mev level is 0+, Cook et al.[3] suggested the following partial widths for these three modes of decay:

$$\Gamma_\alpha \sim 0.5 \text{ ev},$$

$$\Gamma_{3.2\gamma} \sim 0.0014 \text{ ev},$$

$$\Gamma_{e\pm} \sim 5\times 10^{-5} \text{ ev}.$$

Γ_α is 1/10 of the upper limit of 5 ev according to Wigner, $\Gamma_{3.2\gamma}$ is a single-particle estimate, and $\Gamma_{e\pm}$ is calculated from a measurement[4] of $C^{12}(e, e')$. The spectrum of alpha particles from the 7.656-Mev level occurring in the beta decay of B^{12} was observed by Cook et al.,[3] thus proving that the state can be formed in the manner suggested in the astrophysical theories. Neither of the other two decay paths has been firmly established heretofore and the width Γ_α is not known. For astrophysical calculations the ratios of the various widths are required.

By means of an intermediate-image pair spectrometer[5] the 7.656-Mev nuclear pair line has been observed in the $Be^9(\alpha, n)C^{12}$ reaction. For these measurements the instrument was moved to Oak Ridge where it was set up at the large Van de Graaff accelerator. Singly-ionized helium was accelerated and then gas-stripped before entering the 90° deflecting magnet. Runs were made with beams of ~4 μa of He^{++} at energies of 5.38 and 5.81 Mev on thick targets (6-mg/cm^2 Be foil) and with a beam of ~1 μa of He^{++} at 5.81 Mev on a thin target (0.2-mil Be, ~0.7 Mev thick for alpha particles). In all of the runs the 7.656-Mev nuclear pair line was observed with approximately the same intensity relative to the 4.433-Mev internal pair conversion line associated with the 2+ first excited state of C^{12}.

The observed ratio of 7.656- to 4.433-Mev pair line intensities when using the thin Be target and $E_\alpha = 5.81$ Mev is $(5\pm 1.5)\times 10^{-4}$. By applying a factor[6] of 1.26 for the ratio of spectrometer efficiencies for $E2$ to $E0$ pairs and by making use of the theoretical internal pair conversion coefficient[7] of 1.3×10^{-3} for the 4.433-Mev $E2$ transition, the derived ratio of pair to alpha widths for the 7.656-Mev level is

$$\Gamma_{e\pm}/\Gamma_\alpha = 8.2\times 10^{-7}\times R,$$

where R is the ratio of neutron populations, $R = N_{4.433}/N_{7.656}$. A precise number for R under the conditions of the thin target run cited in the present work is not available, and in fact the only information on the relative neutron populations is from a photographic plate measurement at 0° by Guier et al.[8] using 5.3-Mev alpha particles on a thin Be target. Their observed ratio of 4.433- to 7.656-Mev neutron group intensities was 8. As a rough estimate we assume $R\sim 8$ in the present experiment, which gives

$$\Gamma_{e\pm}/\Gamma_\alpha \sim 7\times 10^{-6}.$$

An accurate value of R would be highly desirable in view of the astrophysical importance of this level. Time-of-flight techniques might be one possible approach to this problem.

The above ratio deduced for $\Gamma_{e\pm}/\Gamma_\alpha$ is a factor of ~15 smaller than the estimates given by Cook et al.[3] This could arise from (a) an underestimate of the magnitude of Γ_α, (b) incorrectly assuming that $R\sim 8$, or (c) an incorrect calculation

of $\Gamma_{e\pm}$ from the $C^{12}(e,e')$ measurement. It would seem that (a) is the most likely possibility. This would allow $\Gamma_{3.2\gamma}$, which is probably the dominant path to the ground state, to be in agreement with the single-particle estimate, and it would also explain why attempts to detect the 3.2-Mev gamma ray have not yet met with success.

Full details of these experiments will be published later. The author is greatly indebted to the staff of the Oak Ridge National Laboratory for their hospitality and to Dr. Paul H. Stelson for his invaluable assistance.

†This work was done under the auspices of the U.S. Atomic Energy Commission.

*Permanent address: Brookhaven National Laboratory. This research was carried out at Oak Ridge National Laboratory while the author was a visitor during the summer of 1959.

[1]F. Ajzenberg-Selove and T. Lauritsen, Nuclear Phys. 11, 1 (1959).

[2]E. E. Salpeter, Phys. Rev. 107, 516 (1957).

[3]Cook, Fowler, Lauritsen, and Lauritsen, Phys. Rev. 107, 508 (1957).

[4]J. H. Fregeau, Phys. Rev. 104, 225 (1956).

[5]D. E. Alburger, Rev. Sci. Inst. 27, 991 (1956); Phys. Rev. 111, 1586 (1958).

[6]Alburger, Gallmann, and Wilkinson, Phys. Rev. (to be published).

[7]M. E. Rose, Phys. Rev. 76, 678 (1949).

[8]Guier, Bertini, and Roberts, Phys. Rev. 85, 426 (1952).

POSSIBILITY OF STUDYING THE Λ-HYPERON–NUCLEON FORCE BY LOW-ENERGY SCATTERING

C. G. Gardner and T. A. Welton
Oak Ridge National Laboratory, Oak Ridge, Tennessee
(Received August 24, 1959)

Currently our ideas concerning the Λ-hyperon–nucleon force derive primarily from (a) meson-theoretic static models, together with restrictions imposed by isotopic spin conservation,[1-3] and (b) analysis of the binding energies and decay mode branching ratios of hyperfragments.[2-6] Such considerations have led to the following characterization of the Λ-hyperon–nucleon force: (1) it is of shorter range than the nucleon-nucleon force, most likely having a characterisitc range $a \approx \hbar/2m_\pi c$, corresponding to a 2-pion exchange process; (2) it is "weaker" than the nucleon-nucleon force, being of insufficient strength to bind a Λ hyperon to a single nucleon; (3) it is spin dependent; and (4) the singlet force is somewhat stronger than the triplet force.[7]

We wish to note that the polarization which arises in the production of Λ hyperons may be used in a simple way to explore the spin dependence of the s-state Λ-hyperon–nucleon force. Let us for the moment assume that there is available a beam of low-energy ($\lesssim$25-30 Mev, center of mass)[8] Λ hyperons which are polarized in some direction (specified by the unit vector $\hat{n}$) by an amount $\langle \vec{\sigma}_\Lambda \cdot \hat{n} \rangle = P_\Lambda$, and which are allowed to scatter from unpolarized (free) protons; let us further suppose that the scattering is in fact observed to be isotropic (in the center-of-mass system) so that we are observing the effects of the s-state Λ-hyperon–nucleon force. It is straightforward to show that the polarization $P_{\Lambda(\text{final})}$ of the Λ hyperon after the scattering is related to its initial polarization in the following way:

$$D = \frac{P_{\Lambda(\text{final})}}{P_{\Lambda(\text{initial})}} = \frac{2[\sin^2\delta_t + \sin\delta_t \sin\delta_s \cos(\delta_t - \delta_s)]}{3\sin^2\delta_t + \sin^2\delta_s} . \quad (1)$$

δ_t and δ_s are, respectively, the triplet and singlet state scattering phase shifts. The direction of polarization is, of course, unchanged if the scattering is s-state scattering. One notes that for a spin-independent force ($\delta_t = \delta_s$), $D = 1$, i.e., the polarization is unchanged. If $\delta_t \gg \delta_s$, $D \simeq \frac{2}{3}$; conversely, if $\delta_s \gg \delta_t$, $D \simeq 0$, i.e., the Λ hyperon is strongly depolarized. Hence, one can say that any reduction in polarization of the Λ hyperon is evidence for spin dependence of Λ-hyperon–nucleon force; a reduction by a factor greater than $\frac{2}{3}$ is evidence that the singlet force is "stronger" than the triplet force.

In order to estimate the magnitude of D as a function of the relative strengths of the singlet and triplet forces, we suppose the Λ-hyperon–nucleon s-state potential to be of the following

form:

$$F_{N-\Lambda}(r) = -\frac{692.3 \text{ Mev-fermi}^2}{b^2} \times \exp[-3.541(r/b)](s_t P_t + s_s P_s), \quad (2)$$

where b is the intrinsic range of the well and s_t and s_s are, respectively, the triplet and singlet well-depth parameters[9]; P_s and P_t are, respectively, singlet and triplet projection operators. We assume that the intrinsic range of both wells is the same and corresponds to a 2-pion characteristic range, for which $b = 1.484$ (measured in fermis). For definiteness in computations, we have assumed that $s_s = 0.8$ (an "average" well-depth parameter $\simeq 0.75$ has been suggested on the basis of a variational study of hypertritium)[4]: we then compute phase shifts for $0 \leq (V_{\text{singlet}}/V_{\text{triplet}}) = (s_s/s_t) \leq 5$.

Although an exact analytical expression for the s-state phase shift due to an exponential well can be calculated, we have, for numerical ease, employed the effective-range approximation,[8]

$$k\cot\delta = -\alpha + \tfrac{1}{2}r_0 k^2, \quad (3)$$

which should be satisfactory for energies at which it is safe to neglect p-state scattering. Figure 1 presents the Λ-hyperon depolarization factor D as a function of (s_s/s_t), as given by these computations.

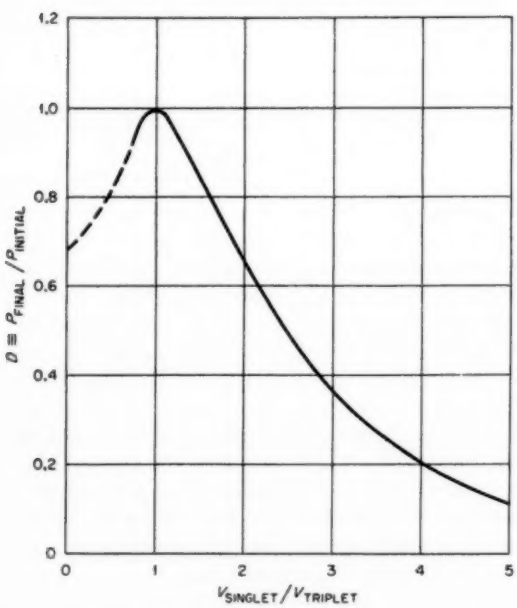

FIG. 1. Depolarization of scattered Λ hyperon of 20-Mev incident kinetic energy (lab) for an assumed singlet well depth parameter $s_{\text{singlet}} = 0.8$.

While no great significance should be attached to the precise numerical values obtained above, it seems safe to conclude that if the singlet well is two to three times as deep as the triplet well, the Λ-hyperon depolarization factor D will be significantly smaller than the ambiguous values $\frac{2}{3} \leq D \leq 1$.

Finally, we note that the above considerations are not necessarily entirely academic. The basic ingredients are: (1) a source of polarized Λ hyperons whose (laboratory) kinetic energy is less than, say, 60 Mev; (2) unpolarized (free) proton scattering centers; and (3) a polarization analyzer. These requirements are all met by associated Λ-hyperon production in a hydrogen bubble chamber. For example, the familiar reaction

$$\pi^- + p \rightarrow K^0 + \Lambda^0 \quad (4)$$

is known to be strongly polarizing at the production energies used heretofore.[10,11] Further, as is well known, the parity-nonconserving features of the Λ-hyperon decay serve as an analyzer of the Λ-hyperon polarization.[10-13] (For our purposes, a measurement of αP, where α is the customary asymmetry parameter in Λ-hyperon decay,[12] is as useful as a measurement of P_Λ itself, since we require only the ratio $P_{\text{final}}/P_{\text{initial}}$.) The hydrogen in the bubble chamber provides the required scattering centers. (A few elastic scattering events of the type $\Lambda + p \rightarrow \Lambda + p$ in a hydrogen bubble chamber have been observed.[14]) Hence, one needs at an appropriate production energy sufficient analyzable events of the type

$$\pi^- + p \rightarrow K^0 + \Lambda^0, \quad \Lambda^0 \rightarrow p + \pi^-, \quad (5)$$

to establish αP as a function of center-of-mass angle of production; one then needs sufficient completely analyzable events of the type

$$\pi^- + p \rightarrow K^0 + \Lambda^0, \quad \Lambda^0 + p \rightarrow \Lambda^0 + p, \quad \Lambda^0 \rightarrow p + \pi^-, \quad (6)$$

to establish αP_Λ after the elastic scattering. As a source of low-energy polarized Λ hyperons, reaction (4) has, for our purposes, obvious kinematical disadvantages; the center-of-mass motion brought about by the fairly high reaction threshold requires that one go to higher production energies in order that the low-energy component in the cone of Λ-hyperon production contain Λ hyperons of sufficiently low energy to be useful. An incident poin momentum of 2 Bev/c

would provide Λ hyperons of energies down to approximately 30 Mev (laboratory), an energy not too high to be useful. Unfortunately, at this incident momentum, a large number of alternative channels are competing.

Although not yet known (to us) to be polarizing, the in-flight reaction

$$K^- + p \rightarrow \pi^0 + \Lambda^0 \qquad (7)$$

is quite favorable kinematically, providing, for example, Λ hyperons of (laboratory) kinetic energy of from 9 Mev to 72 Mev over the cone of production (in addition, of course, there is a much higher energy component), at an incident K-meson momentum of 2 Bev/c. Should reaction (7) prove polarizing at moderate production energies, it would be more useful as a source of low-energy Λ hyperons for scattering than is reaction (4). A third alternative which is kinematically favorable (and which may well prove polarizing)[15] is associated photoproduction of Λ hyperons:

$$\gamma + p \rightarrow K^0 + \Lambda^0. \qquad (8)$$

If reactions (7) and (8) turn out to be polarizing (information important within itself), then the feasibility of a useful study of Λ-hyperon–nucleon scattering as outlined above would be considerably enhanced.

One of us (C.G.G.) wishes to thank G. R. Satchler of the Oak Ridge National Laboratory for instructive conversations.

[1]D. B. Lichtenberg and M. Ross, Phys. Rev. 107, 1714 (1957).
[2]F. Ferrari and L. Fonda, Nuovo cimento 9, 842 (1958).
[3]R. H. Dalitz, Reports on Progress in Physics (The Physical Society, London, 1957), Vol. 20, p.163.
[4]R. H. Dalitz and B. W. Downs, Phys. Rev. 110, 958 (1958); 111, 967 (1958).
[5]M. Leon, Phys. Rev. 113, 1604 (1959).
[6]L. E. Picasso and S. Rosati, Nuovo cimento 11, 711 (1959).
[7]This conclusion now appears to be somewhat weakened [R. H. Dalitz and L. Liu (to be published)]. Hence the experiment suggested in this note perhaps gains in usefulness.
[8]One expects, of course, that only s-state scattering will be important up to 25-30 Mev (center of mass) if the characteristic range of the Λ-hyperon–nucleon force is indeed $\hbar/2m_\pi c \simeq 0.7$ fermi $= 0.7 \times 10^{-13}$ cm.
[9]J. M. Blatt and J. D. Jackson, Phys. Rev 26, 18 (1949).
[10]F. S. Crawford et al., Phys. Rev. 108, 1102 (1957).
[11]F. Eisler et al., Phys. Rev. 108, 1353 (1957).
[12]T. D. Lee et al., Phys. Rev. 106, 1367 (1957).
[13]T. D. Lee and C. N. Yang, Phys. Rev. 108, 1645 (1957).
[14]F. S. Crawford et al., Phys. Rev. Letters 2, 174 (1959).
[15]J. J. Sakurai, Phys. Rev. 108, 491 (1957).

POSSIBLE EVIDENCE FOR A NEGATIVE HEAVY MESON*

T. Yamanouchi and M. F. Kaplon
Department of Physics and Astronomy, University of Rochester, Rochester, New York
(Received August 24, 1959)

Following the report of the High-Energy Conference at Kiev in which evidence was presented for the existence of a heavy positive meson decaying into a π^+ and a K^0,[1] we decided to see if there was any additional evidence relating to the existence of such particles. If such a particle should exist it presumably has strangeness +2 and it would seem reasonable that its antiparticle with strangeness -2 might exist. To this end we re-surveyed the scanning of an emulsion stack exposed to the 300-Mev/c Berkeley K^- beam[2] for stars which might indicate anomalously high-energy release.

We found two events of interest. The first and the one which gives evidence for the possible existence of a new negative meson is shown in Fig. 1 in a schematic sketch. It has a total of 8 prongs, one of which labelled P is the primary particle initiating the event; it lies in the beam direction and the grain density measurements at 0.5 mm and 8.5 mm from the star yield the values 2.89 ± 0.12 and 2.58 ± 0.11 times the minimum, respectively, indicating that the particle is indeed moving in the direction of the star. Of the prongs emitted two are of particular interest. Prong No. 7 is a "picture book" Σ^+ hyperon decaying at rest by the protonic mode; it has an energy at emission of 23.2 Mev and the decay proton an energy of 18.8 Mev. Prong No. 6 is the one which, in conjunction with No. 7, gives the event its pe-

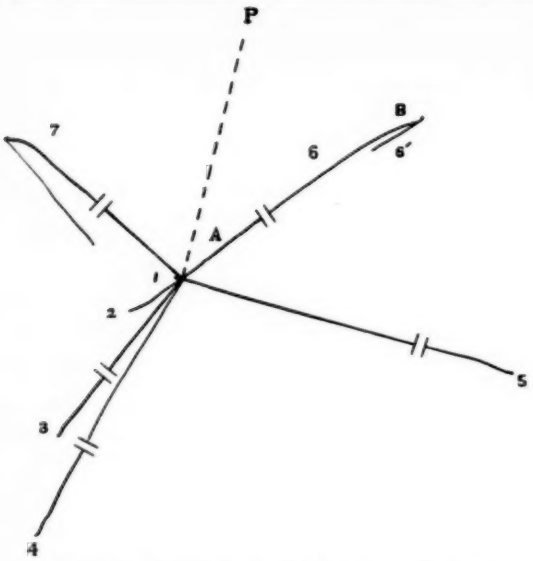

FIG. 1. Schematic drawing of the star, which includes two hyperons. Prong No. 6 is most probably a He hyperfragment decaying by the π^0 mode. Prong No. 7 is a Σ^+ decaying into $p+\pi^0$ at rest.

culiar nature. It appears to come to rest after traversing 628 μ and at this point there is associated with it a singly charged particle (6′) of 101μ range and a recoil of a few grains. Profile measurements made on Prong No. 6 indicate that its charge is ≤ 2 and that its direction of motion is most probably from A to B; its width at A is 10% less than at B. If one assumes this, then the question arises as to the nature of the event of B. One might say that it is a low-energy nuclear interaction of an α particle; however, a direct comparison of the gap density of 6′ and 6 shows that 6 has an ionization $I_6 \geq 5I_{6'}$, and thus its velocity is $\leq 0.08c$. To make the star at B it should supply at least 4 Mev of kinetic energy which implies a velocity $\geq 0.12c$. In addition, the existence of the strong Coulomb barrier would make such an interaction highly improbable.

The other possibilities are that it is the decay of an excited nuclear state which is immediately rejectable, or that it is an event involving a hyperon. The capture of a Σ^- seems unlikely in view of the gap density measurements, and only the decay of a He hyperfragment by π^0 mode seems to be compatible with the observation. Assuming that this represents the event, then the lower limit to the total visible prong energy emitted from A is 565 Mev. Since this represents a production of strangeness -2 in a strong interaction, the incident particle must also have strangeness -2. A lower limit to its mass is obtained by making allowance for the binding energy needed to supply the prongs, allowing for neutrons and subtracting the kinetic energy of the incident particle; this yields an estimate of the lower limit to the mass of 650 Mev. Some supporting evidence for this is the mass as determined by multiple scattering and ionization which yielded 640^{+120}_{-100} Mev.

One could also consider the possibility that prong 6 is in reality travelling from B to A and by coincidence stops just at that point. The probability for this is $\sim 10^{-10}$. If we accept the reality of this event, one can reasonably ask how such a particle was able to pass through the magnetic selection. We have discussed this with W. Barkas who is of the opinion that it is quite difficult to see how such a particle could survive the experimental arrangement. On the other hand, we do have in the same stack an event in flight made by an incident particle in the beam direction which has 17 visible prongs, one of which is an identified π meson. The lower limit to the total visible prong energy in this star is 600 Mev and the incident particle has a velocity $= 0.55c$. This is clearly incompatible with a K^- meson and only barely with a meson as massive as 750 Mev (due to the large amount of energy ≥ 210 Mev which must be attributed to neutrons). On the other hand, a mass measurement yields a value of 1020^{+220}_{-140} Mev indicating that this is an antiproton annihilation in flight. Since the prongs of this event traversed many different emulsions of our stack, they could not have been traced unless it occurred during the exposure as the emulsions are shuffled otherwise. We quote this to illustrate that it is possible for a particle of the wrong mass to survive the focussing arrangement.

We wish to thank Dr. J. B. Marion of the University of Maryland, Dr. W. Barkas of the Lawrence Radiation Laboratory, University of California, and Dr. G. Fazio, Dr. J. Klarmann, and Dr. A. Melissinos of the University of Rochester for helpful discussions, and Mrs. J. Milks and Mrs. V. Miller for their assistance in scanning and tracing.

*This research was supported in part by the U. S. Atomic Energy Commission and the Office of Scientific Research, U. S. Air Force.

[1]Private communication from Professor C. Goebel.

[2]W. Barkas et al., University of California Radiation Laboratory Report UCRL-3627, 1956 (unpublished).

$\bar{p}$-p CROSS SECTIONS FROM 534 TO 1068 Mev

T. Elioff, L. Agnew, O. Chamberlain, H. Steiner, C. Wiegand, and T. Ypsilantis
Lawrence Radiation Laboratory, University of California, Berkeley, California
(Received August 26, 1959)

We report here measurements of the antiproton-proton, elastic, inelastic, and charge-exchange cross sections for antiproton energies of 534, 700, 816, 948, and 1068 Mev. The total cross section remains large with respect to nucleon-nucleon cross sections in the same energy range. It has not yet been possible to determine precisely what fraction of the inelastic cross section is due to annihilation.

The antiproton beam was formed in a manner similar to that of previous experiments.[1,2] A schematic diagram of the experimental area is presented in Fig. 1, and Table I identifies the principal components. The 6-Bev internal proton beam of the Bevatron impinged on a carbon or polyethylene target at one of three different target positions schematically represented by T. Choice of the proper target enabled our mass spectrograph to select antiprotons within the desired energy range at angles from 0° to 5° (lab) with respect to the direction of the incident proton beam. The ratio of antiprotons to other negative particles (mostly pions) transmitted through the spectrograph was about 1/20 000 for the highest antiproton energies.

The antiprotons were distinguished from other particles in the beam by their time of flight between the scintillation counters S_1, S_2, and S_3 in coincidence with a count from the antiproton velocity-selecting Čerenkov counter, *VSC* II. In addition it was required that the meson Čerenkov counter, $\bar{C}$, did not count. The ratio of pions counted accidentally to pions transmitted through the system was less than 10^{-7}.

Identified antiprotons which traversed the magnetic channel entered a target positioned immediately behind S_3. This target could be filled with either liquid hydrogen or deuterium and was completely surrounded by an array of scintillation counters. Figure 2 displays a side view of the target and counter system. Figure 3 shows the counter system from the beam-exit end. Counters S_4 and S_5 detected the transmitted antiprotons. The other 25 counters detected either a scattered antiproton or the products from inelastic antiproton-proton collisions. The coincidence counts between the incident antiproton and the 27 counters were displayed on an oscilloscope and photo-

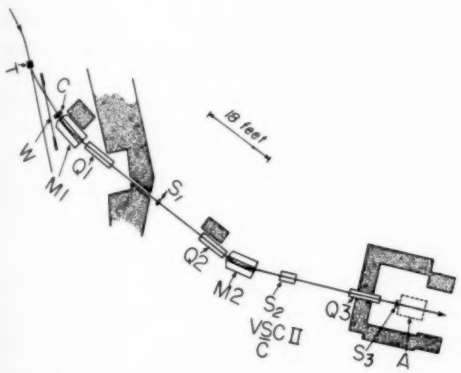

FIG. 1. Schematic view of the Bevatron experimental area. See Table I.

Table I. Experimental components of Fig. 1.

Symbol	Component description
T	Bevatron target area
W	Thin window of Bevatron vacuum system
C	Brass collimator 6-in. diam by 8 in. thick
$M1, M2$	60 in. long deflection magnets with 12- by 7-in. aperture; $\theta_{M1} = 17°$, $\theta_{M2} = 25°$
$Q1, Q2, Q3$	Sets of quadrupole focusing magnets of 8-in. aperture
S_1	Plastic scintillation counter $3\frac{1}{2}$-in. diam by $\frac{1}{4}$ in. thick
S_2	Plastic scintillation counter $3\frac{1}{16}$-in. diam by $\frac{1}{4}$ in. thick
VSC II	Antiproton narrow-band velocity-selecting Čerenkov counter which utilizes a cyclohexene ($n = 1.46$, $\rho = 0.8$) radiator $3\frac{1}{2}$-in. diam and 4.7 in. long. The velocity resolution is $\Delta\beta = 0.03$ in the range $0.95 > \beta > 0.70$
$\bar{C}$	Meson Čerenkov counter which utilizes the same radiator as *VSC* II but views only Čerenkov light that is totally internally reflected, i.e., for $\beta > 0.95$
S_3	Plastic scintillation counter 5-in. diam by $\frac{3}{8}$ in. thick
A	Area for H_2 target and final counter system

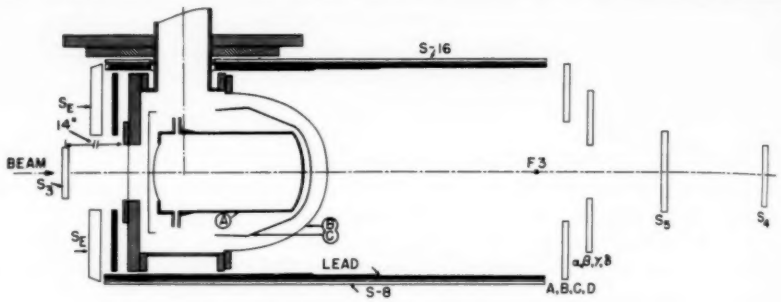

FIG. 2. Side view of target and counter system. For clarity, the figure is not shown precisely to scale. The container A which could be filled with liquid hydrogen or deuterium is a stainless steel cylinder 12 in. long and 6 in. in diameter with 0.008-in. walls except for the beam entrance wall which is 0.010-in. Mylar. Sixteen scintillation counters, S-1 through S-16, cylindrically surround the container A. Each has dimensions 38 by 4.1 by 0.375 in. Scintillators S_E, A, B, C, D, α, β, γ, δ, S_4, and S_5 are shown more explicitly in the next figure. The lead between the target and the scintillators is removable. The heat shield C is 0.003-in. copper; B is a thin region of the vacuum wall which is 0.035-in. aluminum.

graphed whenever an antiproton entered the target.

The pulses photographed on the oscilloscope film were classified as follows:

(a) If S_4 and S_5 counted or if S_5 counted alone, the antiproton did not interact.

(b) Elastic scattering occurred if a single count was detected in one of the counter rings (see Fig. 3) or in counters S-1 through S-16 around the target. For scattering angles greater than 15° in the laboratory system, the recoil proton was also observable.

(c) Inelastic scattering or annihilation occurred when any three or more counters registered or when two counters registered and the kinematics were not consistent with elastic scattering.

(d) A charge-exchange collision occurred when none of the counters registered.

The analysis of 70% of the film data has yielded the cross sections shown in Table II. These cross sections include small corrections for accidentals caused by neutron background in the Bevatron area, annihilations in counters, and the escape of particles through small spaces between

FIG. 3. Schematic view from the beam-exit end of the counter system, which displays counters A, B, C, D, α, β, γ, δ, S_4, and S_5 and their overlapping regions as well as an end view of counters S-1 through S-16.

Table II. $\bar{p}$-p cross sections at various energies.

$\bar{p}$ energy (Mev)	$\bar{p}$-p cross section (mb) Total	Elastic	Inelastic	Charge exchange
534 ± 25	119 ± 6	44 ± 6	69 ± 5	6 ± 2
700 ± 33	114 ± 5	43 ± 5	64 ± 4	8 ± 2
816 ± 37	105 ± 6	37 ± 5	60 ± 5	7 ± 2
948 ± 42	96 ± 3	33 ± 3	56 ± 3	8 ± 2
1068 ± 46	96 ± 4	30 ± 3	58 ± 3	7 ± 1

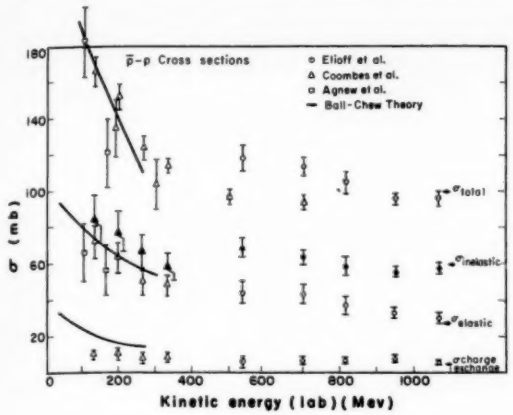

FIG. 4. Antiproton-proton total, elastic, inelastic, and charge-exchange cross sections as a function of antiproton laboratory kinetic energy. The round points are the results of this experiment. The triangular points are from reference 5 and reference 3. The square points are from reference 4. For clarity the inelastic points are darkened.

counters. In the case of the total and the elastic cross sections, an experimental correction has been made to include forward scattering by extrapolating total cross-section measurements at small cutoff angles to zero solid angle.

Figure 4 shows the cross sections given by this experiment and, for comparison, the results of previous experiments.[3-5]

In order to obtain assurance that our system could reproduce known cross sections, a positive proton beam was sent through our apparatus. This was done by scattering a 1.2-Bev internal Bevatron beam from a fourth target positioned near the region T of Fig. 1. We obtained the proton-proton cross sections at 2 energies and the results are tabulated in Table III. Precise agreement was obtained with the results of other experiments.[6,7]

The new antiproton results presented here agree reasonably well with the results of a previous experiment at 457 Mev.[8] An apparent paradox drawn from the information of two prior experiments[8,5] seems to be nonexistent. The somewhat incomplete prior data (incomplete in the sense that the elastic-scattering cross section was never measured) indicated a very large absorption cross section with little or no diffraction scattering—a phenomenon that is difficult to explain.[9] A clarification of the situation can best be seen by the comparisons of Table IV.

The results of this experiment should be more reliable then those of the previous experiments as a more efficient means of distinguishing annihilation events was used and simultaneous measurements of the total, elastic, and charge exchange cross sections could be made. The total cross sections of reference 5 are consistently low compared to later measurements by the same authors at lower energies[3] (see Fig. 4). The H_2O-D_2O-O_2 subtraction procedure of reference 8 inherently limits the accuracy of their results. Thus we conclude from Table IV that the value of the total cross section at 500 Mev [5] is probably 20 mb too low and the inelastic cross section at 457 Mev [8] is perhaps 20 mb too high.

From the 534-Mev data, one observes that more than half of the scattering is strongly

Table III. p^+-p cross sections for two energies.

p^+ energy (Mev)	p^+-p cross sections (mb) Total	Elastic	Inelastic
528	30 ± 7	24 ± 5	6 ± 3
940	49 ± 5	26 ± 3	23 ± 3

Table IV. Comparison of $\bar{p}$-p cross sections near 500 Mev.

Experiment		$\bar{p}$-p cross sections (mb) Total (0°)	Total (14°)	Inelastic	Elastic	Charge exchange
Chamberlain et al.[a]	(457 Mev)		104 ± 8	89 ± 7	. . .	. . .
Cork et al.[b]	(500 Mev)	97 ± 4	. . .	. . .	. . .	. . .
This experiment	(534 Mev)	119 ± 6	93 ± 6	69 ± 5	44 ± 6	6 ± 2

[a]See reference 8. [b]See reference 5.

peaked forward within a 14° laboratory angle. The latest results also indicate that the total elastic-scattering cross section constitutes ~1/3 of the total cross section in the energy range we have measured. This ratio has been indicated by a phenomenological black-sphere model of Koba and Takeda for a sphere radius of $\sim \frac{2}{3}\hbar/m_\pi c$.[10]

It is surprising that the inelastic cross section does not decrease appreciably with increasing energy which may indicate a longer-range annihilation interaction than expected.[9] The Ball-Chew theory,[11] which is in agreement with the low-energy antiproton data, attributes the annihilation interaction to a rather short-range absorbing core. Of course the inelastic cross section as presented here includes both annihilation and meson production. From the partial analysis of the 948-Mev inelastic events, it appears that not more than about 10 mb of the inelastic cross section can be due to meson production. (The remaining 46 mb must then be attributed to annihilation.) This analysis is based on the assumption that production of 2 or more mesons is negligible except in annihilation. The assumption seems warranted because double meson production is known to be very small in nucleon-nucleon collisions at this energy.[7,12,13]

Upon completion of our analysis we hope to discuss more fully the inelastic process. In addition to the antiproton-proton cross sections, we have the antiproton-deuteron cross sections at the same five energies. These results will be presented in a later publication.

We are grateful to Professor Emilio Segre for his interest and advice during the initial stages of the experiment. We thank Dr. Richard Lander, Dr. Norman Booth, and Dr. Jan Button for their help during the course of the experiment.

[1]Chamberlain, Segrè, Wiegand, and Ypsilantis, Phys. Rev. 100, 947 (1955).
[2]Agnew, Chamberlain, Keller, Mermod, Rogers, Steiner, and Wiegand, Phys. Rev. 108, 1545 (1957).
[3]Coombes, Cork, Galbraith, Lambertson, and Wenzel, Phys. Rev. 112, 1303 (1958).
[4]Agnew, Elioff, Fowler, Gilly, Lander, Oswald, Powell, Segrè, Steiner, White, Wiegand, and Ypsilantis, University of California Radiation Laboratory Report UCRL-8822, June, 1959 (unpublished).
[5]Cork, Lambertson, Piccioni, and Wenzel, Phys. Rev. 107, 248 (1957).
[6]References D11, B5, and S1 in W. Hess, Revs. Modern Phys. 30, 368 (1958).
[7]Batson, Culwick, Clepp, and Riddiford, in 1958 International Conference on High-Energy Physics at CERN, edited by B. Ferretti (CERN, Scientific Information Service, Geneva, 1958), p. 74.
[8]Chamberlain, Keller, Mermod, Segrè, Steiner, and Ypsilantis, Phys. Rev. 108, 1533 (1957).
[9]1958 International Conference on High-Energy Physics at CERN, edited by B. Ferretti (CERN, Scientific Information Service, Geneva, 1958), pp. 107, 108.
[10]Z. Koba and G. Takeda, Progr. Theoret. Phys. (Kyoto) 19, 269 (1958).
[11]J. Ball and G. Chew, Phys. Rev. 109, 1395 (1958).
[12]Fowler, Shutt, Thorndike, Whittemore, Cocconi, Hart, Block, Harth, Fowler, Garrison, and Morris, Phys. Rev. 103, 1493 (1956).
[13]W. A. Wallenmeyer, Phys. Rev. 105, 1058 (1957).

SEARCH FOR THE REACTION $\mu^+ + e^- \rightarrow \gamma + \gamma^*$

C. M. York, C. O. Kim, and W. Kernan
Enrico Fermi Institute for Nuclear Studies and Physics Department, University of Chicago, Chicago, Illinois
(Received August 3, 1959)

One of the few reactions in which the direct interaction of two light fermions can be studied is the annihilation process

$$\mu^+ + e^- \rightarrow \gamma + \gamma . \qquad (1)$$

Furthermore, this reaction can be compared directly with the more familiar positron annihilation process.

In this experiment a beam of π^+ mesons is brought to rest in a $\frac{1}{4}$-in.-thick disk of copper, as shown in Fig. 1. This disk is viewed by two, 5-in. diameter by $4\frac{1}{2}$ in. high, sodium iodide counters, I and II, through 2.8-in. diameter holes in lead collimators. The sodium iodide crystals are screened by 6-in. diameter scintillation counters, numbered 1 and 2, placed between the crystals and the exit face of the collimators.

Figure 2 is a block diagram of the electronic circuits used to select the reaction of Eq. (1). Fast pulses were obtained from the 5-in. duMont photomultiplier tubes used with the sodium iodide crystals, by means of a small inductance (about

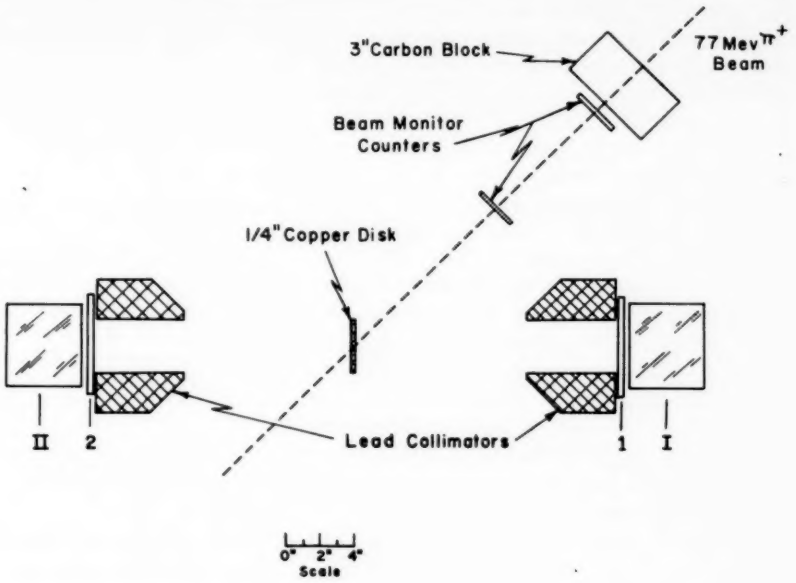

FIG. 1. Geometrical arrangement of the apparatus.

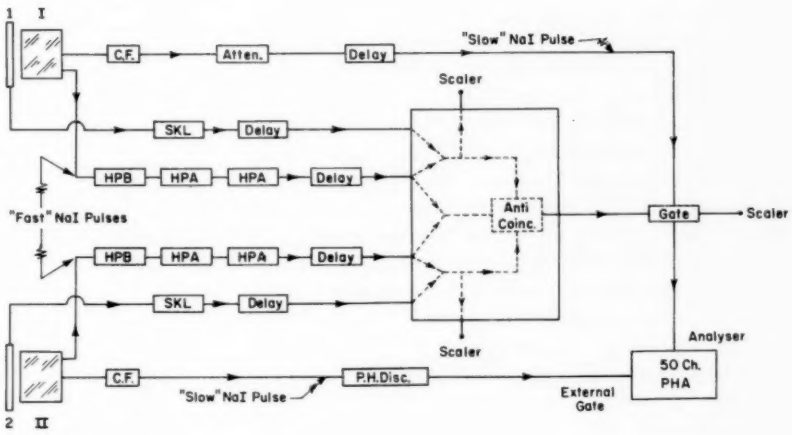

FIG. 2. Block diagram of the electronic circuits (SKL = Spencer-Kennedy amplifier, HPA and HPB = Hewlett-Packard amplifiers, PHA = pulse-height analyzer, C. F. = cathode follower).

3 μh) attached to the last dynode of the tube. The measured resolving time of the twofold coincidence between the two fast sodium iodide pulses is 14 mμsec. Because the gamma rays in Eq. (1) each have an energy of 53 Mev, a pulse-height discrimination on the slow pulse from sodium iodide crystal II was required before analyzing the other in the fifty-channel pulse-height analyzer. With the aid of electron-produced pulses from $\mu - e$ decay, this level was set at approximately 20 Mev. The twofold rates of each sodium iodide counter and its adjacent scintillation counter were used to determine the number of $\mu - e$ decays originating in the copper disk. These two rates were equal throughout the experiment.

Various checks of the apparatus were performed during the course of the experiment. Every eight hours of operation a pulser test was made to check the triggering level of the coincidence circuits and the linearity of the fifty-channel pulse-height analyzer system. Also the $\mu - e$ decay spectrum detected by counter I was recorded by triggering the fast gate and the external gate of the pulse-height analyzer from the twofold coincidence of sodium iodide I and scintillation counter 1. Both of these methods showed that the equipment operated consistently throughout the experiment. Finally, to insure

that pairs of gamma rays of approximately the correct energy could be recorded, the π^+ beam was changed to a π^- beam by reversing the cyclotron field and focusing magnet. The copper disk was replaced by a large block of polyethylene and the 67-Mev gamma-ray pairs from charge-exchange produced π^0's were observed. The pulse-height spectrum was just that which was expected and gave assurance that the electronics performed properly. This check was made at the midpoint of the experiment.

Copper was chosen as a stopping material because it has almost as high an electron density as any of the heavier metals; its Z is sufficiently low so that no appreciable background of gamma rays from the external bremsstrahlung of muon decay electrons is produced[1]; and the possibility of detecting the charge exchange reaction $\pi^+ + n \rightarrow \pi^0 + p$ in the nucleus is minimized. A careful beam scan at the position of the copper disk was made with a $\frac{1}{4}$-in. cubic counter to facilitate an accurate geometrical correction for the difference in detection efficiency for $\mu - e$ decay and the process of Eq. (1). Because low-energy π^+ mesons could scatter into the collimator, a rather large correction was required to determine the true number of $\mu - e$ decays. A small correction for the inefficiency of detection of low-energy muon-decay electrons was made. Although no anticoincidence shield against cosmic-ray events was provided, a test with the beam turned off indicated that several such events could have been recorded during the experiment.

In the course of detecting 546 338 charged particles in the NaI counter, one event of the desired type was detected. After applying a geometric correction of 0.54 ± 0.03, a background correction for scattered π^+ mesons of 0.56 ± 0.07, and an inefficiency correction of 1.11 ± 0.05, this implies a rate of reaction of a μ^+ at rest in copper, measured relative to $\mu - e$ decay, of 1/183 000. Because the one detected event could easily have been due to a cosmic-ray shower, this result must be regarded as an upper limit to the rate of reaction. Thus the rate of the reaction of Eq. (1) is $R_\mu \leq 2.5 \pm 0.4$ (sec^{-1}).

To emphasize how highly forbidden the muon-electron annihilation is, compare it to the positron annihilation

$$e^+ + e^- \rightarrow \gamma + \gamma. \tag{2}$$

The Feynman diagram for this process is shown in Fig. 3(a), and the measured rate of reaction in copper is[2] $R_e = 4 \times 10^9$ (sec^{-1}). The calculated

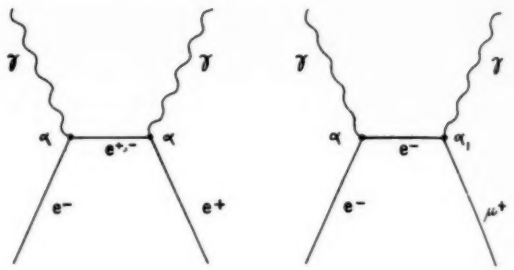

(a) (b)

FIG. 3. (a) Feynman diagram for positron annihilation. (b) Feynman diagram for $\mu - e$ annihilation.

rate is given by[3]

$$R_e = \pi \alpha^2 \lambda\!\!\!^{-}_e{}^2 \rho c / (8\pi a_0^3), \tag{3}$$

where α is the fine structure constant, $\lambda\!\!\!^{-}_e$ is the Compton wavelength of the electron, ρ is the density of electrons in copper, and a_0 is the Bohr radius. If we take the Feynman diagram in Fig. 3(b) as the one most likely to produce the reaction of Eq. (1), its rate of reaction can be written

$$R_\mu = \pi(\alpha/2)\alpha_1 \lambda\!\!\!^{-}_\mu{}^2 \rho c / (\pi a_0^3), \tag{4}$$

where α_1 is the constant characterizing the $e - \mu - \gamma$ vertex and $\lambda\!\!\!^{-}_\mu$ is the Compton wavelength of the μ. The ratio of α_1 to α is

$$\alpha \gtrsim 1.6 \times 10^5 \alpha_1,$$

or

$$\alpha_1 \lesssim 4.5 \times 10^{-8}. \tag{5}$$

The result is consistent with the value of α_1 obtained from the decay mode[4] $\mu \rightarrow e + \gamma$, which is highly forbidden.

The authors are greatly indebted to Professor Henry Primakoff for calling their attention to this problem and for several enlightening comments. Mr. J. Good was of great assistance in preparing the theoretical interpretation. The support of the cyclotron staff and the help of R. Gabriel and W. Stanula are gratefully acknowledged.

---

*Research supported by a joint program of the Office of Naval Research and the U. S. Atomic Energy Commission.

[1]The rate of counting γ's from this reaction was known from an experiment to measure the energy spectrum of gamma rays from the decay mode, $\mu^+ \rightarrow e^+ + \nu + \bar{\nu} + \gamma$. The results of this experiment are being

prepared for publication.

[2]S. de Benedetti and H. J. Richings, Phys. Rev. 85, 377 (1953), and T. R. Gerholm, Arkiv Fysik 10, 523 (1956).

[3]S. de Benedetti, Suppl. Nuovo cimento 4, 1206 (1956).

[4]Berley, Lee, and Bardon, Phys. Rev. Letters 2, 357 (1959); Davis, Roberts, and Zipf, Phys. Rev. Letters 2, 211 (1959); O'Keeffe, Rigby, and Wormald, Proc. Phys. Soc. (London) 73, 951 (1959).

OBSERVATION OF He^4 HYPERFRAGMENTS FROM K^- - He INTERACTIONS; THE K^- - Λ RELATIVE PARITY*

M. M. Block,† E. B. Brucker, I. S. Hughes,‡ T. Kikuchi, and C. Meltzer
Duke University, Durham, North Carolina

F. Anderson‖ and A. Pevsner
The Johns Hopkins University, Baltimore, Maryland

E. M. Harth and J. Leitner
Syracuse University, Syracuse, New York

and

H. O. Cohn
Oak Ridge National Laboratory, Oak Ridge, Tennessee

(Received August 20, 1959)

The Duke University helium bubble chamber was exposed to a separated low-energy K^- beam.[1] Approximately 2500 K^- interactions at rest were obtained. In a partial scan, evidence has been found for the production of He^4 hyperfragments in the reaction

$$K^- + He^4 \rightarrow {}_\Lambda He^4 + \pi^-. \qquad (1)$$

The relative K^- - Λ parity[2,3] can be inferred from the observation of reaction (1), if it is assumed that (a) parity is conserved in reaction (1), (b) the spins of the K^- meson and of the ground state of the ${}_\Lambda He^4$ are zero,[4] and (c) no bound excited states of ${}_\Lambda He^4$ exist.[5]

With the spins of all particles in (1) taken as zero, conservation of angular momentum requires that the orbital angular momentum on the left side of (1) be equal to that on the right. Then, since the pion is pseudoscalar, parity conservation requires the relative K^- - Λ parity to be negative if reaction (1) is observed. It is an advantage of the helium bubble chamber that hyperfragments can be identified from production kinematics and strangeness, baryon, and charge conservation. In particular, in ${}_\Lambda He^4$ production by K^- absorption at rest, the π^- has a unique momentum of 256 Mev/c, the hyperfragment has a unique range[6] of 0.53 mm, and the two tracks are collinear. From our analysis of K^- stars in helium we have computed that the number of background events simulating reaction (1) is negligible. Table I lists the observed He^4 hyperfragments.

The events 39-0760, 41-0312, 47-0563 are those in which no visible prongs are evident at the end of the stub; these events are compatible, e.g., with the decay scheme ${}_\Lambda He^4 \rightarrow \pi^0 + He^4$, since the He^4 range is too short to be detected. Event 83-1404 has the hyperfragment decaying into visible charged prongs, identified as a π^- of

Table I. A list of He^4 hyperfragments.

Event No.	P_π (Mev/c)	Stub length[a] (mm)	Collinearity of the projected angle	Suggested decay mode
39-0760	256 ± 15	0.67 ± 0.15	168° ± 10°	via neutral pion
41-0312	250 ± 23	0.51 ± 0.15	179° ± 10°	via neutral pion
47-0563	225 ± 30	0.47 ± 0.15	180° ± 10°	via neutral pion
83-1404	293 ± 25	0.63 ± 0.15	173° ± 10°	$\pi^- + p + He^3$

[a]Calculated assuming collinearity of pion and stub.

momentum 85 ± 5 Mev/c, a proton of range 3.25 mm corresponding to a momentum of 103 ± 2 Mev/c, and a one-bubble stub. We interpret this event as the decay scheme

$$_{\Lambda}\mathrm{He}^{4} \rightarrow \pi^{-} + p + \mathrm{He}^{3}.$$

Decay kinematics require the He^3 to have a range of 0.24 mm, approximately one bubble diameter. The recoil stub has been observed in the correct hemisphere for momentum conservation. The binding energy obtained is 3.5 ± 3.4 Mev and is compatible with the known binding energy[7] of the $_{\Lambda}He^4$.

Alternate interpretations of event 83-1404 have been considered and rejected. Firstly, charge and baryon conservation at the K-interaction vertex preclude the possibility that the stub is a $_{\Lambda}H^4$. Further, the event cannot be interpreted as a stopping $_{\Lambda}H^3$, since this would require another proton of 3.1-mm range at the K vertex. It might be argued that perhaps the $_{\Lambda}H^3$ decays in flight and that a very low energy proton is present at the K origin, but not visible. Such an interpretation, however, can be ruled out by further kinematical analysis which requires that the $_{\Lambda}H^3$ be unbound by at least 10 ± 3.5 Mev.

In conclusion, our events are sufficiently unambiguous to establish the existence of reaction (1). This requires that the relative $K^- - \Lambda$ parity be negative. We wish to stress that the validity of this conclusion depends on the assumptions (a), (b), and (c).

We would like to thank Dr. W. Fairbank and Dr. H. Blumenfeld for their invaluable aid and cooperation in the construction of the chamber, Dr. J. Murray and Dr. N. Horwitz for their help in using the coaxial separator, Dr. E. Lofgren, H. Heard, and the Bevatron crew, Dr. Alvarez, Dr. Powell, and the many other groups at the Berkeley Bevatron for their assistance during this experiment.

---

*Supported in part by the joint U. S. Atomic Energy Commission-Office of Naval Research program and the Office of Scientific Research.

†John Simon Guggenheim Memorial Fellow 1958-59, on leave of absence at University of Bologna, Italy.

‡Now at Department of Natural Philosophy, The University, Glasgow, Scotland.

‖On leave of absence from University College, Dublin, Ireland.

[1]Horwitz, Murray, Ross, and Tripp, University of California Radiation Laboratory Report UCRL-8269, 1958 (unpublished).

[2]R. H. Dalitz, Proceedings of the Sixth Annual Rochester Conference on High-Energy Physics (Interscience Publishers, New York, 1956).

[3]M. Gell-Mann, Phys. Rev. 106, 1296 (1957).

[4]R. H. Dalitz and B. W. Downs, Phys. Rev. 111, 967 (1958). However, R. H. Dalitz, at the Kiev Conference, 1959 (unpublished), has pointed out that evidence for a spin-zero ground state is now not as conclusive, and the assignment of spin zero rests mainly on the Karplus-Ruderman argument.

[5]R. H. Dalitz, Kiev Conference, 1959 (unpublished); on the basis of new calculations, he concludes that it is very unlikely that the mass-4 hyperfragment has a bound spin-one excited state.

[6]As the slowing-down time of the hyperfragment is of the order of 14% of the lifetime of the free Λ, some decays may occur in flight and the stubs will exhibit a length less than the full range.

[7]Ammar, Levi-Setti, Slater, Limentani, Schlein, and Steinberg, Nuovo cimento (to be published).

LEPTONIC DECAY MODES OF THE K MESON*

K. Chadan and S. Oneda†
University of Maryland, College Park, Maryland
(Received August 26, 1959)

We wish to explore how far the so-called V-A Fermi interaction could account for the strangeness-nonconserving weak reactions. It has been noticed that the observed rates of the decays, $K^0 \rightarrow \pi^{\pm} + e^{\mp} + \nu$ and $K^+ \rightarrow \pi^0 + e^+ + \nu$, seem to be anomalously small compared with the universal rates.[1] Using a dispersion technique,[2] it has also been conjectured that the rate of $K \rightarrow \mu + \nu$ decay is not in contradiction with the experimentally indicated slow rates of hyperon decays into leptons.[3] It may be interesting and instructive to see how the other possible leptonic modes $K \rightarrow 2\pi + e + \nu$ appear. Possible modes will be (a) $K^+ \rightarrow \pi^+ + \pi^- + e^+ + \nu$, (b) $K^+ \rightarrow \pi^0 + \pi^0 + e^+ + \nu$, (c) $K^+ \rightarrow \pi^+ + \pi^+ + e^- + \bar{\nu}$, (d) $K_1^0 \rightarrow \pi^{\pm} + \pi^0 + e^{\mp} + \nu$, and (e) $K_2^0 \rightarrow \pi^{\pm} + \pi^0 + e^{\mp} + \nu$. We write the relevant Fermi interactions with the coupling constant f as follows: $(f/\sqrt{2}) J_{\alpha}^{(\omega)} j_{\alpha} + \mathrm{H.c.}$, $j_{\alpha} = \bar{e}\gamma_{\alpha}(1+\gamma_5)\nu + \bar{\mu}\gamma_{\alpha}(1+\gamma_5)\nu$. $J_{\alpha}^{(\omega)}$ denotes the

strangeness-nonconserving baryonic currents.

If $J_\alpha^{(1)}$ is assumed to satisfy $\Delta S/\Delta Q = 1$,[4] where ΔQ and ΔS denote the change of charge and strangeness, respectively, of the current $J_\alpha^{(1)}$, the mode (c) is forbidden and the rates of the modes (d) and (e) are equal. This is also true when the $J_\alpha^{(1)}$ satisfies the $|\Delta I| = 1/2$ rule,[5] where $\Delta S/\Delta Q = 1$ is automatically guaranteed.

We could write the amplitudes of the various leptonic modes of K meson as follows, neglecting the electromagnetic corrections and the electron mass ($m_e = 0$):

$$K^+ \to \mu^+ + \nu, \qquad (f/\sqrt{2})\bar{\mu}\gamma_\alpha(1+\gamma_5)\nu k_\alpha L; \tag{1}$$

$$K^+ \to \pi^0 + e^+ + \nu, \qquad G(f/\sqrt{2})\bar{e}\gamma_\alpha(1+\gamma_5)\nu k_\alpha M; \tag{2}$$

$$K^+ \to \pi^0 + \pi^0 + e^+ + \nu, \qquad (G^2/\sqrt{2})(f/\sqrt{2})\bar{e}\gamma_\alpha(1+\gamma_5)\nu k_\alpha N. \tag{3}$$

k_α denotes the four-momentum of the K^+ meson. We have extracted the pion coupling G which is responsible for the emission of pions in the final states. L, M, and N are the form factors and their dimensions are different from each other. Since these decays are assumed to proceed through the baryon and antibaryon loops, the characteristic length of the range of interactions would be of the order of the baryon Compton wavelength. (We take $\hbar = c = 1$ and denote this length as $\mathfrak{M}^{-1}$.) Then the dependence of the form factors, M and N, on the secondary pion energies will not be so important.[6] Assuming this, we need only one form factor, N, for the process (3) because of the symmetry with regard to the two final pions. The relations between these form factors will be approximately given by $M\mathfrak{M} \approx L$ and $N\mathfrak{M} \approx M$. Then the branching ratio of the process (2) to (1) will be

$$\frac{W(\pi^0+e^++\nu)}{W(\mu^++\nu)} \approx \left(\frac{G^2}{4\pi}\right)\left(\frac{m_p}{\mathfrak{M}}\right)^2 \times 1.2\times 10^{-2} \approx 1.6\times 10^{-1}\left(\frac{m_p}{\mathfrak{M}}\right)^2. \tag{4}$$

Taking $(G^2/4\pi) \approx 13.5$ and putting $\mathfrak{M} \approx$ baryon mass (m_p is the proton mass), the above ratio is close to the observed value (≈ 0.1). For the ratio in question we have found [using Eq. (7)]

$$\frac{W(\pi^0+\pi^0+e^++\nu)}{W(\pi^0+e^++\nu)} \approx \left(\frac{G^2}{4\pi}\right)\left(\frac{m_p}{\mathfrak{M}}\right)^2 \times 7.4\times 10^{-5} \approx 1.0\times 10^{-3}\left(\frac{m_p}{\mathfrak{M}}\right)^2, \tag{5}$$

which is much reduced compared with the surprisingly large branching ratio (4). The above order-of-magnitude estimate has been confirmed by two different methods. First let us compare directly the various rates in question. For the ratio of the rates the use of perturbation theory would be less controversial and also the unknown K-meson-baryon coupling will not enter. For the $J_\alpha^{(1)}$ current we assume the simplest form[7] $\bar{p}\gamma_\alpha \times(1+\gamma_5)\Lambda^0$ which satisfies $|\Delta I| = 1/2$. The form of the amplitude[6] for the $K^+ \to \pi^+(p_1) + \pi^-(p_2) + e^+(p_3) + \nu(p_4)$ decay is given by

$$(\sqrt{2}\,G)^2(f/\sqrt{2})\,\bar{e}\gamma_\alpha(1+\gamma_5)\nu(p_{1\alpha}N_1 + p_{2\alpha}N_2) + \text{H. c.}, \tag{6}$$

which needs two form factors N_1 and N_2. Then the energy spectrum of the positron with energy p_3 (in the K-meson rest system) will be, except for the irrelevant constant factors,

$$\int_0^{(m_K^2-4m_\pi^2)/2m_K} p_3^2\,dp_3 \int_0^{(E^2-4m_\pi^2)/2E} q_4^2\,dq_4 \left(\frac{m_K}{m_K-2p_3}\right)^{1/2}\left(\frac{E^2-2Eq_4-4m_\pi^2}{E^2-2Eq_4}\right)^{1/2}\left\{(E^2-Eq_4)(N_1+N_2)^2 - 2m_\pi^2(N_1^2+N_2^2) - (E^2-2Eq_4)N_1N_2 + (E^2-2Eq_4-4m_\pi^2)\left[\frac{q_4}{3(E-2q_4)}(N_1-N_2)^2 - N_1N_2\right]\right\}, \tag{7}$$

where $E = [m_K(m_K-2p_3)]^{1/2}$ and q_4 is the neutrino energy in the center-of-mass system of the π^+, π^-, and the neutrino. Now for the $K \to \mu + \nu$ and $K \to \pi + e + \nu$ the results are logarithmically divergent and we must use a cutoff.[8] However, the amplitudes for the $K \to 2\pi + e + \nu$ are convergent. We get the following crude estimates for the pseudoscalar

K meson:

$$W(\mu^+ + \nu):\ W(\pi^0 + e^+ + \nu):\ W(\pi^+ + \pi^- + e^+ + \nu):\ W(\pi^0 + \pi^0 + e^+ + \nu):\ W(K_{1,2}{}^0 \to \pi^\pm + \pi^0 + e^\mp + \nu)$$
$$= 1:\ 1.7\times10^{-1}:\ 8.3\times10^{-4}:\ 3.5\times10^{-4}:\ 2.9\times10^{-4}; \tag{8}$$

and for the scalar K meson:

$$W(\mu^+ + \nu):\ W(\pi^0 + e^+ + \nu):\ W(\pi^+ + \pi^- + e^+ + \nu):\ W(\pi^0 + \pi^0 + e^+ + \nu):\ W(K_{1,2}{}^0 \to \pi^\pm + \pi^0 + e^\mp + \nu)$$
$$= 1:\ 1.0\times10^{-1}:\ 9.0\times10^{-4}:\ 1.7\times10^{-4}:\ 1.2\times10^{-3}. \tag{9}$$

It is seen that the previous estimates (4) and (5) are reproduced. For the same K-meson–baryon coupling constant, the rate of $K \to \mu + \nu$ decay for the scalar K meson is about an order of magnitude smaller than that for the pseudoscalar K meson which is also found in the dispersion theory calculation.[2] However, the same tendency also holds for the other modes and so the above branching ratios are almost independent of the type of K meson. There is also an indication that the result is not so sensitive to the choice of the interactions adopted.[9] Next we shall try a different method. Let us compare the $K^+ \to \pi^+ + \pi^- + e^+ + \nu$ with the $K^+ \to \pi^+ + \pi^- + \pi^+$ decay. We could get[10] the latter process by just replacing the weak vertex (e, ν) in the former process by the weak vertex $\bar{\Lambda}^0 + p \to \pi^+$. We may use the effective weak vertex $g\bar{\Lambda}\gamma_\alpha(1+\gamma_5)p\,\partial_\alpha\varphi_\pi$ $(g^2/4\pi \approx 1.8\times10^{-15})$ which may come from the Fermi interaction $(f/\sqrt{2})J_\alpha{}^{(1)}\bar{p}\gamma_\alpha \times(1+\gamma_5)n$. Then we find for the branching ratio values of around a few percent (these are crude, and also the final-state interactions are neglected):

$$\frac{W(\pi^+ + \pi^- + e^+ + \nu)}{W(\pi^+ + \pi^- + \pi^+)} \approx \begin{cases} 4\times10^{-2} & \text{for } K(\text{pseudoscalar}) \\ 3\times10^{-2} & \text{for } K(\text{scalar}). \end{cases}$$

However, if we accept the fact[3] that the effective Fermi coupling constant for the hyperon decays into leptons is about an order of magnitude smaller than the usual Fermi coupling constant, then the above branching ratio should be reduced by a factor ≈ 10 and is in reasonably good agreement with the values obtained in (8) and (9), since experimentally we have found that $W(\pi^+ + \pi^- + \pi^+) \approx 1.2W(\pi^0 + e^+ + \nu)$.

Thus we would like to conclude that the frequencies of the mode $K^+ \to \pi^+ + \pi^- + e^+ + \nu$ would be approximately in the range between 10^{-2} and 10^{-3}% compared with the $K^+ \to \pi^0 + e^+ + \nu$ or $K^+ \to \pi^+ + \pi^- + \pi^+$ decay.

The positron (or neutrino) energy spectra are shown in Fig. 1 for the case $K^+ \to \pi^+ + \pi^- + e^+ + \nu$. The spectra are very similar for both types of K meson. This is because the spectrum is not sensitive to the value of N_1/N_2. As in the case with the $K^+ \to \pi^0 + \pi^0 + e^+ + \nu$ decay (where $N_1 = N_2 \approx$ constant), the $K^0 \to \pi^\pm + \pi^0 + e^\mp + \nu$ decay has also only one form factor ($N_1 = -N_2 \approx$ constant) since we have assumed the $|\Delta I| = 1/2$ rule for $J_\alpha{}^{(1)}$. So for these cases the spectra are unambiguous (see Fig. 2) and turn out to be almost the same as given in Fig. 1.

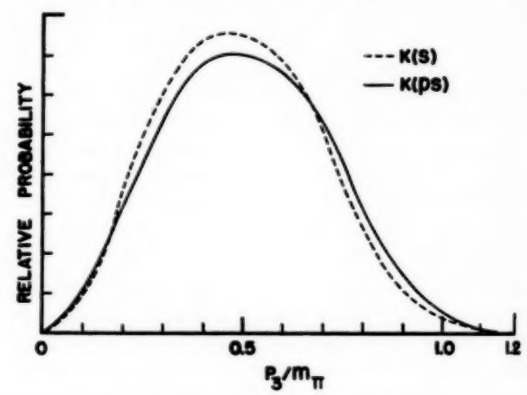

FIG. 1. The energy spectrum of the positron (or the neutrino) in the $K^+ \to \pi^+ + \pi^- + e^+ + \nu$ decay for the pseudoscalar and scalar K meson.

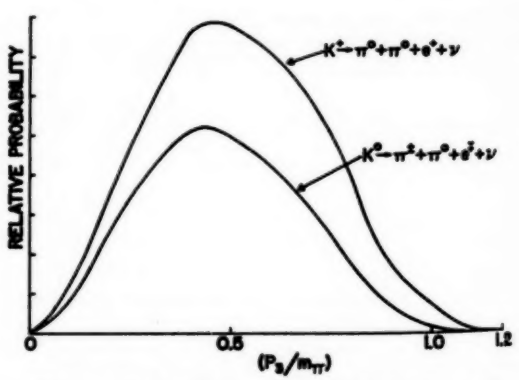

FIG. 2. The energy spectrum of the electron or positron in the decays, $K^+ \to \pi^0 + \pi^0 + e^+ + \nu$ and $K_{1,2}{}^0 \to \pi^\pm + \pi^0 + e^\mp + \nu$.

That is, all the spectra have a broad maximum around 70 Mev.

In the above discussion, no selection rules have been assumed for all the modes.[11] Experimentally there are already about a thousand events of the $K\to 3\pi$ decays. So far three noncoplanar events which look like anomalous $K^+\to\pi^++\pi^-+\pi^+$ decays have been reported and interpreted as the $K^+\to\pi^++\pi^-+\pi^++\gamma$ decay.[12,13] Dalitz has shown[14] that the ratio of the $K^+\to\pi^++\pi^-+\pi^++\gamma$ to the $K^+\to\pi^++\pi^-+\pi^+$ decay would be about 1.2×10^{-3} for emission of a photon whose energy is greater than 10 Mev. According to our estimate the frequency of the $K^+\to\pi^++\pi^-+e^++\nu$ decay seems to be slightly larger than the $K^+\to\pi^++\pi^-+\pi^++\gamma$ decay. As the decay $K^+\to\pi^++\pi^-+e^++\nu$ is not so difficult a process to detect, experimental clarification may be possible in the future. Although the rates turn out to be not so large, they are still more than an order of magnitude larger than the predicted rates of the $K^+\to e^++\nu$ decay which is an important process to prove the success of the V-A Fermi interaction.

---

*This research was supported in part by the U. S. Air Force through the Air Force Office of Scientific Research of the Air Research and Development Command.

†On leave of absence from the Institute of Theoretical Physics, Kanazawa University, Japan.

[1]S. Oneda, Nuclear Phys. 9, 476 (1958/59).

[2]B. Sakita, Phys. Rev. (to be published); C. H. Albright, Phys. Rev. (to be published).

[3]F. S. Crawford et al., Phys. Rev. Letters 1, 377 (1958); P. Nordin et al., Phys. Rev. Letters 1, 380 (1958); J. Leitner et al., Bull. Am. Phys. Soc. 4, 356 (1959).

[4]R. P. Feynman and M. Gell-Mann, Phys. Rev. 109, 193 (1958). The possible existence of this selection rule was once noticed by one of us from a slightly different standpoint. S. Oneda, Nuclear Phys. 4, 21 (1957).

[5]I. Yu. Kobzarev and L. B. Okun, Proceedings of the Padua-Venice Conference on Mesons and Recently Discovered Particles, 1957 (unpublished); S. Okubo et al., Phys. Rev. 112, 665 (1958).

[6]In the following calculations we neglect terms of the order $Q^2/\mathfrak{M}^2$ (Q is the available energy of the decays) which amounts to (at most) less than 20%.

[7]This will be reasonable especially if the Λ is a more fundamental particle than other hyperons. See, for instance, S. Sakata, Prog. Theoret. Phys. (Kyoto) 16, 686 (1956).

[8]We have made use of the results of S. Oneda and Y. Tanikawa, Phys. Rev. 113, 1354 (1959), where an intermediate boson with mass $\approx 2300m_e$ plays a role of relativistic cutoff. The result is not sensitive to the choice of the cutoff.

[9]Using the form of Fermi interaction proposed by Feynman and Gell-Mann[4] and assuming a global symmetric model of strong interactions, quite similar results were also obtained for the ratio (4). Lee, Shih, Ho, and Chu, Chinese Academy of Atomic Research, Phys. J. 15, 33 (1959).

[10]This seems to be the most important diagram for this decay.

[11]If we insist on the universality, we might introduce weak selection rules for the $K\to\mu+\nu$ and $K\to\pi+e+\nu$ decays. See, for instance, R. P. Feynman, Bull. Am. Phys. Soc. 4, 84 (1959). In this case, however, the branching ratios of $K\to2\pi+e+\nu$ would be enhanced by a factor ≈ 10 unless we also forbid these processes. However, the $K\to2\pi+e+\nu$ modes are allowed in the above model of Feynman.

[12]R. R. Daniel and Y. Pal, Proc. Indian Acad. Sci. A40, 114 (1954). Introductory summary by L. Leprince-Ringuet, Proceedings of the Sixth Annual Rochester Conference on High-Energy Physics, 1956 (Interscience Publishers, New York, 1956).

[13]τ-meson-like phenomena, in which two charged pions and a μ meson appear, have also been reported. K. R. Dixit, Z. Naturforsch. 90, 335 (1954). In this note we have not discussed the μ-meson modes. The μ-meson modes will be as frequent as the electron modes. The phase space volume favors the latter, but the former modes have one more form factor since the muon mass cannot be neglected.

[14]R. H. Dalitz, Phys. Rev. 99, 915 (1955).

FIELD THEORY COMMUTATORS

Julian Schwinger
Harvard University, Cambridge, Massachusetts
(Received August 24, 1959)

There are some paradoxical contradictions between the formal commutation relations and the nature of the energy spectrum which serve to emphasize that localized field operator products must be understood as the singular limit of products defined for noncoincident points. Thus, it is customary to assert that the electric charge density of a Dirac field commutes with the current density at equal times, since the current vector is a gauge-invariant bilinear combination of the Dirac fields. It follows from the conservation of charge that the charge density and its time derivative, referring to any pair of spatial points at a common time, are commutative. But this is impossible if a lowest energy state—the vacuum—is to exist. For any Hermitian operator F, here an arbitrary linear functional of the charge density, the vacuum expectation value of such a commutator is

$$\langle [i\partial_0 F, F]\rangle = \langle [[F, P^0], F]\rangle = 2\langle FP^0F\rangle > 0,$$

since the operator F in general will possess nonvanishing matrix elements between the vacuum state of zero energy and other states of necessarily positive energy. The exceptional circumstance, that the vacuum state is an eigenvector of F, is excluded physically for the example of the charge flux vector. A related example appears on deriving F from a component of the electric field by choosing the zero wave number Fourier transform. It is the advantage of this special choice that the time derivative of F is then proportional to the same Fourier component of the electric current vector, which enables us to conclude that the electric field and the current vector cannot commute. Invariance considerations and an existence hypothesis show that

$$x^0 = x^{0\prime}: \quad \langle i[E_k(x), j_l(x')]\rangle = \delta_{kl}\delta(\vec{x} - \vec{x}')K^2,$$

where K is a real constant with the dimensions of inverse length or mass. Since the longitudinal part of the electric field is related to the charge density, we learn that

$$\langle i[j^0(x), j_l(x')]\rangle = \nabla_l \delta(\vec{x} - \vec{x}')K^2.$$

The independent nonvanishing commutator expectation value involving the transverse electric field is also in apparent contradiction with the formal commutation properties of the Maxwell and Dirac fields.

Electromagnetic field commutation relations inferred from invariance requirements must be realized by any model of the charge-bearing field. For a spinless field $\phi(x)$, $\phi^\dagger(x)$,

$$j_k = \tfrac{1}{2}e[\phi^\dagger\left(\frac{1}{i}\nabla_k - eA_k\right)\phi + (i\nabla_k - eA_k)\phi^\dagger\phi],$$

in which symmetrization of the $\phi^\dagger\phi$ products is understood, and the application of the formal commutation relations now yields the anticipated result, with

$$K^2 = e^2\langle \phi^\dagger\phi\rangle .$$

The electric current vector of the Dirac field is generally defined as the limit of a time-ordered product,

$$j_\mu(x) = \lim_{x'\to x} e(\psi^\dagger(x)\gamma^0\gamma_\mu\psi(x'))_+ \epsilon_+(x - x'),$$

but for the purpose of evaluating the commutator with the charge density, it suffices to consider the operator product at distinct spatial points[1] and equal times, as in

$$i[\int(d\vec{x})\phi(x)j^0(x), e\psi^\dagger(x' - \tfrac{1}{2}\vec{\epsilon})\gamma^0\gamma_k\psi(x' + \tfrac{1}{2}\vec{\epsilon})]$$
$$= -(\phi(x' + \tfrac{1}{2}\vec{\epsilon}) - \phi(x' - \tfrac{1}{2}\vec{\epsilon}))ie^2\psi^\dagger(x' - \tfrac{1}{2}\vec{\epsilon})\gamma^0\gamma_k\psi(x' + \tfrac{1}{2}\vec{\epsilon}).$$

If the limit $\vec{\epsilon} \to 0$ is performed symmetrically in space, the required expectation value form is obtained, with

$$K^2 = -\tfrac{1}{3}ie^2 \lim_{\vec{\epsilon}\to 0} \mathrm{tr}\gamma^0\vec{\gamma}\cdot\vec{\epsilon}\langle\psi(x + \tfrac{1}{2}\vec{\epsilon})\psi^\dagger(x - \tfrac{1}{2}\vec{\epsilon})\rangle .$$

The conventional treatment of the commutator evidently assumes that the field product expectation value remains bounded as $\vec{\epsilon} \to 0$, whereas the structure of the energy spectrum provides assurance to the contrary. In one simple situation, that of the noninteracting Dirac field, it is well known that

$$\langle\psi(x + \tfrac{1}{2}\vec{\epsilon})\psi^\dagger(x - \tfrac{1}{2}\vec{\epsilon})\rangle \sim \frac{1}{2\pi^2}\frac{i\gamma^0\vec{\gamma}\cdot\vec{\epsilon}}{(\vec{\epsilon}^2)^2}, \quad \vec{\epsilon} \to 0$$

and K^2 is the divergent limit of $(2e^2/3\pi^2)(\vec{\epsilon}^2)^{-1}$.

The implications of this discussion for the

structure of the photon Green's function will be considered elsewhere.

[1]An additional factor involving the line integral of the vector potential should be understood. It is needed to maintain gauge invariance and accounts for the non-vanishing commutator with the transverse electric field.

$K^+ - K^0$ MASS DIFFERENCE

P. T. Matthews and J. L. Uretsky*
Imperial College, London, England
(Received June 1, 1959)

It has recently been established[1] that, in contrast to the π mesons, the K^0 is heavier than the $K^\pm$. This is in contradiction with perturbation theory,[2] and with the naive classical argument that the charged components of a mass multiplet should be heavier in proportion to the work done in assembling the charge. We wish to draw attention to the important difference that, whereas the π^0 has a vanishing charge density, the K^0, like the neutron, is a concentration of positive and negative charge,[3] giving total charge zero, but with a nonvanishing charge density. It is quite simple to construct physically reasonable charge distributions for K^0 and K^+ such that the neutral particle has the greater electrostatic energy. We produce such a model and show further that this classical interpretation of the self-energy is very closely related to the leading term in the field-theoretic calculation.

The familiar relation[4] between electric charge, isotopic spin, I, and hypercharge, Y, can be expressed in terms of the corresponding current densities, in an obvious notation, as

$$j_\mu^{el}(x) = j_\mu^{I_3}(x) + \tfrac{1}{2} j_\mu^{Y}(x). \tag{1}$$

The static charge distribution for a particular multiplet, χ, is the expectation value of the "zero" component of this operator for single-particle states in the rest system:

$$\rho(x) = \langle \chi | j_0^{el}(x) | \chi \rangle = I_3 \rho_I(x) + \tfrac{1}{2} Y \rho_Y(x), \tag{2}$$

where I_3 is the matrix appropriate to the multiplet and Y is the single-particle value.

For π^0 it follows that

$$\rho(x) = 0. \tag{3}$$

The neutral pion has a vanishing charge density, and the fact that the charged pions are heavier is consistent with the simple classical argument.[5]

For the case of the K meson ($Y = 1$) the situation is quite different. Rewriting Eq. (2),

$$\rho_K(x) = \tfrac{1}{2}(1 + \tau_3)\rho_1(x) + \rho_2(x), \tag{4}$$

it is seen that ρ_2 describes the charge density of the neutral K meson. We argue that by choosing a suitable charge distribution, say a negative "cloud" around a sufficiently small positive "core", one can easily give the neutral K meson a greater self-mass than the charged one. Choose, for example,

$$\rho_+(x) = (e^2/4\pi)\lambda^2 e^{-\lambda r}/r = \rho_1 + \rho_2, \tag{5a}$$

$$\rho_0(x) = (e^2/4\pi)[\lambda^2 e^{-\lambda r} - \mu^2 e^{-\mu r}]/r = \rho_2. \tag{5b}$$

Recalling that the classical self-mass is given (for the charged particle for example) by

$$\delta M_+ = \frac{e^2}{(2\pi)^2} \int d\vec{q} \frac{\lambda^2}{\lambda^2 + \vec{q}^2} \frac{1}{k^2} \frac{\lambda^2}{\lambda^2 + \vec{q}^2}, \tag{6}$$

it is found that the observed mass splitting is reproduced by taking λ to be a pion Compton wavelength and μ, the "core" radius, a little greater than two Σ-hyperon Compton wavelengths.

In the field-theoretic calculation, it is reasonable to suppose that the main contribution comes from intermediate states of the least possible energy, and this is borne out by the dispersion relation approach.[6] We need to calculate the contribution from the graph of Fig. 1. The cor-

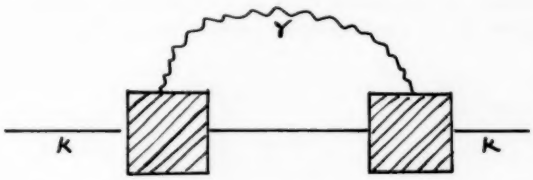

FIG. 1. Feynman diagram of the K-meson electromagnetic self-energy.

responding expression is ($q^2 = q^\mu q_\mu$, $p^2 = -M^2$)

$$\delta(M^2) = \frac{2e^2}{(2\pi)^3}\int d^4q \Gamma_\mu(p, p-q)\Delta_F'(p-q) \times \Gamma_\mu(p-q, p)\frac{1}{q^2}. \quad (7)$$

We make the choice (which is discussed further below)

$$\Gamma_\mu^{+}(p, p') = (p_\mu + p_\mu')\frac{\lambda^2}{\lambda^2 + (p-p')^2}, \quad (8a)$$

$$\Gamma_\mu^{0}(p, p') = [(p-p')^2(p_\mu + p_\mu') - (p_\mu - p_\mu')(p^2 - p'^2)] \times \left[\frac{\lambda^2}{\lambda^2 + (p-p')^2} - \frac{\mu^2}{\mu^2 + (p-p')^2}\right]\frac{1}{(p-p')^2}. \quad (8b)$$

These are the covariant quantum mechanical equivalents of the charge distributions (5a) and (5b). It will be shown below that it is consistent with the spirit of the proceedings to approximate the exact Feynman propagator by

$$\Delta_F'(p) = (p^2 + M^2 - i\epsilon)^{-1}. \quad (9)$$

The integral (7) is readily evaluated by standard techniques. Choosing the inverse "cloud" radius, λ, equal to m_π, as before, we obtain the following results:

$$\mu/\lambda = 8 \ , 9$$

$$M_0 - M_+ = 2.7, 4.5 \text{ (Mev)}.$$

Recalling that the observed splitting[1] is about 3.5 Mev we see that the "core" radius corresponds to about one baryon Compton wavelength and that the classical and quantum mechanical estimates differ by a factor of about two.

We have stated that the two self-mass calculations are very closely related to each other. In fact the integral of Eq. (6) comes naturally out of the expression (7) in the limit that the K-meson mass, M, becomes very large. To see this we write Eq. (7) in the form comparable to Eq. (6),

$$\delta M_+ = \frac{e^2}{(2\pi)^3}\frac{1}{M}\int d^4q \frac{\lambda^2}{\lambda^2 + q^2}\frac{1}{q^2} \times \frac{q^2 - 4p\cdot q - 4M^2}{(p-q)^2 + M^2}\frac{\lambda^2}{\lambda^2 + q^2}, \quad (10)$$

and perform the q_0 integration by closing the contours in the upper half-plane. Consider only the pole at

$$(p-q)^2 = -M^2.$$

Evaluating the residue and keeping only the leading term in $1/M$, we are led back to the expression (6). This is not a surprising result. It says, merely, that the classical self-mass is the static limit of that part of the quantum mechanical expression where the (intermediate) K meson is restricted to the mass shell.

It remains now to justify our choice of vertex function and our use of the bare propagator, Δ_F. We construct the most general possible vertex from the two vectors,

$$A_\mu = (p_\mu + p_\mu')q^2 - q_\mu(p^2 - p'^2),$$

$$B_\mu = q_\mu/q^2 + (p_\mu + p_\mu')/(p^2 - p'^2). \quad (11)$$

Gauge invariance is identically satisfied by writing

$$\Gamma_\mu(p, p') = \tfrac{1}{2}(1+\tau_3)\{B_\mu[\Delta_F'^{-1}(p^2) - \Delta_F'^{-1}(p'^2)] + A_\mu F\} + A_\mu G, \quad (12)$$

where F and G are functions of the three scalars

$$p^2 + M^2, \ p'^2 + M^2, \ q^2 = (p-p')^2.$$

In the absence of any knowledge of the functions $\Delta_F'(p^2)$ and F, it is convenient to rewrite Γ_μ as

$$\Gamma_\mu(p, p') = \tfrac{1}{2}(1+\tau_3)\{(p_\mu + p_\mu')F_1 + q_\mu F_2\} + A_\mu G. \quad (13)$$

It is clear that $G(0, 0, q^2)$ is just the charge structure of the K^0 meson as would be seen, say, in an electron scattering experiment. Similarly $F_1(0, 0, q^2)$ describes the charge and charge structure of the charged K meson. On the other hand $F_2(0, 0, q^2)$ must vanish as the interaction of a K^+ with an external field would not be gauge invariant. We now introduce the supposition that there is little probability that the meson can emit very energetic photons. That is to say, we suppose that the intermediate line in Fig. 1 is almost always near the physical meson mass. In this approximation we take F_1 and G as functions of q^2 only, and set F_2 equal to zero. This assumption also justifies our use of the "bare" propagator in the integral of Eq. (7).

The foregoing argument will not conceal from the astute reader the fact that we have attempted to construct the simplest possible field-theoretic

model with a minimum number of arbitrary parameters and a ready classical interpretation. This we have done and shown that it leads to physically sensible results.

The last listed author is indebted to the National Science Foundation for its support and to Professor A. Salam for the hospitality of Imperial College. We are both grateful to Dr. Burhop, who asked the right question, and Professor Y. Yamaguchi, who suggested the correct answer.

---

*National Science Foundation post-doctoral fellow.

[1]Rosenfeld, Solmitz, Tripp, Crawford, and Cresti, Phys. Rev. Letters 2, 110 (1959); Crawford, Cresti, Good, Stevenson, and Ticho, Phys. Rev. Letters 2, 112 (1959).

[2]S. Gasiorowicz and A. Petermann, Phys. Rev. Letters 1, 457 (1958). The basis of our calculation is rather different in spirit from that of this reference. These authors performed lowest-order perturbation calculations with a cutoff introduced on a purely ad hoc basis, and made some estimates of the effect of higher-order corrections. We construct what seems to us a very plausible classical model and assume that the field-theoretic calculation will be dominated by the terms which correspond most closely to this classical model.

[3]This was apparently first observed by T. Nakano (unpublished). We are indebted to Professor Y. Yamaguchi for informing us of this work. See also G. Feinberg, Phys. Rev. 109, 1381 (1958).

[4]M. Gell-Mann, Phys. Rev. 92, 833 (1953); T. Nakano and K. Nishijima, Progr. Theoret. Phys. (Kyoto) 10, 581 (1953); J. Prentki and B. d'Espagnat, Phys. Rev. 99, 328 (1955).

[5]Actually the two-pion, one-photon vertex part vanishes identically, on or off the mass shell, as can be seen immediately from invariance under particle antiparticle conjugation. Quantum mechanically the neutral pion does have an electromagnetic self-energy, but this is either of higher order in e^2 or involves rather massive intermediate states.

[6]Riazzudin (to be published).

ERRATUM

OSCILLATORY MAGNETO-ACOUSTIC EFFECT IN METALS. T. Kjeldaas, Jr., and T. Holstein [Phys. Rev. Letters 2, 340 (1959)].

In Eq. (6) the expression in brackets should read

$$\left[\frac{\sigma_0\sigma_{yy}}{\sigma_{xx}\sigma_{yy}+\sigma_{xy}^2}-1\right].$$

On page 340, the first line of the right-hand column should read, "the numbers shown as ordinates by $mM^{-1}\tau^{-1}C_s^{-1}$."

ABSTRACTS

In this section are printed the abstracts of Articles that have been forwarded to The American Institute of Physics for publication in THE PHYSICAL REVIEW. In quoting information obtained from this section before the appearance of the corresponding Article, reference should be made to "Physical Review (to be published)" rather than to this Journal.

WEAK-COUPLING EXPANSION FOR THE GROUND-STATE ENERGY OF A MANY-BOSON SYSTEM. M. Girardeau, Institute for Advanced Study, Princeton, New Jersey (Received April 14, 1959).

The pair theory of many-boson systems is used to obtain a weak-coupling expansion for the ground-state energy correct to third order in the coupling constant. The relationship of this expansion to the formal Rayleigh-Schrödinger perturbation expansion is discussed, with particular reference to the relationship between the divergent third-order term in the formal perturbation expansion and the terms of 5/2 and third orders in the correct weak-coupling expansion. The excitation energy is discussed briefly; it is pointed out that the lowest-order "nonpair" correction to the phonon energy is of the right order of magnitude to cancel the spurious energy gap of the pair theory.

GROUND STATE OF A BOSE SYSTEM OF HARD SPHERES. Tai Tsun Wu, Institute for Advanced Study, Princeton, New Jersey, and Bell Telephone Laboratories, Murray Hill, New Jersey (Received April 3, 1959).

It is shown that the pseudopotential method can be extended to yield further terms in the low-density expansion of the ground-state energy of a system of Boltzmann or Bose particles with hard-sphere interaction. Two terms beyond the known result are found, and the expansion is no longer a power series in $(a^3\rho)^{1/2}$. Other related properties of the system are discussed.

FOURTH VIRIAL COEFFICIENT FOR THE SQUARE-WELL POTENTIAL. Shigetoshi Katsura, Department of Applied Science, Tôhoku University, Sendai, Japan (Received September 24, 1958).

The fourth virial coefficient D and its component D_1, D_2, D_3 for molecules interacting with a square-well potential have been obtained as functions of the temperature by the use of Fourier transformation and the addition theorem of Bessel functions. Each component and their sum are nearly constant above the Boyle temperature and tend to negative infinity as the temperature tends to zero. The total D is expressed by

$$D/b^3 = 0.28642 + 1.5397f - 23.554f^2 + 53.645f^3 + 69.859f^4 - 170.01f^5 - 14.777f^6,$$

where $f = e^{\epsilon/kT} - 1$. Corrections of the critical data and some related problems are discussed.

IONIZED-IMPURITY SCATTERING MOBILITY OF ELECTRONS IN SILICON. Donald Long and John Myers, Honeywell Research Center, Hopkins, Minnesota (Received April 13, 1959).

Curves have been obtained of the temperature dependence of the electron mobility in a set of n-type silicon samples of varying impurity content and compensation between about 30° and 100°K by combining data from electrical resistivity and Hall effect measurements. The curves have been used in an experimental test of the applicability of the Brooks-Herring formula to the ionized-impurity scattering of electrons in silicon under conditions for which the Born approximation is valid. Impurity concentrations in the samples were determined by analysis of the Hall vs temperature data. It was necessary to correct for the lattice-scattering contribution to the observed mobility in comparing the Brooks-Herring formula with the experimental results. It is found that the formula gives a good quantitative description of the results when an electron effective mass of 0.3 of the true mass is used, provided that the ion scattering is not too strong. When ion scattering is dominant, however, such as at low temperatures in relatively impure samples, there is a discrepancy between formula and results which may be due to electron-electron interactions.

HALL EFFECT AND IMPURITY LEVELS IN PHOSPHORUS-DOPED SILICON. Donald Long and John Myers, Honeywell Research Center, Hopkins, Minnesota (Received April 13, 1959).

An experimental study has been made of the energy level structure of a phosphorus donor impurity in silicon, using Hall coefficient and Hall mobility measurements on six samples of widely varying impurity content and compensa-

tion. The main purpose was to test the Kohn-Luttinger theoretical model which predicts a splitting of the sixfold-degenerate (excluding spin) ground "1s" level, with a single state being depressed in energy by between 0.009 and 0.015 ev relative to the remaining five-fold degenerate level. The splitting energy can be measured by comparing carrier concentration vs temperature curves corresponding to this energy level scheme with experimental curves derived from Hall data. The curves for our samples all agree well with the Kohn-Luttinger model for splitting energies of between 0.009 and 0.012 ev, in agreement with the theoretical prediction.

VARIATIONAL APPROACH TO DEVIATIONS FROM OHM'S LAW. I. Adawi, RCA Laboratories, Princeton, New Jersey (Received December 15, 1958; revised manuscript received April 23, 1959).

In a perturbation framework, Kohler's variational method has been extended to obtain deviations from Ohm's law for a nondegenerate electron gas. Solution for the distribution function reduces to solving sets of linear algebraic equations. It is shown that, to second order in the field strength, the "popular" Maxwellian distribution (with a new temperature) is only a first-order variational solution. The method becomes extremely simple if the diffusion approximation is introduced and a relaxation time can be defined. Under these conditions, the second-order term in the mobility is expressed as the ratio of two infinite determinants using the usual representation, in which the unknown function is expressed as an energy polynomial. This ratio can be expressed by an infinite series.

INFRARED ABSORPTION FROM $\vec{L}\cdot\vec{S}$ SPLITTINGS IN Co^{2+} SALTS. R. Newman* and R. M. Chrenko, General Electric Research Laboratory, Schenectady, New York (Received April 9, 1959).

A line absorption spectrum has been observed at about 0.15 ev in CoO, $CoBr_2$, $CoCl_2$, and CoF_2 crystals. For the halides, the line has a complex structure. No absorption is observed in Cs_3CoCl_5 crystals. The absorption arises from transitions between various energy levels of the $\vec{L}\cdot\vec{S}$ fine structure multiplet. In CoF_2 some of the lines show changes in intensity on passing through the Néel temperature. Optical polarization effects are also observed in the CoF_2 spectrum.

*Present address: Materials Research Laboratory, Hughes Products, Newport Beach, California.

FURTHER EXPERIMENTS ON THE SIDWISE MOTION OF 180° DOMAIN-WALLS IN $BaTiO_3$. Robert C. Miller and Albert Savage, Bell Telephone Laboratories, Murray Hill, New Jersey (Received April 2, 1959).

Techniques have been developed to extend the measured electric-field dependence of the sidewise 180° domain-wall velocity in liquid-electroded $BaTiO_3$ crystals. The wall velocity data now cover about eight decades of velocity. The wall velocity is given by $v_\infty \exp(-\delta/E)$ where δ is found to increase slightly with field. The temperature dependence of v has been measured over a limited temperature range and the data show that δ varies with temperature faster than T^{-1}. The shapes and orientations of the reversed domains are field dependent. As the electric field is increased, the approximately square reversed domains observed in the low-field region go over into octagonal domains. At still higher fields, approximately square domains rotated by 45° about the ferroelectric axis with respect to the low-field domains are observed. Several of the important features of the sidewise wall motion are consistent with a nucleation-controlled model which is currently under investigation.

PHOTOCONDUCTIVITY OF GALLIUM SELENIDE CRYSTALS. Richard H. Bube and Edward L. Lind, RCA Laboratories, Princeton, New Jersey (Received April 10, 1959).

Single crystals of GaSe have been prepared by reaction of the elements, followed by gradient freeze crystallization. Crystals as grown were p-type, probably because of Cu acceptors, with hole mobility of 15 cm^2/volt sec, hole concentration of 10^{16} cm^{-3}, and acceptor ionization energy of 0.12 ev. In many ways the properties of GaSe crystals are very similar to those of ZnTe crystals. The absorption edge of GaSe is at 6310 A, corresponding to a band gap of 1.97 ev; the temperature coefficient of band gap is

about -4×10^{-4} ev/deg. Insulating and photosensitive GaSe crystals can be prepared by compensating the acceptor impurities by incorporated donors from Groups VII or IV. Rectification tests indicate p-type photoconductivity. Thermal quenching of photoconductivity corresponds to an ionization energy of about 0.5 ev, whereas optical quenching corresponds to an ionization energy of about 1.0 ev; thus a large Franck-Condon shift is indicated. Below the temperature at which thermal quenching of photoconductivity occurs, the sensitivity is within the range of sensitive CdS or CdSe crystals.

THERMAL EXPANSION COEFFICIENTS OF MANGANESE FLUORIDE. D. F. Gibbons, Bell Telephone Laboratories, Murray Hill, New Jersey (Received April 1, 1959).

The expansivity $(\Delta l/l_{273.2})$ and linear thermal expansion coefficient $[l^{-1}(dl/dT)_p]$ have been measured for the a and c axes of manganese fluoride. There is a marked anomaly in the linear thermal expansion coefficients at the Néel temperature; the Néel temperature was found to be $67^\circ\pm1^\circ$K. The anomaly has the characteristic shape associated with order-disorder transformations.

ENERGY LEVELS OF CONDUCTION ELECTRONS IN A MAGNETIC FIELD. Y. Yafet, Westinghouse Research Laboratories, Pittsburgh, Pennsylvania (Received March 26, 1959).

The energy levels of an electron in a periodic potential and a constant magnetic field are found as the solutions to a secular determinant when the following approximations are made: (a) The energy band of interest is spherically symmetric, and (b) lattice broadening of the levels is neglected. Inclusion of spin-orbit coupling gives the g factor as function of position in the band. Perturbation theory is used to treat the effect on the free energy of small departures of the band from spherical symmetry.

MAGNETIC SUSCEPTIBILITY OF InSb. R. Bowers and Y. Yafet, Westinghouse Research Laboratories, Pittsburgh, Pennsylvania (Received March 26, 1959).

The magnetic susceptility of n-InSb has been measured for a range of extrinsic carrier densities extending from 10^{16} to 6×10^{18} cm^{-3}. Measurements were made in the temperature range 300°K to 1.3°K. The degenerate conduction electron susceptibility was determined from the data. The deviation of the conduction band from parabolic form is clearly exhibited in the susceptibility. A theoretical analysis has been made using Kane's band structure calculation. The mixing of the conduction and valence bands resulting from the magnetic field has been treated exactly. Consideration of these two bands alone will not explain the dependence on concentration of the observed susceptibility; at the higher carrier densities, higher bands are important and a perturbation-theoretical treatment of these indicates that the observed susceptibility is consistent with Kane's model.

CRYSTALLINE IMPERFECTIONS AND $1/f$ NOISE. James J. Brophy, Physics Division, Armour Research Foundation, Chicago, Illinois (Received April 1, 1959).

The $1/f$ noise of single-crystal silicon and germanium has been examined as a function of naturally occurring imperfection densities, dislocations produced by plastic deformation, and imperfections resulting from fast-neutron irradiation. In all cases the noise power decreases with increasing crystalline imperfection. The results may be quantitatively explained by assuming that $1/f$ noise is proportional to the square of the minority carrier lifetime and accounting for the decrease in lifetime due to imperfections.

ELECTRON IRRADIATION OF INDIUM ANTIMONIDE. L. W. Aukerman,* Purdue University, Lafayette, Indiana (Received March 16, 1959).

The effects of 4.5-Mev electron bombardment on the electrical properties of n- and p-type InSb are studied. Isochronal annealing experiments carried out on samples bombarded at 80°K indicate three regions of rapid annealing, the first two between 80°K and 200°K and the third near room temperature. It is shown that the distribution of bombardment-produced energy levels is altered by heating a bombarded specimen to 200°K. The changes which occur as a result of this heat treatment suggest that energy levels are shifted as defects rearrange them-

selves into positions of greater stability. For samples bombarded at 200°K the positions of energy levels and the rates at which they are generated are determined from careful studies of the temperature dependence of carrier concentration. Mobility changes are utilized to identify donor or acceptor behavior. The levels introduced into the forbidden band appear to be multiply ionized.

*Present address: Battelle Memorial Institute, Columbus, Ohio.

ELECTRON IRRADIATION OF INDIUM ARSENIDE. L. W. Aukerman,* Purdue University, Lafayette, Indiana (Received March 16, 1959).

The carrier concentration of n-type InAs increases during irradiation with 4.5-Mev electrons. The increase is followed to a carrier concentration of $10^{17}/cm^3$. The carrier concentration of p-type samples decreases with irradiation. The increase in the electron concentration suggests that bombardment-produced donors are at least doubly ionized, even when the Fermi level is in the conduction band. Initially p-type samples exhibited anomalies which may result from n-type conduction in the vicinity of dislocations.

*Present address: Battelle Memorial Institute, Columbus, Ohio.

MAGNETORESISTANCE IN A MULTIVALLEY MODEL WITH ⟨110⟩ ELLIPSOIDS OF GENERAL SHAPE. Robert S. Allgaier, United States Naval Ordnance Laboratory, White Oak, Silver Spring, Maryland (Received April 13, 1959).

Expressions are derived for the three weak-field magnetoresistance coefficients b, c, and d, using a multivalley model having ellipsoids of general shape along the ⟨110⟩ directions in k-space. The results are given in terms of statistical and scattering integrals and of the two mass ratios K and L needed to specify the relative values of the three effective-mass components characterizing the ellipsoids. The properties of b, c, and d as functions of K and L are discussed, including in particular the fact that the symmetry conditions which are appropriate for each of the three ellipsoid-of-revolution models are satisfied along certain lines in the K-L plane.

MANY-PARTICLE APPROACH TO THE ONE-ELECTRON PROBLEM IN INSULATORS AND SEMICONDUCTORS. Abraham Klein, University of Pennsylvania, Philadelphia, Pennsylvania (Received April 10, 1959).

A formal theory of one-electron states in insulators and semiconductors is developed from a many-particle point of view. The techniques of second quantization are utilized for this purpose in a manner analogous to that introduced recently for the study of Fermi liquids, i.e., by the study of matrix elements of the electron field operator which describe the propagation of particles or holes. Both types of motion are described symmetrically by means of the one-particle Green's function or propagator. The utility of these constructs for the present study derives from the existence of a gap against single-particle excitation.

The basic result of this paper is that the motion of electrons near the bottom of the conduction band in the presence of external electric and magnetic fields whose spatial variation over one lattice spacing is small and which contain no frequencies comparable with the gap frequency is governed by a simple Schrödinger equation. The latter contains as parameters only the effective mass (as measured in a cyclotron resonance experiment) and the static dielectric constant and magnetic permeability of the solid. Our proof, within the restriction of a fixed, perfect lattice, takes into account all many-body effects. A similar theorem obtains for the motion of holes.

THEORY OF BLOCH ELECTRONS IN A MAGNETIC FIELD: THE EFFECTIVE HAMILTONIAN. Walter Kohn, Department of Physics, Carnegie Institute of Technology, Pittsburgh, Pennsylvania (Received February 26, 1959).

The Hamiltonian of a Bloch electron in a static magnetic field is $H = \frac{1}{2}\vec{P}^2 + V(\vec{r})$, where $V(\vec{r})$ is the periodic potential, $\vec{P} = \vec{p} + (1/c)\vec{A}$, and $\vec{A}$ is the vector potential giving rise to the magnetic field $\vec{\mathcal{H}}$. We consider the case of a nondegenerate band m. It is then shown that, with an error vanishing with $\mathcal{H}$ like $\mathcal{H}^{N+1}$ (N arbitrary), the eigenstates of H can be calculated from an equivalent Hamiltonian $\bar{H}_m(\vec{P})$ with the following properties: (1) It is a one-band Hamiltonian, obtained by transforming away all relevant interband matrix elements. (2) It depends only on the gauge-covariant

operators P^α. (3) It has the periodicity property $\bar{H}_m(\vec{P}+\vec{K})=\bar{H}_m(\vec{P})$, where K_ν is an arbitrary reciprocal lattice vector. (4) It can be written as a series $\bar{H}_m(\vec{P})=\sum_i s^i \bar{H}_{m;i}(\vec{P})$ $(i=0,1,\cdots,N)$, where $s\equiv\mathcal{H}/c$ and the functions $\bar{H}_{m;i}(\vec{P})$ are completely symmetrized in the noncommuting operators P^α. Properties (3) and (4) can also be summarized in the equations $\bar{H}_m(\vec{P})=\sum_l a^{(l)}\exp[i\vec{R}^{(l)}\cdot\vec{P}$ where the $\vec{R}^{(l)}$ are lattice vectors and the $a^{(l)}$ can be expanded as $a^{(l)}=\sum_i s^i a_i^{(l)}$. An algorithm is given for the construction of the $\bar{H}_{m;i}$ and carried through for $i=0,1,2$. The formalism is not restricted to the neighborhood of the bottom and top of the band. We believe that the equivalent Hamiltonian $\bar{H}_m(\vec{P})$ provides a sound basis for a discussion of wave functions and energy levels of Bloch electrons in a magnetic field.

ELECTRON AFFINITY OF O_2. R. S. Mulliken, Laboratory of Molecular Structure and Spectra, University of Chicago, Chicago, Illinois (Received April 8, 1959).

It is shown by using molecular orbital theory and experimental data that 0.15 ev is much the more probable of two alternative values for the electron affinity of O_2 which have been considered. Thermochemical evidence favoring a value of 0.9 ev is rather uncertain and should be given less weight.

$1\,^1S$ AND $2\,^3S$ STATES OF HELIUM. C. L. Pekeris, Department of Applied Mathematics, Weizmann Institute, Rehovot, Israel (Received April 15, 1959).

The method described previously for the solution of the wave equation of two-electron atoms has been applied to the $1\,^1S$ and $2\,^3S$ states of helium, with the purpose of attaining an accuracy of 0.001 cm^{-1} in the nonrelativistic energy values. For the $1\,^1S$ state we have extended our previous calculations by solving determinants of orders 252, 444, 715, and 1078, the last yielding an energy value of -2.903724375 atomic units, with an estimated error of the order of 1 in the last figure. Applying the mass-polarization and relativistic corrections derived from the new wave functions, we obtain a value for the ionization energy of 198312.0258 cm^{-1}, as against the value of 198312.011 cm^{-1} derived previously from the solution of a determinant of order 210. With a Lamb-shift correction of -1.339, due to Kabir, Salpeter, and Sucher, this leads to a theoretical value for the ionization energy of 198310.687 cm^{-1}, compared with Herzberg's experimental value of $198310.8_2 \pm 0.015$ cm^{-1}.

For the $2\,^3S$ state we have solved determinants of orders 125, 252, 444, and 715, the last giving an energy value of -2.17522937822 atomic units, with an estimated error of the order of 1 in the last figure. This corresponds to a nonrelativistic ionization energy of 38453.1292 cm^{-1}. The mass-polarization and relativistic corrections bring it up to 38454.8273 cm^{-1}. Using the value of 74.9 ry obtained by Dalgarno and Kingston for the Lamb-shift excitation energy K_0, we get a Lamb shift correction to the ionization energy of the $2\,^3S$ state of -0.16 cm^{-1}. The resulting theoretical value of 38454.66 cm^{-1} for the ionization potential is to be compared with the experimental value, which Herzberg estimates to be 38454.73 ± 0.05 cm^{-1}. The electron density at the nucleus $D(0)$ comes out 33.18416, as against a value of 33.18388 ± 0.00023 which Novick and Commins deduced from the hyperfine splitting. We have also determined expectation values of several positive and negative powers of the three mutual distances, which enter in the expressions for the polarizability and for various sum rules.

APPLICATION OF WAVE FUNCTIONS CONTAINING INTERELECTRON COORDINATES. I. GROUND-STATE ENERGY OF LITHIUM. Peter Walsh, Westinghouse Electric Corporation, Research Department, Lamp Division, Bloomfield, New Jersey, and Sidney Borowitz, Physics Department, New York University, New York (Received April 3, 1959).

Several years ago, Pluvinage made a substantial advance in the use of interelectron coordinates in atomic systems by illustrating how the Schrödinger equation can be partially separated in such a way that the interelectron potential no longer appears as the perturbing term. His method gave excellent results when used to obtain variational energies of helium-like systems. In this paper, the Pluvinage method is modified in such a way that it can be applied with a reasonable amount of labor to more complex systems. In this modification, the nuclear coordinates act like Fermi-Dirac "particles" filling the energy levels pairwise, while the interelectron coordi-

nates act like Bose "particles," all of which pile into the lowest energy continuum state. An accurate approximation technique is also developed for use in integrating functions containing three or more interelectron coordinates over the space of the nuclear coordinates. The modified Pluvinage approach is used in conjunction with the approximation technique to calculate the ground-state energy of neutral lithium. Internal evidence indicates that the approximation technique is better than 99% accurate in evaluating the individual integrals which appear. Although the wave function used here has no adjustable parameters, it yields an energy value for lithium which is slightly better than the two-parameter value of Wilson.

ISOTOPE SHIFT OF He $2P$. Gentaro Araki, Koichi Mano, and Masao Ohta, Department of Nuclear Engineering, Kyoto University, Yosida, Kyoto, Japan (Received April 2, 1959).

The isotope shift of the deepest ^3P and ^1P levels of the helium atom is calculated by making use of the wave functions which were reported by one of the authors. The theoretical values of the specific isotope shift of ^3P and ^1P levels are -636.00×10^{-3} cm^{-1} and 453.83×10^{-3} cm^{-1}, respectively, which are in fairly good agreement with the observed values $(-642\pm5)\times10^{-3}$ cm^{-1} (2^3P) and $(461\pm5)\times10^{-3}$ cm^{-1} (2^1P).

ELECTRONIC POLARIZABILITIES OF IONS. R. M. Sternheimer, Brookhaven National Laboratory, Upton, New York (Received April 9, 1959).

The dipole polarizability α_d has been calculated for several ions by solving the Schrödinger equation for the first-order perturbation of the wave functions of the core electrons. General results have been obtained for the number of nodes of the various types of perturbed wave functions $(nl-l')$ in terms of the principal quantum number n. Tables of the perturbed wave functions for the Na^+ and Cl^- ions are presented. The results for α_d of Na^+, K^+, Rb^+, and Cs^+ are in reasonable agreement with those obtained in previous work. Calculations have also been carried out for the electric field at the nucleus due to the charge distribution induced in the ion by an external charge. Values of the quadrupole shielding constant γ_∞ have been obtained for several helium-like ions.

NUMBER OF PROMPT NEUTRONS EMITTED PER THORIUM-232 FISSION. A. B. Smith, R. G. Nobles, and S. A. Cox, Argonne National Laboratory, Lemont, Illinois (Received April 9, 1959).

The number of prompt neutrons emitted per Th^{232} fission $[\nu_{Th^{232}}]$ is compared to the number emitted per U^{238} fission $[\nu_{U^{238}}]$. At a bombarding neutron energy of 1.4 Mev the ratio $\nu_{Th^{232}}/\nu_{U^{238}} = 0.98\pm0.08$.

MEASUREMENT OF SPIN POLARIZATION BY NUCLEAR SCATTERING. G. C. Phillips and P. D. Miller,* The Rice Institute, Houston, Texas (Received April 13, 1959).

Accurate measurements of differential cross sections for elastic scattering of protons from He^4 and C^{12}, and of He^3 from He^4 in the energy range 2 - 6 Mev have been phase-shift analyzed and the expected spin polarization of scattered particles calculated. The results, plotted as contours of equal spin polarization versus energy and angle, should be useful in accurate measurements of spin polarization and in addition show a number of rather striking complexities due to interference effects.

*Now at the Oak Ridge National Laboratory, Oak Ridge, Tennessee.

MEASUREMENT OF THE FISSION THRESHOLDS OF Pu^{239}, U^{233}, U^{235}, AND U^{238} USING THE (d,p) REACTION. John A. Northrop, Richard H. Stokes, and Keith Boyer, Los Alamos Scientific Laboratory, Los Alamos, New Mexico (Received April 6, 1959).

An experiment is described which measures the fission thresholds of thermally fissionable nuclides. In contrast to fission induced by neutron capture, use of the (d,p) reaction allows compound nuclei to be produced with excitations less than the binding energy of the last neutron. Measurements of the energy spectra of protons in coincidence with fission, normalized by the energy spectra of all emitted protons, have allowed the thresholds of Pu^{239}, U^{233}, and U^{235} to be observed. It should be emphasized that the compound nucleus is stable against neutron emission in the region of these fission thresholds, thus avoiding distortions by this competing reac-

tion. The threshold of U^{238} was also obtained for comparison with neutron data. In the case of the even-even compound nuclei, the observed step structure of the fission threshold is a clear indication of a multiple fission barrier. This multiple barrier is predicted by the collective model of fission and is correlated with the experimental data. The equivalent neutron energies at the center of the first threshold are as follows: $Pu^{239} = -1.61 \pm 0.02$ Mev, $U^{233} = -1.47 \pm 0.02$ Mev, and $U^{235} = -0.60$ Mev. The second thresholds are observable only for the first two: $Pu^{239} = -0.72 \pm 0.03$ Mev, and $U^{233} = -0.72 \pm 0.03$ Mev. The threshold of U^{238} agrees well with the data from neutron excitation. In each case the fission probability decreases in the region of positive neutron energies. This would result either if neutron emission were to compete with fission or if there were a significant contribution to the proton spectrum from the electric breakup of the deuteron.

LOW-ENERGY CAPTURE GAMMA RAYS OF Eu^{152} AND Eu^{154}. Eugene T. Patronis, Jr.,* and Harvey Marshak, Brookhaven National Laboratory, Upton, New York (Received April 14, 1959).

The low-energy capture gamma-ray spectra of Eu^{152} and Eu^{154} have been examined up to an energy of 300 kev by the use of a scintillation spectrometer. Eu^{152} was found to exhibit gamma lines at 81 ± 4 kev and 92 ± 3 kev while Eu^{154} exhibited gamma lines at 75 ± 3 kev and 91 ± 3 kev. Coincidence measurements were made on a composite spectrum produced by thermal-neutron capture in natural Eu. The data are consistent with the interpretation that the Eu^{154} lines are members of a rotational band while the Eu^{152} lines are not.

*On leave from Georgia Institute of Technology, Atlanta, Georgia.

PROTON-PROTON SCATTERING AT 90° FROM 28 to 68 Mev. Lawrence H. Johnston and Yung Su Tsai,* School of Physics, University of Minnesota, Minneapolis, Minnesota (Received April 1, 1959).

Proton-proton scattering cross sections are measured at 45° in the laboratory system, from 28 Mev to 68 Mev, with an accuracy of about $\pm 1.2\%$. These measurements fill the energy gap between the work of Cork on the low-energy end, and that of Ramsey et al. at higher energies. In the region of overlap with these experiments there is reasonable agreement. The cross section falls monotonically with increasing energy.

*Now at the High-Energy Physics Laboratory, Stanford University, Stanford, California.

EXCITATION FUNCTION FOR THE $V^{51}(\gamma, \alpha)Sc^{47}$ REACTION. Palmer Dyal and John P. Hummel, Department of Physics and Department of Chemistry and Chemical Engineering, University of Illinois, Urbana, Illinois (Received March 23, 1959).

Yields of the $V^{51}(\gamma, \alpha)Sc^{47}$ reaction have been determined by measuring the Sc^{47} radioactivity produced in metallic vanadium targets irradiated with bremsstrahlung of maximum energy varying from 10.5 to 25 Mev. The reaction was not observed below 15.5 Mev because of the severe effect of the Coulomb barrier on the outgoing alpha particles. The excitation function derived from these measurements has a maximum value of 0.81 mb at 23 Mev, and the integrated cross section to 24.5 Mev is 4.3 Mev-mb. The observed excitation function agrees very well with one calculated from a statistical theory for the decay of a compound nucleus. This appears to be a general feature of (γ, α) reactions in medium-weight nuclei.

MIRROR NUCLEI RADII UTILIZING SELF-ENERGY TERM AND NONUNIFORM CHARGE DISTRIBUTIONS. R. D. Cherry, Department of Physics, University of Cape Town, Rondebosch South Africa (Received December 17, 1957; revised manuscript received May 21, 1959).

The nature of the self-energy term in the mirror nucleus energy-difference formula is investigated. Two approaches are used. In the first this self-energy term is assumed to be a constant equal to the Coulomb self-energy of a single proton, and in the second a more refined quantum-mechanical approach based on the Swamy and Green Coulomb exchange energy calculations is used. Both approaches yield r_0 values which possess the correct general trend with increasing A, but which disagree with theoretical values for very low A. The effect of nonuniform charge distributions on the values of

nuclear radii obtained from mirror nuclei is investigated, and expressions for the Coulomb energy for various charge distributions are given. A direct comparison between the mirror-nucleus radii and those obtained from electron scattering is made in the few cases where this is possible. Finally, the possible validity of a suggested value of 0.58 Mev for the Coulomb self-energy of the proton is discussed briefly.

RADIATIVE CAPTURE OF PROTONS BY Be^9. W. E. Meyerhof, Department of Physics, Stanford University, Stanford, California, N. W. Tanner,* Kellogg Radiation Laboratory, California Institute of Technology, Mount Wilson and Palomar Observatories, Carnegie Institute of Washington, California Institute of Technology, Pasadena, California, and C. M. Hudson, Office of the Chief of Ordnance, Department of the Army, Washington, D. C. (Received April 13, 1959).

The gamma rays from the capture in Be^9 of protons of energy between 0.27 and 1.2 Mev have been studied using large scintillation crystals. Excitation functions of the gamma rays leading to the 0-, 0.72-, 1.74-, 2.15-, 3.58-, and 5.16-Mev states of B^{10} were computed from the measured gamma-ray spectra. In addition to the resonances previously known to exist at 0.33-, 0.99-, and 1.086-Mev proton energy [corresponding to (1^-) 6.88-, (2^-) 7.48-, and (0^+) 7.56-Mev states in B^{10}], evidence was found only for the p-wave resonance near 1 Mev [(2^+) 7.5-Mev state in B^{10}] postulated by Mozer and by Dearnaly and for the influence of higher lying states. This work leaves unexplained the large isotopic spin impurity of the 6.88-Mev level. Appreciable nonresonant capture was found for the transitions to the 0-, 0.72-, 3.58-, and 5.16-Mev states, which is probably not s-wave for the latter two transitions. Accurate energy measurements and coincidence work showed that the 5.16-Mev level of B^{10} is populated in preference to the 5.11-Mev level, contradicting earlier work of Clegg. Also, experimental evidence has been found which appears to be in contradiction to the 0^+ spin assignment for the 7.56-Mev level of B^{10} and raises doubts about the 2^+ spin assignment of the 5.16-Mev level.

*Present address: Clarendon Laboratory, Oxford, England.

DETERMINATION OF THE BETA-DECAY INTERACTION FROM ELECTRON-NEUTRINO ANGULAR CORRELATION MEASUREMENTS. J. S. Allen, R. L. Burman, W. B. Herrmannsfeldt,* and P. Stähelin,† University of Illinois, Urbana, Illinois, and T. H. Braid, Argonne National Laboratory, Lemont, Illinois (Received April 13, 1959).

The angular correlation coefficients in the allowed beta decays of He^6, Ne^{19}, Ne^{23}, and A^{35} have been experimentally determined from measurements of the energy spectra of the recoil ions. The form of the beta-decay interaction has been deduced from these measurements. The experimental results are summarized in the following table together with the beta-decay interaction forms which are indicated by each measurement.

Isotope	Selection rules	Correlation coefficient	Interaction forms
He^6	G-T	-0.39 ± 0.05	A
Ne^{19}	F and G-T	0.00 ± 0.08	ST or VA
Ne^{23}	G-T	-0.37 ± 0.04	A
A^{35}	Mostly F	$+0.97 \pm 0.14$	VT or VA

It is apparent from the last column that the experimental results are consistent if we assume that the dominant beta-decay interaction is the VA combination.

*Now at Los Alamos Scientific Laboratory, Los Alamos, New Mexico.

†Now at the Swiss Institute of Technology, Zürich, Switzerland.

THEORETICAL STUDIES OF THE ALPHA DECAY OF U^{233}. R. R. Chasman* and J. O. Rasmussen, E. O. Lawrence Radiation Laboratory and Department of Chemistry, University of California, Berkeley, California (Received April 9, 1959).

The alpha decay of a deformed odd-mass nucleus, U^{233}, is treated by the use of numerical integration on an IBM-650 computer. The results of this treatment are compared with the theory of Bohr, Fröman, and Mottelson.

Approximate analytic methods are developed for predicting the intensities of the higher members of the ground rotational band.

A comparison is made between the numerical integration and the experiments of Roberts, Dabbs, and Parker, in which they examine the

angular distribution of alpha particles from aligned U^{233} nuclei.

The results of the numerical integration of U^{233} are presented in matrices analogous to those of Fröman, and numerical values of the functions are given for selected values of r.

*Present address: Division of Chemistry, Argonne National Laboratory, Lemont, Illinois.

SIMPLE MODEL FOR GIANT-RESONANCE EFFECTS IN NUCLEAR REACTIONS. W. Tobocman and D. E. Bilhorn, Rice Institute, Houston, Texas (Received April 6, 1959).

A simple model for the scattering of s-wave neutrons is discussed. The scattering interaction is a square-well potential modified by allowing transmission through the origin to a mode of motion characterized by many narrow resonances. When coupling out of the incident channel is weak, the cross section is found to have a resonant part which shows the giant-resonance behavior observed in nuclear scattering.

TOTAL NEUTRON CROSS SECTION OF Xe^{135} AS A FUNCTION OF ENERGY. E. C. Smith,* G. S. Pawlicki,† P. E. F. Thurlow,‡ G. W. Parker, W. J. Martin, G. E. Creek, and P. M. Lantz, Oak Ridge National Laboratory, Oak Ridge, Tennessee (Received April 10, 1959).

The total neutron cross section of Xe^{135} as a function of energy has been remeasured at Oak Ridge National Laboratory under more favorable conditions than obtained in earlier measurements. A sample thickness of 2.5×10^{18} atoms of Xe^{135} gas per cm^2 was procured from the gases generated by a homogeneous reactor. A mechanical time-of-flight chopper was used to select neutrons in the energy range from 0.01 ev to several kev. The number of Xe^{135} atoms in the sample was determined by means of mass spectrometer measurements on the long-lived daughter, Cs^{135}. The data of the low-energy resonance were fitted to the single-level Breit-Wigner formula, taking into account Doppler corrections, equally well with the following two sets of parameters: statistical weight factor $g=3/8$, resonance energy $\epsilon_0=0.084\,72\pm0.000\,27$ ev; neutron width at energy ϵ_0, $\Gamma_n^0=0.034\,77\pm0.000\,21$ ev; capture width, $\Gamma_a=0.083\,303\pm0.000\,62$ ev; for $g=5/8$, $\epsilon_0=0.084\,15\pm0.000\,28$ ev; $\Gamma_n^0=0.020\,57\pm0.000\,12$ ev; $\Gamma_a=0.094\,93\pm0.000\,71$ ev. The errors quoted are the standard deviations derived from the statistics of the measurements. Systematic errors are discussed in the body of the paper. No evidence for resonances at energies greater than 0.085 ev was observed. The results described are interpreted in terms of recent considerations on the statistics of the properties of nuclear energy levels.

*Now at Lockheed Aircraft Corporation, Marietta, Georgia.

†Now at Argonne National Laboratory, Lemont, Illinois.

‡Now at American Machine and Foundry Company, Greenwich, Connecticut.

OPTICAL-MODEL ANALYSIS OF EXCITATION FUNCTION DATA AND THEORETICAL REACTION CROSS SECTIONS FOR ALPHA PARTICLES. George Igo, Los Alamos Scientific Laboratory, Los Alamos, New Mexico, Institute for Theoretical Physics, University of Heidelberg, and Max Planck Institute for Nuclear Physics, Heidelberg, Germany (Received April 7, 1959).

The complex alpha particle-nuclear potential is determined with small uncertainty at the nuclear surface by experiments with alpha particles in the range of bombarding energies up to 50 Mev in conjunction with this optical model analysis which assumes that the shape of the complex potential is exponential at the nuclear surface. The potential is given by the expression

$$V_\alpha + W_\alpha = -1100\exp\left[-\left(\frac{r-1.17A^{1/3}}{0.574}\right)\right] - i\,45.7\exp\left[-\left(\frac{r-1.40A^{1/3}}{0.578}\right)\right]\ \text{Mev},$$

for values of r (in units of 10^{-13} cm) where the real part is $\gtrsim -10$ Mev. The elastic scattering data have been used to determine the potential. The calculated reaction cross sections are found to be in satisfactory agreement with excitation function data.

The total reaction cross section σ_R for alpha particles in the energy range 0-50 Mev on nuclei with charge $Z=10$, 20, 30, 50, 70, and 90 has been calculated using the potential $V_\alpha+iW_\alpha$ obtained from the analysis of elastic scattering data. The calculated values may be interpolated to obtain σ_R for other values of Z.

COULOMB EXCITATION OF STATES IN Pt^{195}. F. K. McGowan and P. H. Stelson, Oak Ridge National Laboratory, Oak Ridge, Tennessee (Received April 9, 1959).

Gamma rays of 99, 110, 130, 140, 210, and 240 kev have been observed from Coulomb excitation of Pt^{195} (platinum target containing 60.1% Pt^{195}) with 3.0- to 5.5-Mev protons and α particles. The energy dependence of the gamma-ray yields indicates direct excitation of states at 99, 130, 210, and 240 kev. The 140-kev gamma ray is a cascade transition between states at 240 and 99 kev. These results do not agree with the conclusions of Bernstein and Lewis who measured the Coulomb excitation functions of the internal conversion electrons and found evidence for direct excitation of levels at 31 and 130 kev but no evidence for direct excitation of a level at 99 kev. The angular distributions of the 240- and 210-kev gamma rays and the 140-kev gamma ray in coincidence with K x-rays from internal conversion of the 99-kev transition have been measured with respect to the incident ion beam on a thick target. These measured distributions are consistent with an assignment of $\frac{5}{2}(E2)\frac{1}{2}$, $\frac{3}{2}(E2+M1)\frac{1}{2}$ with $(E2/M1)^{1/2}=0.37\pm0.02$, and $\frac{3}{2}(E2+M1)\frac{3}{2}$ with $(E2/M1)^{1/2}=-(0.13\pm0.03)$ for the 240-, 210-, and 140-kev transitions, respectively. The $B(E2)$ and $B(M1)$ for decay of these states have been determined.

DIRECT PAIR PRODUCTION BY MUONS. Byron P. Roe* and Seinosuke Ozaki,† Laboratory for Nuclear Studies, Cornell University, Ithaca, New York (Received April 3, 1959).

A measurement has been made of the direct pair production cross section for muon primaries between about 8 and 120 Bev. The muons were selected by a magnetic spectrometer and interactions were observed in a multiplate expansion cloud chamber. Results indicate that in the transferred energy range above about 200 Mev, the direct pair production cross section is somewhat less than that predicted by the Murota-Ueda-Tanaka theory. This result does not, however, necessarily indicate any breakdown of fundamental electromagnetic theory. Possible theoretical inadequacies are discussed in the text.

*Now at University of Michigan, Ann Arbor, Michigan.
†On leave from the Institute of Polytechnics, Osaka City University, Osaka, Japan.

INELASTIC SCATTERING OF 500-Mev ELECTRONS FROM Li^6 AND Li^7. Ulrich Meyer-Berkhout,* High-Energy Physics Laboratory, Stanford University, Stanford, California (Received April 6, 1959).

500-Mev electrons have been scattered from enriched Li^6 and ordinary Li (92.5% Li^7) between scattering angles of 60° and 135° in the laboratory system. The cross section integrated over the inelastic continuum at these large momentum transfers has been compared with the free-proton cross section at the corresponding angles. The results, when compared with those obtained for other light nuclei, may be used to yield some insight as to the extent to which the scattering from the individual nucleons can be considered as incoherent.

*Now at I Physikalisches Institut der Universität, Heidelberg, Germany.

INTERFERENCE EFFECTS OF THE RETARDATION TERM IN PION PHOTOPRODUCTION. A. M. Wetherell, California Institute of Technology, Pasadena, California (Received April 13, 1959).

It is shown that the difference in behavior of the high-energy (>450 Mev c.m.) total photoproduction cross sections for π^+ and π^0 can be explained by the presence of the retardation term in the case of the π^+ production. The analogy with the behavior at the (3/2, 3/2) resonance is noted. The discussion naturally provides an explanation for the difference in c.m. energies of the lower high-energy peak found in π^--p scattering and the corresponding peak in the π^+ photoproduction. It is felt that the discussion contributes some evidence for the resonance nature of the peaks.

CHARGE-EXCHANGE SCATTERING OF 128-Mev NEGATIVE PIONS ON HYDROGEN. E. Garwin, W. Kernan, C. O. Kim, and C. M. York, Enrico Fermi Institute of Nuclear Studies and Physics Department, University of Chicago, Chicago, Illinois (Received April 13, 1959).

The charge exchange scattering of negative pions by liquid hydrogen has been measured at 128±2 Mev bombarding energy. A lead glass Čerenkov counter was used to measure the energy

spectrum of the gamma rays emitted in the decay of the neutral pions. The gamma rays were detected at four angles relative to the incident beam: 45°, 80°, 116°, and 135°. If the charge-exchange scattering cross section is expanded as a sum of Legendre polynomials which are functions of the π^0 scattering angle in the center-of-mass system, we find that

$$\frac{d\sigma}{d\Omega}(\pi^-,\pi^0) = (1.00 \pm 0.04)[(2.04 \pm 0.06) + (-1.61 \pm 0.13)P_1 + (1.43 \pm 0.24)P_2],$$

when only s and p waves are considered. The confidence level for the least-squares fit used to determine the coefficients inside the square brackets is 65%. The integrated cross section is $\sigma_{tot}(\pi^-,\pi^0) = 25.6 \pm 1.3$ mb, which is in good agreement with other work.

MESON-MESON SCATTERING TERM IN PSEUDOSCALAR-PSEUDOSCALAR MESON THEORY. M. Sugawara, Purdue University, Lafayette, Indiana, and A. Kanazawa, Hokkaido University, Sapporo, Japan (Received March 17, 1958; revised manuscript received July 2, 1959).

The meson-meson scattering term has been investigated within the static approximation for a nucleon. First a static Hamiltonian is constructed from the renormalizable covariant meson theory in a manner similar to that proposed by one of the present authors. Improvements are that the meson-meson scattering term is included besides the ps-ps coupling term and that an argument is presented to show that the Foldy transformation is the unique one generating a valid static Hamiltonian, though it was left undetermined before. The resulting static Hamiltonian is than analyzed, for the cases of low-energy S- and P-wave pion-nucleon scattering and threshold photomeson production, in terms of the one-meson approximation of the Chew-Low-Wick formalism, without recourse to perturbation expansion. It is shown in particular that the meson-meson scattering term modifies the Chew-Low effective range plot of the δ_{33}-phase shift, making the renormalized P-wave coupling constant smaller than the conventional plot gives, for a positive coefficient of the meson-meson scattering term in the Hamiltonian. Empirical values of the coupling constant determined through the conventional Chew-Low plot and threshold photomeson extrapolation are shown to be interpretable in terms of the renormalized P-wave coupling constant of 0.08 and the meson-meson scattering term with coefficient of $\approx +4(\hbar = c = 1)$. The present treatment of threshold photomeson production, however, does not agree with the relativistic dispersion relation. General features of the static model resulting from the ps-ps meson theory are summarized in the final section, together with the conclusions obtained. The effects of strange particles and of renormalization have been neglected.

PION-PION INTERACTION IN τ^+-MESON DECAY. Billy S. Thomas* and W. G. Holladay, Physics Department, Vanderbilt University, Nashville, Tennessee (Received April 6, 1959).

The deviations of the π^- spectrum in τ^+-meson decay from the Dalitz-Fabri distribution in the 0^- state are analyzed on the assumption of a π^+-π^+ short-range interaction. Agreement with experiment is found if the absolute value of the π^+-π^+ scattering length $|a|$ is 1.4×10^{-13} cm. The π^+ spectrum is also calculated on the basis of this scattering length and found to agree with the experimental results.

*Now at Argonne National Laboratory, Lemont, Illinois.

USEFUL SYMMETRIES OF STRONG INTERACTIONS. J. J. Sakurai,* Institute for Advanced Study, Princeton, New Jersey (Received April 15, 1959).

An attempt is made to deduce "useful" relations among strange particle reactions slightly stronger than those implied by charge independence in the conventional sense. As Pais has shown, there are no such relations that hold to all orders aside from those already contradicted by experiments. However, for the relative $\Lambda\Sigma$ parity even and $G_{K\Lambda N} = (\pm)\, G_{K\Sigma N}$, $G_{K\Xi\Lambda} = (\pm)\, G_{K\Xi\Sigma}$, there exist relations that are valid as long as virtual pions play no role (as is evident from a recent unpublished work of Feynman). In particular, if we have, in addition, $G_{\pi\Lambda\Sigma} = (\mp)\, G_{\pi\Sigma\Sigma}$ (which means that the π couplings and the K couplings exhibit opposite four-dimensional symmetries), the weaker condition that pions emitted by N and Ξ (Λ and Σ) be not absorbed by Λ and Σ (N and Ξ) is sufficient for the validity of such relations.

Empirical examples are given. The question of the baryon mass spectrum is discussed.

*Now at The Enrico Fermi Institute for Nuclear Studies and the Department of Physics of the University of Chicago.

ANOMALOUS MAGNETIC MOMENTS OF BARYONS IN A STATIC CUTOFF PERTURBATION THEORY. W. G. Holladay, Department of Physics and Astronomy, Vanderbilt University, Nashville, Tennessee (Received February 17, 1959).

A universal coupling between pions and baryons should lead to anomalous moments comparable in magnitude for all the baryons except for the Λ and Σ^0 whose anomalous moments for reasons of isotopic spin symmetry should receive no direct contribution from the pion field. To estimate the influence of the K-mesonic field on these moments, a static, cutoff, second-order pertubation calculation is made on the assumption that all baryons have spin $\frac{1}{2}$, the same parity, that the K meson is a pseudoscalar, and that the K-mesonic interaction with the baryons is charge independent. Along the same lines a fourth-order calculation of the pionic contributions to these moments is also made. Baryon currents are neglected in these calculations and cutoff momenta based on the rest mass of the baryon emitting the meson were uniformly used for all processes. The Λ and Σ^0 moments are negative with a value of only about 0.5 nuclear magneton even if the K-meson coupling constants are large and judiciously chosen, a value which is therefore indicated as an upper limit, if no special enhancement effect is considered. If the K-meson couplings are all considerably smaller than the universal pion-baryon coupling, then the Λ and Σ^0 moments are quite small but the other hyperons have moments of comparable magnitude as is generally to be expected. If all K-coupling constants are large, our considerations show that p, n, Σ^+, and Ξ^- may still have comparable anomalous moments but the Σ^- is indicated to have a somewhat larger and the Ξ^0 a somewhat smaller moment than these. A pion coupling to the hyperons different from that to the nucleons would manifest itself in characteristic ways in terms of anomalous magnetic moments, for large or small values of the K-coupling constants.

SPHERICAL GRAVITATIONAL WAVES. John Boardman and Peter G. Bergmann, Department of Physics, Syracuse University, Syracuse, New York (Received April 14, 1959).

The field equations of the general theory of relativity are solved in the linear approximation for all cases of spherical waves with quadrupole symmetry. Energy is radiated outward by all these waves as determined by the canonical expression for the energy flux. A qualitative check of the validity of this method of calculation is made by the application of the same approximation to cylindrical gravitational radiation, for which an exact solution is known. In this case the exact and the linearized calculations lead to corresponding results.

RECIPROCAL STATIC METRICS AND SCALAR FIELDS IN THE GENERAL THEORY OF RELATIVITY. H. A. Buchdahl,* Institute for Advanced Study, Princeton, New Jersey (Received April 10, 1959).

In the first part of this paper a variant of the idea of reciprocal static solutions of the gravitational field equations is developed. Thus, given any static solution of Einstein's vacuum equations $R_{kl}=0$, a one-parameter family of pairs of solutions of the field equations with scalar field, viz., $R_{kl}=-\mu V_{;k}V_{;l}$, $g^{kl}V_{;kl}=0$, can be written down by inspection. The special cases of spherical symmetry and axial symmetry are treated as explicit examples. In the former case all the solutions of the field equations are obtained in this way. In the second part of the paper the theory is discussed from a physical point of view, for which purpose the motion of a test particle in the spherically symmetric field is treated in some detail.

*On leave from the Physics Department, University of Tasmania, Hobart, Tasmania, Australia.